Northwest African Sahel climate variations during Holocene/Late Pleistocene:

Insights from plant wax stable hydrogen (δD) and carbon ($\delta^{13}C$) isotopic composition and sea-surface temperature

Dissertation zur Erlangung des akademischen
Grades eines Doktors der Naturwissenschaften

Dr. rer. nat.

im Fachbereich 05 (Geowissenschaften)
der Universität Bremen

Eva Maria Niedermeyer

Bremen, 2009

Tag des öffentlichen Kolloquiums

23.10.2009

MARUM 2070, 10 Uhr c.t.

Gutachter der Dissertation

Prof. Dr. Gerold Wefer

Prof. Dr. Michael Schulz

Weitere Mitglieder des Prüfungsausschusses

Prof. Dr. Kai-Uwe Hinrichs

Prof. Dr. Gerhard Bohrmann

Dr. Enno Schefuß

Hiske Fink

ERKLÄRUNG

Name: Eva Niedermeyer **Datum**: 11.09.2009

Anschrift: Neckarstraße 90, 28199 Bremen

Hiermit versichere ich, dass ich

1. die Arbeit ohne unerlaubte fremde Hilfe angefertigt habe
2. keine anderen als die von mir angegebenen Quellen und Hilfsmittel benutzt habe und
3. die den benutzten Werken wörtlich oder inhaltlich entnommenen Stellen als solche kenntlich gemacht habe.

Bremen, den 11.09.2009

Eva M. Niedermeyer

(Unterschrift)

ACKNOWLEDGEMENTS

Firstly I would like to thank my advising committee Prof. Dr. Gesine Mollenhauer, Dr. Stefan Mulitza, Dr. Enno Schefuß and Prof. Dr. Gerold Wefer (in alphabetical order). Formerly trained as a biologist, I did not know much about marine sediments and how to read them as climate archives. With their individual expertise they greatly contributed to the completion of this thesis. Despite their full schedules they ALWAYS took their time to deal with my questions, to discuss about science and to assist me with writing. They also encouraged me to "non-office" science like presenting at several conferences, going for a trip onboard a research vessel and two research stays abroad.

A great thank-you goes to Prof. Dr. Alex Sessions from Caltech who introduced me to the secrets of compound specific stable hydrogen isotope analysis. I had the pleasure to spend several months benefiting from his tuition and advice, and I learned an incredible amount. Thank you Gesine for initiating my stay at Caltech! I further want to thank Dr. Alon Amrani for sharing his office with me as well as for all the any-time chats and lunch-time pizzas!

I thank Prof. Dr. Michael Schulz for constructive discussions that stimulated the interpretation of my results in a broader context and greatly enlarged my horizon. Dr. Jan-Berend Stuut for numerous discussions about the provenance of eolian dust off West Africa, Dr. Mahyar (Marco) Mohtadi for diverse ☺ support, not forgetting Dr. Markus Raitzsch & Christian Svenson for tackling numerous software problems. And, very importantly, Dr. Ed Hathorne and Robert J. Holmes for reading most parts of this thesis and transferring them to proper English.

Dear Uli, Markus R. & E., Lalitha, Ed, Jeroen, Petra, Steijn, Katrin, Marco, Stefan, Jan-Berend, Ines, Julio, Flo, Sergios, Marcos, Marius, and Christian, you've brought me great (after) work times and made Bremen a lively place to live for me. I thank Nicole Plöghoff and the Carabao-Bremen team for after-hour power! And of course I want to mention my two office dream-teams, my first office mate Dr. Uli Alt-Epping for a lot (!) of fun, and my current office crew Markus Eisele, Hiske Fink and Inka Meyer –you are the perfect combo!

I am grateful to the Bremen International Graduate School GLOMAR for accepting me as member and for all the numerous courses I had the pleasure to attend as well as for funding support. Thank you Uta and Gabi for your open ears for all troubles and for your dedicative support! Thank you Carmen for navigating through the administrative jungle.

This work was funded by the DFG through the Research Center/Excellence Cluster "The Ocean in the Earth System" at MARUM. Additional funding support for international conference contributions was provided by IMAGES for the 9th International Conference on Paleoceanography in Shanghai, and by the DFG through a Young Scientist travel grant for the SCOR 50th Anniversary Symposium in Woods Hole. The German Academic Exchange Service and GLOMAR are acknowledged for funding of two research stays at Caltech.

TABLE OF CONTENTS

ABBREVIATIONS **3**

ABSTRACT **5**

ZUSAMMENFASSUNG **7**

1 INTRODUCTION **9**

1.1 West African Monsoon 10
1.2 North Atlantic Circulation 12
1.3 Late Quaternary Climate Change 14

2 SCIENTIFIC OBJECTIVES AND APPROACH **16**

2.1 Objectives 16
2.2 Approach 17

3 OUTLINE **18**

4 MATERIAL AND REGIONAL SETTING **20**

4.1 Study material 20
4.2 Oceanographic Setting 20
4.3 Environmental setting 21
4.4 Regional controls of the δD value of precipitation 23

5 METHODS **24**

5.1 Sea-surface temperature – Alkenones ($U^{K'}_{37}$) 24
5.2 Deepwater ventilation – $\delta^{13}C$ of benthic foraminifera tests 25
5.3 C_3 or C_4 type photosynthesis – $\delta^{13}C$ of individual long-chain *n*-alkanes 25
5.4 Precipitation variability – leaf wax δD 26

6 MANUSCRIPTS **28**

6.1 Extratropical forcing of Sahel aridity during Heinrich stadials 28
6.1.1 Introduction 28
6.1.2 Material and environmental setting 29
6.1.3 Methods 30
6.1.4 Results 31
6.1.5 Discussion 32
6.1.6 Conclusions 33

6.2 Orbital- and millennial-scale changes in the hydrologic cycle and vegetation in the western African Sahel: Insights from plant wax δD and $\delta^{13}C$ 34

6.2.1 Introduction 34

6.2.2 Study area 35

6.2.3 Methods 37

6.2.4 Results 39

6.2.5 Discussion 40

6.2.6 Conclusions 45

6.3 18th century onset of aridification toward modern drought in the western Sahel Region 47

7 SYNTHESIS 57

7.1 West African monsoon and tropical northeast Atlantic SST 57

7.2 Vegetation feedbacks 58

7.3 Plant wax δD 58

8 OUTLOOK 60

9 REFERENCES 63

ABBREVIATIONS

AABW	Antarctic bottom water
AAIW	Antarctic intermediate water
AMOC	Atlantic meridional overturning circulation
BP	Before present
C_3	C_3 type photosynthesis
C_4	C_4 type photosynthesis
CAM	Crassulacean acid metabolism
CE	Current era
D	Deuterium
HS	Heinrich stadial
ITCZ	Intertropical convergence zone
ka	Thousand years before present
kyr	Thousand years
NADW	North Atlantic Deep Water
SST	Sea-surface temperature in degree centigrade (°C)
WP	Wet period
YD	Younger Dryas interval
Yr	Year(s)
$\delta^{13}C$	Stable carbon isotopic composition in per mill (‰) relative to the Vienna-Pee Dee Belemnite (V-PDB)
δD	Deuterium/Hydrogen ratios in per mill (‰) relative to the Vienna-Standard Mean Ocean Water (V-SMOW)

ABSTRACT

Intertropical convergence and tropical monsoon generation are important features of global atmospheric circulation and the hydrologic cycle. Understanding the mechanisms that drive tropical climate variability is of great interest within the context of modern climate change. The present study compiles the results of a three-year project presented as three manuscripts dealing with climate variability in the African western Sahel and the adjacent ocean during the Late Quaternary. This time interval is characterized by a number of abrupt climate changes (e. g. during Heinrich stadials) of global impact which makes it well suited to examine potential controls of global climate.

The aim of this PhD thesis is to document changes in West African monsoon intensity and vegetation, and to examine their potential link to the Atlantic meridional overturning circulation (AMOC) and sea-surface temperatures (SST) of the adjacent ocean. Analyses were done using marine cores retrieved from the continental slope off the coast of Senegal. Their vicinity to the modern northernmost position of the Intertropical convergence zone (ITCZ) makes them sensitive recorders of past variability of tropical northwest African climate. Deepwater ventilation at the study site was assessed through the stable carbon isotopic composition ($\delta^{13}C$) of benthic foraminifera tests and SST was estimated using alkenone paleothermometry. Changes in West African monsoon intensity and vegetation composition (that is C_3 vs. C_4 plants) were estimated using Deuterium/Hydrogen ratios (δD) and $\delta^{13}C$ of higher plant wax *n*-alkanes. The δD value of plant wax *n*-alkanes has been found to relate to the isotopic composition of rainwater which in turn relates to the amount of rainfall at the study site. The analytic technique has become available recently, and few paleo-studies that apply this proxy as an indicator for changes in the wet season exist so far.

The data indicate that tropical northeast Atlantic SSTs are not the trigger of millennial-scale drought in the western Sahel during Heinrich stadials. Instead, these droughts were presumably induced by substantial coolings of the extratropical North Atlantic in response to a slowdown of the AMOC (MANUSCRIPT I). The asynchronous temporal evolution of SST and rainfall variability as suggested by the Late Quaternary record also holds true for climate change during the Late Holocene (the past 2900 years), indicating this to be a robust feature of western Sahel climate on a centennial- and multi-decadal time scale.

The pattern of Late Quaternary plant wax δD variability suggests permanent local insolation forcing of the West African monsoon during the past 44 kyr. Moreover, it is indicated that climate change during Heinrich stadials also affected the rainy season, in addition to the dry season. Vegetation type, however, reveals only small changes throughout the past 44 kyr and shows low correlation to hydrology changes. This suggests that strong vegetation feedbacks

were of minor importance for Late Quaternary climate change in the western Sahel (MANUSCRIPT II). In contrast, the Late Holocene δD record suggests, in conjunction with historical documentation of land-use change, that agricultural clearing induced vegetation-precipitation feedbacks that triggered western Sahel aridification 250 years ago (MANUSCRIPT III). This suggests that the relative importance of feedback-mechanisms within the climatic system is highly dynamic.

ZUSAMMENFASSUNG

Die tropische Konvergenz von Luftmassen und die Erzeugung des Monsuns sind bedeutende Bestandteile der globalen atmosphärischen Zirkulation sowie des globalen Wasserkreislaufs. Klimatische Veränderungen in den niederen Breiten sind daher von potentiell globalem Ausmaß. Es ist essenziell die zugrunde liegenden Prozesse zu verstehen, insbesondere vor dem Hintergrund des erwarteten anthropogenen Klimawandels. Als Beitrag zum Verständnis von Klimaprozessen befasst sich die vorliegende Arbeit mit Klimaschwankungen im westlichen Teil des afrikanischen Sahel und des angrenzenden Ozeans während des späten Holozäns sowie des späten Quartärs. Dieser Zeitraum ist durch zahlreiche abrupte Klimaveränderungen von weltweitem Ausmaß gekennzeichnet (z. B. während sogenannter „Heinrich Stadiale“) und eignet sich somit zur Analyse globaler Klimamechanismen.

Das Ziel der vorliegenden Doktorarbeit ist Veränderungen des westafrikanischen Monsuns und der Vegetation der letzten 44 000 Jahre zu dokumentieren, sowie mögliche (kausale) Verbindungen zur Oberflächenwasser-Temperatur des angrenzenden tropischen Atlantiks und dessen Zirkulation herauszuarbeiten. Studienobjekt hierfür waren marine Sedimente von Schelf und Kontinentalhang vor der Küste des Senegal. Das Arbeitsgebiet liegt im Bereich der nördlichsten Position der Intertropischen Konvergenz (ITCZ) und ist somit gut geeignet, Schwankungen in der Intensität des Monsuns aufzuzeichnen. Die Rekonstruktion der örtlichen Tiefenwasser-Zirkulation erfolgte über den Gehalt stabiler Kohlenstoffisotope ($\delta^{13}C$) in Gehäusen bentischer Foraminiferen. Oberflächenwasser-Temperaturen wurden mit Hilfe von Alkenonen abgeschätzt. Veränderungen des westafrikanischen Monsuns sowie der Vegetation in Bezug auf C_3 und C_4 Pflanzen wurden über den Gehalt stabiler Wasserstoffisotope (δD) und $\delta^{13}C$ pflanzlicher *n*-Alkane angenähert. Der δD Wert pflanzlicher *n*-Alkane korreliert mit dem des Niederschlags, welcher in der Studienregion an die Regenmenge gekoppelt ist. Die Möglichkeit der komponenten-spezifischen Analyse des δD Wertes von Pflanzenwachsen gibt es erst seit Kurzem, und wenige paläo-Studien wenden diesen Proxy bisher an.

Die Resultate der ersten Teilstudie (spätes Quartär, MANUSKRIPT I) deuten darauf hin, dass Oberflächenwasser-Temperatur des tropischen nordöstlichen Atlantiks nicht der Auslöser für Trockenheit im westlichen Sahel während Heinrich Stadialen ist. Es scheint eher so, dass diese Trockenheiten durch erhebliche Abkühlung der Oberflächenwasser-Temperaturen des Nordatlantiks in höheren Breiten verursacht wurden, welche wiederum an die nordatlantische Zirkulation gekoppelt ist. Die Resultate der dritten Teilstudie (spätes Holozän, MANUSKRIPT III) weisen ebenfalls darauf hin, dass Oberflächenwasser-Temperaturen des angrenzenden Ozeans nicht der Auslöser für Klimaschwankungen im westlichen Sahel

sind. Dies legt den Schluss nahe, dass das Klima im westlichen Sahel auf großen Zeitskalen (im Bereich von einigen Jahrhunderten bis zu mehreren Jahrzehnten) in wesentlichen Teilen vom Klima des Nordatlantiks bestimmt wird.

Die Untersuchung zur Intensität des westafrikanischen Monsuns im späten Quartär (die letzen 44 000 Jahre, MANUSKRIPT II) weist auf einen kontinuierlichen Einfluss der lokalen Insolation auf das Regenregime hin. Des Weiteren zeigt sich, dass sich Klimaschwankungen während der Heinrich Stadiale nicht nur auf die Trockenzeit auswirken, sondern ebenfalls einen vermindernden Einfluss auf die Regenzeit haben. Die Analyse des Vegetationstyps deutet darauf hin, dass der westliche Sahel während der letzen 44 000 Jahre weitestgehend durch C_4 Pflanzen bestimmt wurde. Des Weiteren scheinen kleinere Veränderungen unabhängig vom Niederschlag zu sein. Dies deutet darauf hin, dass ausgeprägt Wechselwirkungen zwischen Vegetation und Niederschlag im westlichen Sahel von geringer Bedeutung waren für Klimaschwankungen der letzten 44 000 Jahre. Im Gegensatz dazu lassen die Ergebnisse der dritten Teilstudie vermuten, dass frühe landwirtschaftliche Aktivitäten vor etwa 250 Jahren eine bis heute andauernde Austrocknung im westlichen Sahel verursacht haben. Dies deutet darauf hin, dass der Einfluss verschiedener Rückkopplungsmechanismen innerhalb des Klimasystems höchst dynamisch ist.

1 INTRODUCTION

The African Sahel is a semi-arid ecosystem in tropical North Africa. It stretches from the Red Sea in the East to the Atlantic coast in the West forming a latitudinal band oriented almost parallel to the equator of varying width between 10-20°N. Vegetation of the Sahel forms the transition between the Sahara desert in the north and the humid savannah to the south with decreasing tolerance of drought with decreasing latitude. During the past century, the western Sahel has experienced a series of droughts with the most recent dry period in the 1970s and 1980s. During this time, precipitation over the western Sahel was 25–40 % lower than in 1931-60 (Nicholson 2000) with dramatic social and economic consequences for the local population. Further, Saharan dust export is believed to have various impacts on global climate in terms of the Earth's radiation balance (e. g. Prospero and Lamb, 2003), the global hydrologic cycle (e. g. Kaufman et al., 2002), marine phytoplankton productivity (e. g. Singh et al., 2008), and sea-surface temperatures (e. g. Lau and Kim, 2007). Understanding the mechanisms that trigger expansion or retreat of the Sahel is of great interest in the context of modern climate change in order to better predict and prepare for the impacts of future climate variability.

Western Sahel climate is characterized by seasonal rainfall brought by the West African monsoon. Sea-surface temperature gradients between the North and South Atlantic (Folland et al., 1986, Rowell et al., 1995, Fontaine et al., 1998, Hoerling et al., 2006) as well as tropical Atlantic sea-surface temperature variability (Hastenrath, 1984, Lamb and Peppler, 1992), and Indian Ocean temperatures (Bader and Latif, 2003, Giannini et al., 2003) have been found to considerably influence West African monsoon intensity. Further control is exerted by vegetation cover through its impact on soil-moisture-albedo feedbacks and evapotranspiration affecting continental rainwater recycling that feeds the monsoon (Xue and Shukla, 1993, Kutzbach et al., 1996, Ganopolski et al., 1998). Moreover, human induced vegetation change through agricultural clearing and herding is suggested to contribute to the recent Sahel drought (Otterman, 1974, Charney, 1975, Schlesinger et al., 1990).

The time interval covered by instrumental records does not capture large changes in global climate that could be analyzed to test the different hypotheses. One way to overcome this problem is the study of past climate variability. Late Quaternary climate, for example, is characterized by a number of millennial-scale abrupt climate changes of global extent (GRIP, 1993). There is evidence that they coincided with changes in the Atlantic meridional overturning circulation (AMOC) and sea-surface temperatures (SSTs), suggesting a central role of Atlantic Ocean circulation and its associated heat transport for global climate (e. g. Mix et al., 1986, Sarnthein et al., 1994, McManus et al., 2004). The goal of this thesis is to

reconstruct time series of western Sahel climate and contemporaneous conditions of the adjacent tropical northeast Atlantic during the Late Quaternary (the past 44,000 years) in order to identify potential causal links. Moreover, the Late Holocene (the past 2900 years) climate is focused upon to examine recent western Sahel climate variability in high resolution and link paleo-climate studies and modern climate. In addition to climate aspects, this study also focuses upon the application of Deuterium/Hydrogen ratios of plant waxes as paleo-proxy for rainfall variability, a technique that has been developed recently.

The following chapters aim to briefly introduce the general concept of the West African Monsoon system (CHAPTER 1.1), the basic features of Atlantic meridional overturning circulation (CHAPTER 1.2), and to provide an overview of global climate change during the Late Quaternary (CHAPTER 1.3). Specific scientific objectives and approach can be found in CHAPTER 2 and the thesis outline is given in CHAPTER 3 followed by a description of sample material and the study site in CHAPTER 4. The methods are briefly introduced in CHAPTER 5 (with a more detailed description of plant wax δD), whereas the analytical procedures can be found in the manuscripts (CHAPTER 6). This study ends with a synthesis of the three studies (CHAPTER 7) and an outlook for future research (CHAPTER 8).

1.1 West African Monsoon

The most prominent feature of atmospheric circulation over tropical Africa is the Intertropical Convergence Zone (ITCZ), a low-pressure trough separating the northern and the southern Hadley cells (Fig. 1.1-1). It refers to the location of surface convergence of the dry northeastern trade winds and the humid low-level southwestern monsoon flow to high atmospheric levels. The position of the ITCZ moves between 5° and 20°N (Nicholson 2000) over the West African continent following the seasonal migration of maximum insolation. This leads to a north-south precipitation gradient between the Sahara desert and the Guinea coast with increasing annual precipitation toward the equator. The generation of rainfall in the tropical rain belt occurs south of the ITCZ at higher atmospheric levels within a second zone of convergence of the mid-troposphere African Easterly Jet and the upper-troposphere Tropical Easterly Jet (Nicholson, 2009) (Fig. 1.1-2). The African Easterly Jet is characterized by a series of westward propagating waves (“easterly waves”) (Reed et al., 1977) that provide the energy that is required to develop rain-bearing disturbances (Nicholson and Grist, 2003). As a result, the intensity of the West African monsoon at a given geographic location depends on the position of the ITCZ and the associated rain belt, the precipitation potential of the monsoonal air masses, the frequency of cloud clusters modulated by easterly waves (Thompson et al., 1979, Nicholson and Grist, 2003), and on features of the rain-producing wind systems in the mid- and upper troposphere convergence (Nicholson, 2009). Rainfall

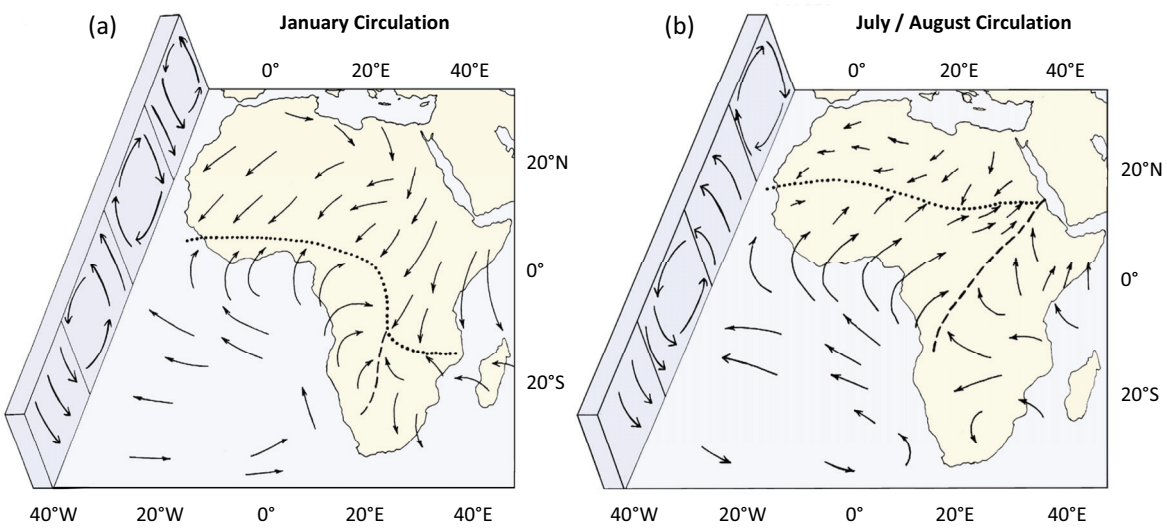

Fig. 1.1-1: Schematic of the general patterns of winds and convergence over Africa (adapted from Nicholson, 2000). (a) Atmospheric circulation in northern hemisphere winter with the ITCZ at its southernmost position (b) Atmospheric circulation during northern hemisphere summer when the ITCZ reaches its northernmost position. Arrows in the left panel indicate 3-dimensional atmospheric circulation; arrows on the screen indicate surface winds. Dotted lines denote position of the Intertropical Convergence Zone (ITCZ); dashed lines represent other zones of convergence.

directly resulting from the surface convergence is of minor importance compared to precipitation generated within the tropical rain belt (Nicholson, 2009).

The controls on the position of the ITZC and West African monsoon intensity are not yet understood in detail, and the relative importance of the different driving forces of course depends on the timescale in focus. On orbital timescales (10^4 to several 10^5 years), the intensity of the West African monsoon has been linked to the precessional cycle of summer season insolation through associated changes in SST and the land-sea contrast (e. g. Kutzbach, 1981, Rossignol-Strick, 1983, Prell and Campo, 1986, Pokras and Mix, 1987, Gasse, 2000, Weldeab et al., 2007). Modelling studies suggest that non-linear biogeophysical feedbacks between precipitation and vegetation cover may cause abrupt transitions from savannah vegetation to desert conditions within few centuries (Ganopolski et al., 1998, Claussen et al., 1999) despite a gradual orbital forcing. Millennial-scale variability of West African monsoon intensity is indicated during intervals of cooling in the northern North Atlantic realm (Adegbie et al., 2003, Jullien et al., 2007, Mulitza et al., 2008, Tjallingii et al., 2008, Itambi et al., 2009). This suggests an additional sensitivity of West African monsoon intensity to high-latitude climate processes such as changes in the AMOC (Zhang and Delworth, 2005, Mulitza et al., 2008, Tjallingii et al., 2008) and associated SST variability.

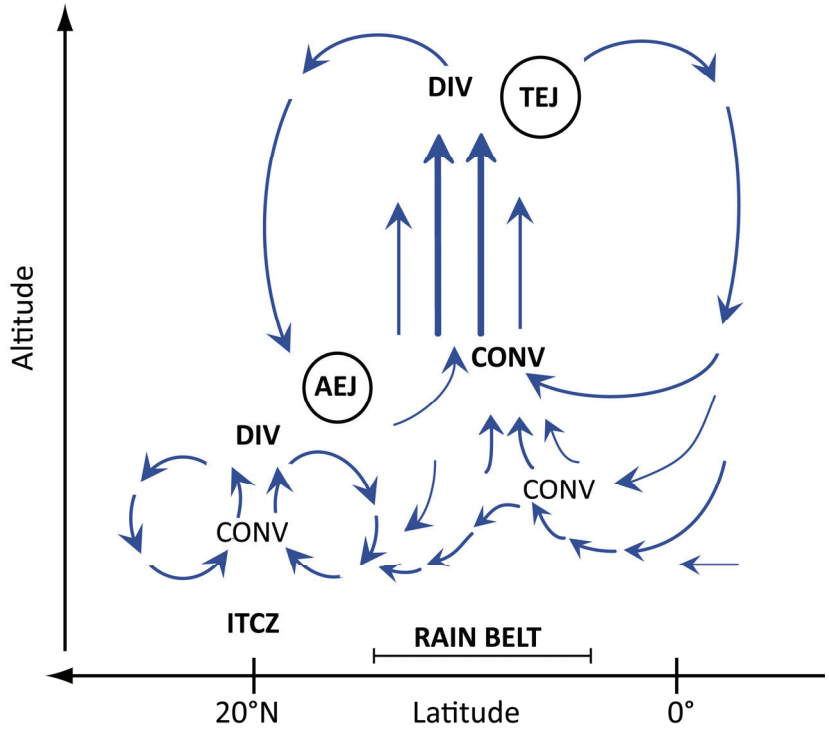

Fig. 1.1-2: Schematic picture of air mass convergence (CONV) and divergence (DIV) within the West African monsoon (after Nicholson 2009). The Intertropical Convergence Zone (ITCZ) is the location of surface convergence of the northern and southern Hadley cells. Rainfall generation occurs south of the ITCZ within a zone of convergence of the mid-tropospheric African Easterly Jet (AEJ) and the upper tropospheric Tropical Easterly Jet (TEJ).

1.2 North Atlantic Circulation

The global ocean circulation plays an important role for the energetic teleconnection between the latitudes (Ganachaud and Wunsch, 2000). For example, the heat transport associated with the North Atlantic circulation is responsible for the relatively mild temperatures Western Europe experiences, even in winter. This transport occurs by surface currents resulting from the overlying atmospheric circulation and the density driven deepwater formation at high latitudes (Fig. 1.2-1). The tropical easterly trade winds and the mid-latitude westerlies, together with deflection by the Coriolis force and the bordering continents, result in the formation of a subtropical gyre. This is a cyclonic circulation cell that connects the water masses of the eastern and western Atlantic basin. Within its western northward moving branch the Gulf Stream transports warm surface waters to mid-latitudes. There, the North Atlantic current detaches from the North Atlantic subtropical gyre introducing warm and salty surface waters into the high-latitude North Atlantic where they cool and sink. At present, most of this deepwater formation takes place in the Norwegian Sea and in the Greenland Sea. Depending on their relative density the down-dwelled waters form the so-

called Intermediate Waters (>1 km) or the North Atlantic Deepwater (NADW) (>2 km) (Duplessy et al., 1988) which both flow southward compensating for the fluxes in the upper mixed layer. Deepwater formation also takes place in the South Atlantic in areas of sea ice formation adjacent to the Antarctic continent, leading to the very dense Antarctic Bottom Water (AABW) and the less dense Antarctic Intermediate Water. The AABW has the highest density and enters the North Atlantic as the deepest bottom current. The different densities of the water masses lead to a stratification of the Atlantic Ocean with the NADW flowing as a tongue between the AABW and the Antarctic Intermediate Water. Depending on the strength of the Atlantic meridional overturning and associated NADW formation, the Atlantic Ocean basin is filled with more or less NADW or AABW (Sarnthein et al., 1994, Vidal et al., 1997).

Time slice compilations of deep sea sediments suggest that three distinct circulation modes have prevailed in the Atlantic during the past 30,000 years: the "stadial mode", the "interstadial mode" and the "Heinrich mode" (Sarnthein et al., 1994). In the interstadial mode, NADW formed in the Nordic sea, whereas during the stadial mode it formed further south in the subpolar North Atlantic south of Iceland. The Heinrich mode is thought to represent a slowdown of Atlantic overturning caused by high-latitude freshwater input (McManus et al., 2004), resulting in reduced NADW formation and deepwater of Antarctic origin extending into the northern North Atlantic basin (Sarnthein et al., 1994, Vidal et al., 1997, Elliot et al., 2002).

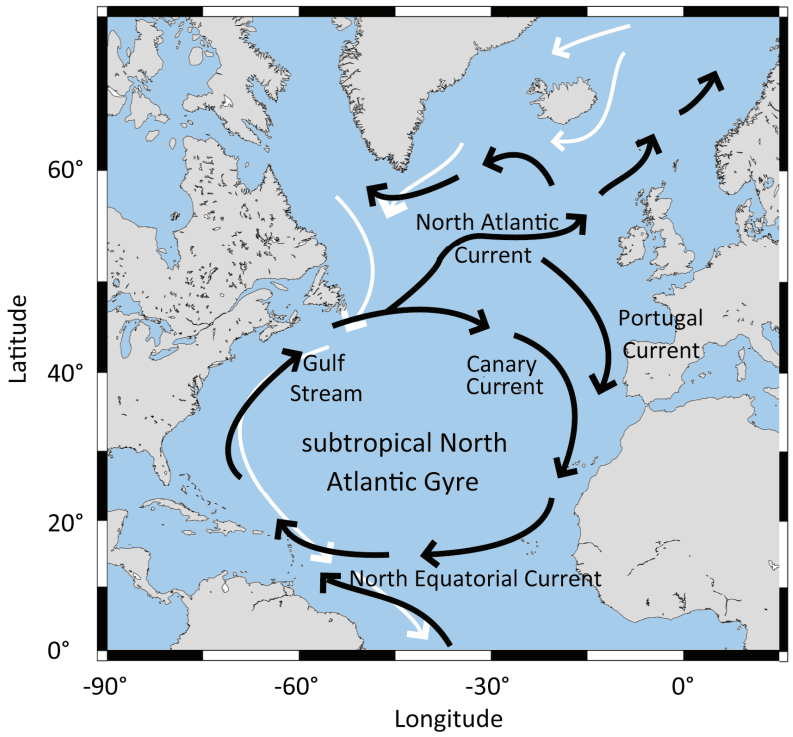

Fig. 1.2-1: Schematic of North Atlantic circulation after Tomczak and Godfrey (1994) and Stramma and Schott (1999). Tropical warm and saline surface waters are transported northward within the western branch of the subtropical north Atlantic Gyre (Gulf stream) and the North Atlantic current. North Atlantic deepwater (NADW) formation occurs north of Iceland and in the Greenland Sea. Black arrows indicate surface circulation; white arrows indicate NADW flow. Map was drawn using the generic mapping tool (http://www.aquarius.geomar.de)

1.3 Late Quaternary Climate Change

Climate archives obtained from Greenland ice cores (GRIP, 1993) reveal that the last glacial cycle (~100,000 years) was marked by a variety of millennial-scale climate fluctuations in the North Atlantic realm (Johnsen et al., 1992, Daansgard et al., 1993, Grootes et al., 1993). The so-called Dansgaard-Oeschger cycles comprise recurring warm and cold periods (referred to as interstadials and stadials) over Greenland that are characterized by abrupt warming of up to ~10°C (Severinghaus et al., 1998) within a few decades followed by gradual cooling over a longer period. The coldest phases of subsequent cooling cycles (Bond et al., 1993) are associated with the occurrence of ice rafted debris, the so-called Heinrich events (Heinrich, 1988), that culminated in enormous discharge of icebergs and meltwater into the North Atlantic (Bond et al., 1992, Broecker et al., 1992). Additional strong coolings over Greenland occurred during the Younger Dryas interval and the "8.2 kyr" event (Alley et al., 1997).

Climate variability during cold stadials is recorded in climate archives all over the world revealing opposite interhemispheric responses with cooling the northern and warming in the southern hemisphere (see Voelker, 2002). Antarctic ice core records from the Dronning Maud Land show warming during Greenland stadials, with the amplitude of the Antarctic warm events linearly related to the length. While the Younger Dryas and Heinrich stadials are reflected by surface cooling of the high latitude North Atlantic realm (Bond et al., 1992, Bond et al., 1993, Elliot et al., 2002), a reverse pattern is found in the high latitude southern hemisphere. Cold and dry conditions during Heinrich stadials are recorded basin-wide in the North Atlantic realm e.g. along Iberia (Bard *et al.*, 2000, Sánchez-Goñi et al., 2000, Sánchez-Goñi et al., 2008), the western Mediterranean (Combourieu Nebout et al., 2002) and subtropical northwest Africa (Zhao et al., 1995, Moreno et al., 2002, Jullien et al., 2007, Mulitza *et al.*, 2008). In contrast, concurrent warmer and moister conditions are suggested for the subtropical North Atlantic realm around e.g. Florida (Grimm *et al.*, 1993, Grimm *et al.*, 2006) and Barbados (Rühlemann et al., 1999) as well as for the southern hemisphere e.g. around Bolivia (Baker et al., 2001) and Brazil (Wang et al., 2004).

This bipolar see-saw (warming of the southern hemisphere with cooling in the northern hemisphere) has been linked to a slowdown of the AMOC during Heinrich stadials. A reduced northward transport of tropical warm surface waters leads to a cooling in the North Atlantic and an accumulation of heat in the South Atlantic. Sediment cores show that NADW formation was strongly reduced during Heinrich events (Sarnthein et al., 1994, Oppo and Lehman, 1995, Elliot et al., 2002) which is in agreement with a concurrent freshwater release into the North Atlantic (Stocker and Wright, 1991, Manabe and Stouffer, 1995). This reduces sea-surface salinity so that surface waters are not dense enough to sink, preventing the formation of NADW. This is reasonably well established for the Younger Dryas and at least Heinrich event

1 (Boyle and Keigwin, 1987, McManus et al., 2004, Rühlemann et al., 2004), and evidence points to changes in the AMOC (albeit different from the Heinrich mode) being a general feature of Dansgaard-Oeschger stadials (Sarnthein et al., 1994, Oppo and Lehman, 1995, Elliot et al., 2002).

The initial trigger causing AMOC variation during Heinrich stadials remains elusive. Hypotheses involve high-latitude forcing e. g. through internal oscillations of AMOC strength (Schmittner et al., 2002), ice sheet dynamics (MacAyeal, 1993, Hulbe et al., 2004) and variation in atmospheric CO_2 linked to ocean overturning changes (Marchal et al., 1998, Toggweiler et al., 2006). Low-latitude climate processes appear to be responsive to high-latitude temperature change (Chiang et al., 2003, Broccoli et al., 2006) and are suggested to amplify, perpetuate or even trigger millennial-scale climate variation. Climate change in the tropics may affect atmospheric circulation and composition through changes in the ITCZ position, surface water evaporation and greenhouse gas emissions (CO_2, N_2O CH_4) (Altabet et al., 2002, Stott et al., 2002, Ivanochko et al., 2005). Tropical ocean conditions may further impact the oceanic and heat distribution through e. g. heat convection and salinity changes (McIntyre and Molfino, 1996, Peterson et al., 2000, Turney et al., 2004).

In recent years, many studies have focused on millennial-scale climate change in the high- and mid-latitude North Atlantic realm, whereas timeseries covering tropical climate variability during Heinrich stadials are rare. Detailed information about tropical climate variation and its relation to high-latitude climate processes is needed to better understand the driving forces of global climate.

2 SCIENTIFIC OBJECTIVES AND APPROACH

2.1 Objectives

Studies of northwest African climate suggest numerous swings between dry and wet climate conditions in Northwest Africa on orbital (e. g. Kutzbach, 1981, Gasse, 2000, Tjallingii et al., 2008) and millennial timescales (Jullien et al., 2007, Mulitza et al., 2008, Tjallingii et al., 2008, Itambi et al., 2009) during the last glacial cycle. Studies of SST off northwest Africa (Mauritania) (Zhao et al., 1995, Romero et al., 2008) indicate surface cooling concurrent with millennial scale aridity (Heinrich stadials) but they do not reveal whether millennial-scale Sahel drought is triggered by the adjacent ocean SST or if it is linked to high-latitude climate instead. Further, although studies off Mauritania (Jullien et al., 2007, Tjallingii et al., 2008) and Senegal (Mulitza et al., 2008, Itambi et al., 2009) indicate an abrupt onset of dry conditions prevailing during Heinrich stadials, no continuous multi-millennial timeseries of northwest African monsoon intensity exists so far. The proxies applied in the previous studies most likely reflect variations of the dry season; congruent variations during the rainy season has been inferred but not shown yet. Variations of the rainy season, such as duration and precipitation rate, further may affect vegetation type and density. An impact of vegetation dynamics on monsoon intensity and, hence, on climate (Kutzbach, 1981, Ganopolski et al., 1998, Claussen et al., 1999) appears reasonable, given the importance of continental rainwater recycling for monsoon feeding (Gong and Eltahir, 1996, Nicholson, 2000). These feedbacks have been suggested to act as amplifying mechanisms of modern Sahel drought (Charney, 1975, Ganopolski et al., 1998) but remain poorly understood. Furthermore, the evolution of modern Sahel climate is not well understood. Pollen studies (Senegal) (Lézine, 1989, Lézine and Casanova, 1989) indicate the onset of modern dry conditions 2000 years ago, whereas archaeological and historical studies (McIntosh and McIntosh, 1983, Webb, 1994) indicate humid excursion during this period and aridification of the western Sahel starting about 300 years ago.

The scientific questions in detail are:

- How do tropical northeast Atlantic SSTs vary with high latitude climate changes during Heinrich stadials, and how do they relate to variations of the AMOC?
- What is the potential role of tropical northeast SST as a trigger of climate in the Sahel?
- How does West African monsoon intensity vary on orbital, millennial and centennial timescales, and what are possible forcing factors?

- How does vegetation vary with monsoon intensity?
- How does the modern Sahel drought relate to the climate of its recent past (Late Holocene)?
- How do tropical northeast Atlantic SST and West African monsoon intensity during the Late Holocene compare to Late Quaternary variability?

2.2 Approach

This study addresses the temporal evolution of tropical northeast Atlantic SST and deepwater ventilation as well as West African monsoon intensity and vegetation composition of the past 44,000 years, and with higher temporal resolution, of the past 2900 years. Analyses were done on marine sediment cores retrieved off the coast of Senegal, tropical northwest Africa. They are located close to the modern northernmost extension of the West African monsoon and consist of material deriving from both marine and terrestrial sources. This allows a direct comparison of ocean conditions to climate on land without stratigraphic and dating uncertainties. Further, the terrestrial material deposited off tropical West Africa integrates climate conditions over a broader area in comparison to many terrestrial archives like lacustrine sediments. Studies of Late Quaternary climate were done on gravity core GeoB9508-5 extending to 60,000 years before present. Holocene climate was reconstructed using cores GeoB9504-3 (gravity core) and GeoB9504-4 (multi core) which together cover the past 2900 years.

Marine conditions such as SST and deep ocean ventilation were approximated using $U^{K'}_{37}$ based alkenone paleothermometry and $\delta^{13}C$ of benthic foraminifera tests (Dr. Stefan Mulitza). Climate conditions on land were approximated through changes in vegetation (C_3 vs. C_4 plants) based on $\delta^{13}C$ and sedimentary abundance of plant wax *n*-alkanes. However, during the time interval assessed by this study, pCO_2 has varied considerably (Monnin et al., 2001) therefore potentially biasing the interpretation of vegetation changes in terms of humidity vs. pCO_2 changes. A new tool to directly assess changes in rainfall is provided by Deuterium/Hydrogen ratios of individual plant wax *n*-alkanes. The δD value of plant material has been found to record the isotopic composition of the growth water (Epstein et al., 1977, Sessions et al., 1999, Sachse et al., 2004) which in turn is linked to precipitation (Dansgaard, 1964). The recording of the isotopic signature needs no hydrologic thresholds as required for vegetation change and is therefore potentially a direct and sensitive proxy for rainfall variability. The analytical technique to measure plant wax δD compound specifically has only recently been developed and only a few paleo-studies exist so far (e. g. Schefuß et al., 2005, Makou et al., 2007, Tierney et al., 2008).

3 OUTLINE

The scientific objectives were addressed within three different studies. The results of these studies are presented in CHAPTER 6 as three manuscripts as follows:

CHAPTER 6.1: Extratropical forcing of Sahel aridity during Heinrich stadials

Eva M. Niedermeyer, Matthias Prange, Stefan Mulitza, Gesine Mollenhauer, Enno Schefuß, and Michael Schulz

This manuscript addresses millennial-scale variability of tropical northeast Atlantic SST and local deepwater ventilation of the past 44,000 years. A tight coupling of the temporal structure of the SST record and deepwater ventilation at the study site indicates a link to the AMOC. The hypothesized relation is assessed by a freshwater hosing experiment (Dr. Matthias Prange). Furthermore, the role of tropical northeast Atlantic SST as a potential trigger of climate variation in the western Sahel during Heinrich stadials is investigated. Comparing the SST record to Fe/K ratios (a proxy for aridity on land) from the same core (Mulitza et al., 2008) reveals a lag between SST variation and the onset of drought, suggesting that tropical northeast Atlantic SST is not the trigger for Sahel drought during Heinrich stadials.

CHAPTER 6.2: Orbital- and millennial-scale changes in the hydrologic cycle and vegetation in the western African Sahel: Insights from plant wax δD and $\delta^{13}C$

Eva M. Niedermeyer, Enno Schefuß, Alex L. Sessions, Stefan Mulitza, Gesine Mollenhauer, Michael Schulz, and Gerold Wefer

This study deals with variability of the West African monsoon intensity in the western Sahel and vegetation changes on orbital and millennial timescales during the past 44,000 years and discusses potential driving forces. For this, individual plant wax *n*-alkanes were analyzed for their Deuterium/Hydrogen ratios (δD) in collaboration with Prof. Dr. Alex Sessions at Caltech (California Institute of Technology, USA), as well as for their $\delta^{13}C$ and abundance. Vegetation variability shows little correlation with hydrologic changes indicating additional controls on plant type growth such as atmospheric pCO_2. The pattern of δD variability indicates permanent insolation forcing of the West African monsoon and additional control during Heinrich stadials.

CHAPTER 6.3: 18th century onset of modern drought in the Sahel Region

Eva M. Niedermeyer, Enno Schefuß, Stefan Mulitza, Alex L. Sessions, Gesine Mollenhauer, and Gerold Wefer

The third study addresses western Sahel precipitation and adjacent SST of the past 2900 years. This is done working on a gravity core and a multi core retrieved from the mud belt of the Senegal River. The climate record of the gravity core (2900 to 600 years BP) is used to validate plant wax δD as a proxy for precipitation changes and to show the coupling of 'natural' western Sahel precipitation changes to the central West African monsoon. This is done by comparing variations of the δD record to earlier studies and to a recent $\delta^{18}O$ record from Lake Bosumtwi (Shanahan et al., 2009), respectively. The record obtained from the multi core links the paleo-record to modern climate and provides evidence for a decoupling of western Sahel rainfall from central African precipitation about 400 years ago. The data show that modern drought in the western Sahel is part of a multi-centennial aridification trend starting 250 years ago. It is suggested that aridification was triggered by vegetation-precipitation feedbacks that were induced through anthropogenic agricultural clearing.

4 MATERIAL AND REGIONAL SETTING

4.1 Study Material

Analyses were done on marine sediment cores (gravity cores GeoB9508-5 and GeoB9504-3 and multi core GeoB9504-4) that were retrieved during RV METEOR cruise 65/1 (Mulitza et al., 2006) off Senegal (Fig. 4-1). Gravity cores (multi core) are stored at 4°C (-20°C) the in the MARUM core repository. All cores consist of undisturbed sediments and provide high resolution climate archives of their respective time intervals. The terrigenous fraction of sediments at the study site derives from both Senegal River suspension and eolian dust (Sarnthein et al., 1981, Mulitza et al., 2008).

Sampling of the gravity core was done using PET syringes (ø ~1 cm) with the tip cut off lowered 10 cm into the sediment. Samples were taken every 5 cm from GeoB9504-4 and every 4-12 cm from the upper 692 cm of GeoB9508-5. The multi core was sampled shipboard into 1 cm slices stored in Petri-dishes, samples were analyzed every 5 cm.

4.2 Oceanographic Setting

Surface waters of the tropical northeast Atlantic off the coast of Africa are dominated by the southward flowing Canary Current (the eastern branch of the subtropical North Atlantic gyre, Fig. 4-1) which is a wind driven cold surface current flowing southward along the West African coast all year round (Mittelstaedt, 1991). At about 21°N, the Canary Current detaches from the continental margin and turns westward into the North Equatorial Current. South of 20°N, the cool southward African Coastal Current flows along the West African shoreline in winter and spring. During summer and fall, a northward flow (the Mauritania Current, gray arrows in Fig. 4-1) exists along the coast (e. g. Stramma and Schott, 1999) which transports warm surface waters and is fed by the North Equatorial Counter Current and the Guinea Dome. Surface waters are submerged by a poleward flowing undercurrent transporting South Atlantic Central Water which encounters the Canary Current between 21° and 22°N. It is vertically bordered by the southward moving North Atlantic deepwater.

Wind driven upwelling of the nutrient rich South Atlantic Central Water occurs within a 20 to 30 km band inshore along the coast in winter and spring, and no upwelling is recorded throughout the rest of the year (Mittelstaedt, 1991). Seasonally averaged SSTs range from 19°C during winter (Jan-Mar) and 21°C in spring (Apr-Jun) to 28°C during summer (Jul-Sep) and 26°C in fall (Oct-Dec). (National Virtual Ocean Data System, http://ferret.pmel.noaa.gov/NVODS).

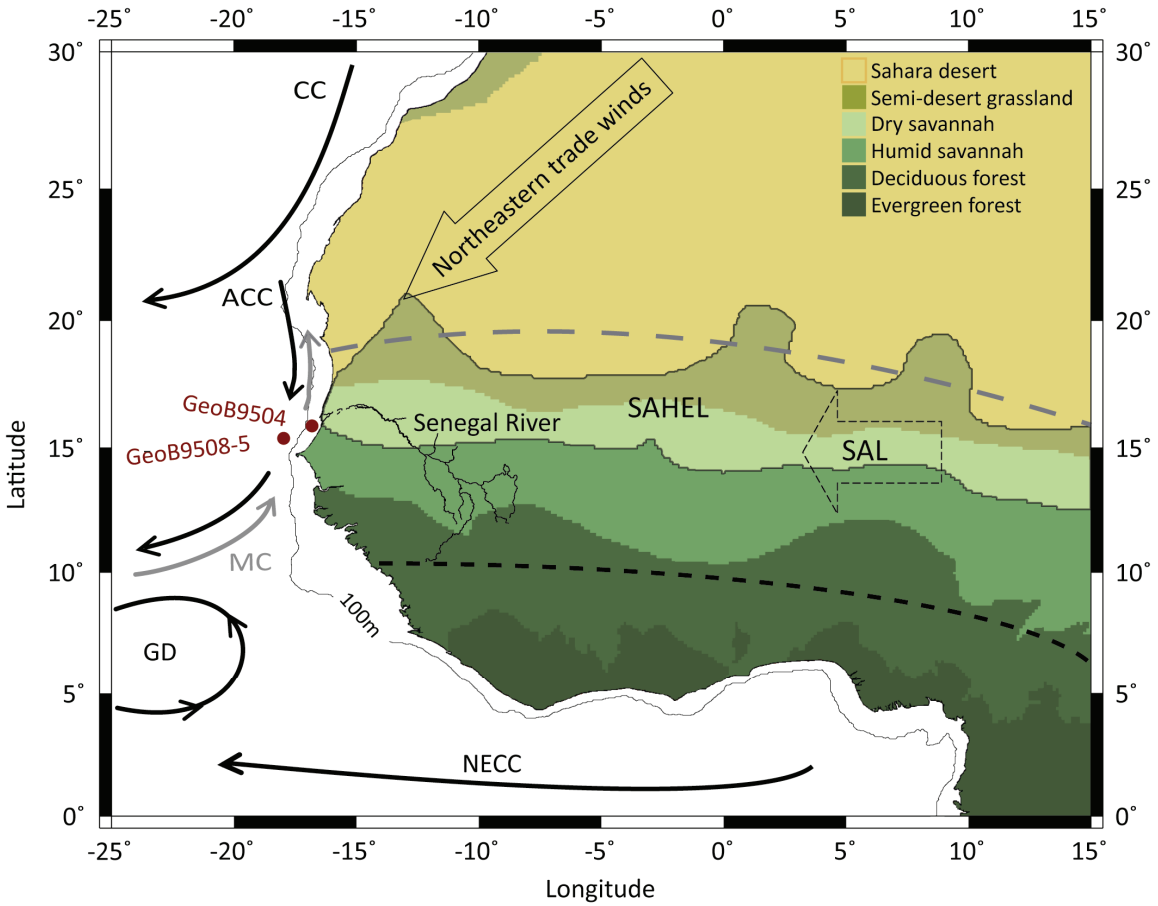

Fig. 4-1: Map indicating study site and regional setting. Black (gray) curved arrows indicate surface currents during northern hemisphere winter (summer) (adapted from Stramma and Schott, 1999). Black (gray) dashed line represents southernmost (northernmost) ITCZ position in winter (summer). Broad arrows indicate direction of the northeastern trade winds and the Saharan Air Layer (SAL). Vegetation changes gradually from Sahara desert to tropical rainforest as depicted by colour coding (White, 1983). CC: Canary Current; ACC: African Coastal Current; MC: Mauritania Current; GD: Guinea Dome; NECC: North Equatorial Counter Current.

4.3 Environmental Setting

Rainfall over tropical northwest Africa is linked to the position of the ITCZ and its associated rain belt. The seasonal migration of the ITCZ leads to a seasonal precipitation pattern over northwest Africa (Fig. 4-2) with increasing precipitation [mm yr^{-1}] and extension of the rainy season toward the equator (http://climate.geog.udel.edu/~climate). Maximum precipitation over the western Sahel occurs during the northern hemisphere summer from July to September when the ITCZ reaches its northernmost position, followed by a dry season for the rest of the year when the ITCZ moves back southward. During the dry season, the northwest African continent is dominated by the low-level dry northeastern trade winds (Sarnthein et al., 1981) that blow almost parallel to the West African coast, transporting large amounts of dust to the ocean (Swap et al., 1996, Stuut et al., 2005). Further dust transport occurs in high atmospheric levels within the Saharan Air Layer. These two regimes provide the most

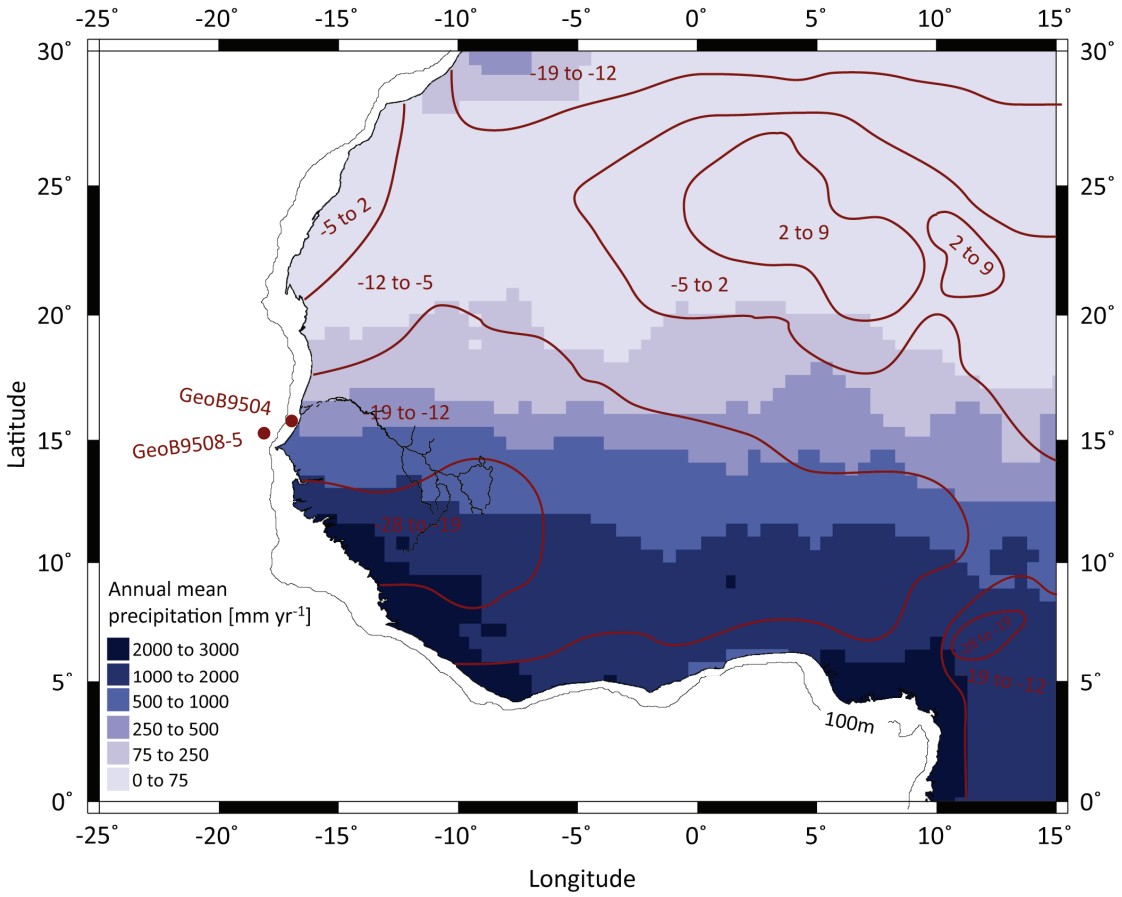

Fig. 4-2: Mean annual rainfall [mm yr^{-1}] and growing season precipitation δD [‰] of northwest Africa. Precipitation after Willmott, Matsuura and collaborators from http://climate.geog.udel.edu/~climate/ as indicated by colour coding. Red lines indicate distribution of growing season precipitation δD after Bowen and Revenaugh (2003) and Bowen (2009) from www.waterisotopes.org.

important sources of eolian input for plant waxes (Huang et al., 2000) deposited in marine sediments offshore West Africa.

Additional plant wax transport occurs within Senegal River discharge. The Senegal River is located between 11-16°N and 10-16°W (Fig. 4-1) and has a total drainage area of approximately 350,000 km^2. Following the north-south precipitation gradient the major part of the river discharge is generated in the tropical deciduous forests (>1250 mm) of the Guinea Mountains and southern Mali, whereas the contribution from higher tropical latitudes is small. The sediment flux is closely related to the water discharge (Gac and Kane, 1986) and is highest during the rainy seasons from June to October, and drops to almost zero during the end of the dry season. The yearly flux of organic matter accounts for less than 2 % of total sedimentary flux (Gac and Kane, 1986).

Vegetation gradually changes from desert to dense tropical vegetation (Fig. 4-1), following the seasonal migration of the tropical rain belt and the associated precipitation gradient (White, 1983) (Fig. 4-2). The Sahara desert is sparsely vegetated by few C_4-type grasses and

CAM type plants. The adjacent Sahel consists of semi-desert grassland dominated by short C_4 grasses and dry savannah with sporadic trees (C_3 type). Vegetation changes progressively to the humid savannah which receives sufficient rainfall to maintain a higher vegetation cover consisting of both tall C_4 grasses and trees (C_3). It widens up to tropical deciduous forests toward the equator that become evergreen forests at the Guinea coast.

4.4 Regional controls of the δD value of precipitation

Ocean water provides the initial source of most rainwater. In the tropics, ocean surface water evaporates, is lifted to cloud height by convection and is transported poleward (Gat, 1996). Because the lighter isotope evaporates preferentially (the saturation vapour pressure of HDO is lower than for H_2O), the initial water vapour is depleted in deuterium (D) when compared to its oceanic origin (Gat, 1996). Due to the preferential removal of the heavier isotope during condensation (rainfall), the atmospheric water vapour gets progressively depleted with increasing distance from its source and toward higher elevations (Dansgaard, 1964). Additionally, rainwater gets further depleted by continental rainwater recycling, that is the cycle of rainfall and subsequent cloud formation due to continental evapotranspiration (Worden et al., 2007). The isotopic composition of rainfall also strongly depends on the degree of re-evaporation of raindrops which in turn depends on ambient relative humidity (Worden et al., 2007, Risi et al., 2008a, Risi et al., 2008b). In the tropics, such as the study area, atmospheric humidity varies considerably with the precipitation gradient leading to "heavier" rain (D enriched) in dry areas compared to "lighter" rain (D depleted) in humid areas (Fig. 4-2). This so called "amount effect" (Dansgaard, 1964) controls the δD value of precipitation over tropical northwest Africa, dominating the continental effect over a wide area (Bowen and Revenaugh, 2003, Bowen, 2009).

5 METHODS

Ocean conditions such as SST and deepwater sources (North or South Atlantic) were estimated by analyses of Alkenones based on the $U^{K'}_{37}$ index and $\delta^{13}C$ of benthic foraminifer tests. Climate changes on land associated with vegetation type and rainfall variability were approximated by $\delta^{13}C$ and δD of terrigenous higher-plant wax *n*-alkanes. Long-chain *n*-alkanes are characteristic products of higher plants with typical chain lengths ranging from C_{25} to C_{35}. They are integral parts of epicuticular waxes from vascular plant leaves (Eglinton and Hamilton, 1967), protecting the leaf from uncontrolled evaporative loss of water and microbial attack. Leaf waxes are produced throughout the growing season and may record climate conditions on land.

In the following, the proxies applied within this study will be briefly introduced. A more detailed description will be provided for the application of plant wax δD as a proxy for rainfall variation since this is a new technique and still subject to intense research with considerable depleyment over the past three years.

5.1 Sea-surface temperature – Alkenones ($U^{K'}_{37}$)

Alkenones are long chained unsaturated mono-ketones that are mainly produced by the coccolithophore *Emiliania huxleyi*, a unicellular marine green algae found in almost all marine environments except the Arctic Ocean and high-latitude Southern ocean. It is still uncertain what role alkenones play in haptophyte physiology, but it has been found that the number of double bonds built in the C_{37} ketone (unsaturation index, $U^{K'}_{37}$) relates to the growth temperature of the algae (Brassel et al., 1986). *E. huxleyi* lives in the photic zone (between 10 and 50m) and is an important primary producer in the world's ocean forming large blooms in spring and early summer (Tyrrell and Merico, 2004). Calibration studies revealed that the alkenone index is best correlated with annual mean surface temperatures (Brassel et al., 1986, Prahl and Wakeham, 1987, Prahl et al., 1988, Müller et al., 1998, Müller and Fischer, 2001, Conte et al., 2006). However, this relationship is potentially biased by the seasonal occurrence of the algae toward spring (Conte et al., 1992) or winter (Herbert et al., 1998). Further, depth of alkenone production (and therefore SST) may vary depending on water turbidity. Additionally, growth rate can affect $U^{K'}_{37}$ as well as lateral advection and diagenetic processes (Teece et al., 1998, Müller and Fischer, 2001, Conte et al., 2006). At the study site, growth temperature has been shown to dominate the $U^{K'}_{37}$ signal and SST estimates are found to relate best to annual mean temperature of the upper mixed layer (Müller and Fischer, 2001).

5.2 Deepwater ventilation – $\delta^{13}C$ of benthic foraminifera tests

The $\delta^{13}C$ of tests from the (epi-) benthic foraminifera *Cibicidoides wuellerstorfi* was used to trace the isotopic composition of dissolved inorganic carbon in bottom water ($\delta^{13}C_{\Sigma CO2}$) as a proxy for changes in deepwater ventilation (Duplessy et al., 1988, Sarnthein et al., 1994). This method is based on fractionation processes during primary production (which discriminates against ^{13}C) resulting in surface waters with high productivity being enriched in ^{13}C compared to areas with low primary production. Since deepwater forms from surface water, this signal is transferred into the deep ocean. NADW forms from surface waters that are enriched in ^{13}C (and depleted in nutrients) by photosynthesis at subtropical latitudes compared to AABW which is depleted in $\delta^{13}C_{\Sigma CO2}$ (and enriched in nutrients) because it forms from low productivity surface waters (Curry et al., 1988). The $\delta^{13}C$ value of deepwater may be further modified by oxidation of organic matter settling from the surface, leading to progressive depletion of low-ventilated water masses and nutrient release (Kroopnick, 1985). (Therefore, strictly speaking $\delta^{13}C_{\Sigma CO2}$ is a nutrient proxy.)

The isotopic characteristic of deepwater is preserved in the tests of benthic foraminifera using the dissolved inorganic carbon of the ambient water for calcification, and can be used to trace the presence and distribution of NADW and AABW over glacial-interglacial cycles (Curry et al., 1988, Raymo et al., 1990). However, some physiological and inorganic conditions exist that may exert additional control on the correlation between the $\delta^{13}C$ value of the benthic tests and the nutrient content in the upper water column like seasonal production of phytodetritus ("Mackensen effect"). Other factors which can influence the $\delta^{13}C$ of benthic foraminera include species specific habitat, temperature and variability of the $\delta^{13}C$ of atmospheric CO_2 over time (for a review see Mackensen and Bickert, 1999).

5.3 C_3 or C_4 type photosynthesis – $\delta^{13}C$ of individual long-chain n-alkanes

The geographic distribution of C_3 and C_4 plants depends on climate parameters such as water availability, atmospheric pCO_2, insolation intensity and temperature (Larcher, 2001). The $\delta^{13}C$ value of plant wax *n*-alkanes is a well established tool to distinguish C_3- from C_4-type photosynthesis. The isotopic difference results from physiological differences during CO_2 acquisition for photosynthesis (O'Leary, 1981) and varies between -21 ‰ (C_4 type) and -36 ‰ (C_3 type) (values are for the C_{31}-*n*-alkane, Rieley et al., 1993, Collister et al., 1994). The range of variation in $\delta^{13}C$ of atmospheric pCO_2 is much smaller (Indermühle et al., 1999), making the photosynthetic pathway the dominant control on the isotopic signature of plant waxes. In tropical northwest Africa, C_4-type grasses are the dominant species of the semi-desert and savannah grasslands with increasing contribution of C_3-type species (mainly

shrubs and trees) with increasing humidity towards the equator (White, 1983). The growing season of tropical C_4 grasses is characterized by higher minimum temperatures and a shorter rainy season compared to that required for C_3 plants (Larcher, 2001). The competitive advantage of C_4 over C_3 plants in hot and dry environments is due to their ability to internally concentrate CO_2 prior to photosynthetic CO_2 fixation. This allows for lower stomatal conductivity reducing the transpirational loss of water (Larcher, 2001). In addition, low atmospheric pCO_2 such as during the last glacial may control the dispersal of C_3 plants (even under humid conditions) as a limiting factor of photosynthesis (Collatz et al., 1998, Bond et al., 2003). Therefore, the competition between C_4 and C_3 plants may not depend on humidity only, but also on atmospheric pCO_2 with low pCO_2 suppressing C_3 photosynthesis and vice versa.

5.4 Precipitation variability – leaf wax δD

The Deuterium/Hydrogen ratio of plant material incorporates the δD value of the source water (Epstein et al., 1977). Although this has been known for several years, it has only been recently that the δD of leaf wax became accessible for paleo-climatologists as a potential proxy for past rainfall variability. The traditional technique did not allow compound specific conversion of organic analytes to the gaseous form needed for isotope analysis which is essential for the application of organic proxies. In the 1990s, a pyrolysis interface was developed that couples a conventional gas chromatograph to an isotope-ratio mass spectrometer (for a review see Sessions, 2006). This allows the δD value of individual compounds in small sample sizes (in the range of 50ng total hydrogen) to be analyzed precisely. This development opened the field to investigating the biochemical and environmental controls of plant wax δD which is still subject to intense research.

The δD value of plant wax *n*-alkanes has been shown to record to the δD value of precipitation (Sessions et al., 1999, Sauer et al., 2001, Huang et al., 2004, Sachse et al., 2004, Smith and Freeman, 2006, Hou et al., 2008). However, strictly speaking it is not the isotopic composition of precipitation that is recorded by plant waxes but rather that of leaf water (e.g. Pendall et al., 2005). This water source may be D-enriched relative to precipitation by soil evaporation and leaf transpiration (Dongmann et al., 1974, Epstein et al., 1977, Flanagan et al., 1991), suggesting an additional influence of relative humidity on leaf wax δD. Such a link has been proposed in several studies (Sachse et al., 2004, Sachse et al., 2006, Smith and Freeman, 2006, Hou et al., 2007, Hou et al., 2008), and the question to what extend relative humidity influences D enrichment in leaf waxes is focus of ongoing research. There is also debate about whether vegetation characteristics have influence on leaf wax δD through differences in photosynthetic pathway, leaf anatomy, or rooting depth (e. g. Chikaraishi and

Naraoka, 2003, Liu et al., 2006, Smith and Freeman, 2006, Hou et al., 2007, Liu and Yang, 2008) but no specific pattern can be extracted yet. However, despite interspecific differences, the δD values of plant waxes extracted from surface sediments agree well with the δD of precipitation. They show better correlation to precipitation δD than do individual plants (Sachse et al., 2004), indicating that species-specific differences are smoothed in the integrated signal.

The application of δD of individual plant wax compounds as a proxy for past rainfall variation has produced valuable results (e. g. Schefuß et al., 2005, Makou et al., 2007, Tierney et al., 2008) contributing to a more detailed understanding of climatic mechanisms.

6 MANUSCRIPTS

6.1 Extratropical forcing of Sahel aridity during Heinrich stadials

Eva M. Niedermeyer[1], Matthias Prange[1,2], Stefan Mulitza[1], Gesine Mollenhauer[1,2,3], Enno Schefuß[1], Michael Schulz[1,2]

[1] *MARUM–Center for Marine Environmental Sciences, University of Bremen, P.O. Box 330 440, D-28334 Bremen, Germany (eniedermeyer@marum.de)*

[2] *Department of Geosciences, University of Bremen, P.O. Box 330 440, D-28334 Bremen, Germany*

[3] *Alfred Wegener Institute, Am Handelshafen 12, D-27570 Bremerhaven, Germany*

Submitted to *Geophysical Research Letters*

(accepted for publication by the associate editor with minor revisions)

In order to investigate a possible link between tropical Northeast (NE) Atlantic sea-surface temperature (SST), Atlantic meridional overturning circulation (AMOC), and drought in the Sahel during the past 44 thousand years (kyr) we used alkenone paleothermometry and $\delta^{13}C$ of *C. wuellerstorfi* of a marine sediment core from the continental slope off Senegal. Our data show periods of low SST and reduced AMOC that coincided with drought in the Sahel during North Atlantic Heinrich stadials (HS). The coldest period was HS1 (ca. 15-18 kyr before present, BP) when SST decreased by more than 2°C. Moreover, the SST off Senegal lagged variations in Sahel aridity which is in agreement with results from a freshwater hosing experiment. We conclude that variations in tropical NE Atlantic SST were not the initial trigger of millennial-scale Sahel droughts of the past 44 kyr. Instead, it is thought that these droughts were induced by substantial coolings of the extratropical North Atlantic.

6.1.1 Introduction

It is generally accepted that the distribution pattern of SSTs of the Atlantic and the Indian Oceans is critical for interannual and interdecadal Sahel rainfall variability (e. g. Folland et al., 1986, Fontaine and Bigot, 1993, Giannini et al., 2003, Lu and Delworth, 2005). Using an atmosphere general circulation model, Sutton and Hodson (2005) investigated the role of the Atlantic SST pattern in forcing Northern Hemisphere summer climate. In particular, their model predicted that an anomalously warm tropical North Atlantic (0°N to 30°N, excluding the Gulf of Guinea; their Figure S1B) leads to a substantial increase in rainfall over the West African Sahel (their Figure 3B), whereas SST anomalies in the extratropical North Atlantic (>30°N) were inferred to have no significant effect on Sahel climate. Particularly cold tropical SSTs along the West African coast between Mauritania and Guinea (i.e. ~20°N to 10°N) associated with Sahel droughts were identified by Hastenrath (1984) and Druyan (1991). On longer timescales, Mulitza et al. (2008) argued that millennial-scale

Sahel "mega-droughts" during the past 50 kyr were primarily triggered by strong coolings of the extratropical North Atlantic during HS which, in turn, were induced by perturbations of the AMOC and its associated northward heat transport.

In this study, we examine a possible link between tropical NE Atlantic SST and AMOC and further investigate the potential role of tropical NE Atlantic SST in triggering drought in the Sahel through the past 44 kyr. For this purpose, we analyzed a gravity core from the continental slope off Senegal. This site allows reconstructing SST through alkenone paleothermometry, deep ocean ventilation through benthic carbon isotopes, and direct comparison to a continental aridity record from the same core as depicted by changes in XRF elemental abundances (Mulitza et al., 2008). Our data show that tropical NE Atlantic SST lags Sahel aridity and therefore likely is not the initial trigger for the onset of millennial-scale Sahel drought.

6.1.2 Material and environmental setting

Marine sediment core GeoB9508-5 was retrieved from the continental slope off Senegal during RV Meteor cruise M65/1 about 160 km southwest (15°29.90'N 17°56.88'W) of the Senegal River mouth at a water depth of 2,384 m (Fig. 6.1-1).

Surface waters at the site are indirectly influenced by the southward flowing Canary Current. At about 21°N, the Canary Current detaches from the continental margin and turns westward into the North Equatorial Current. South of 20°N, the cool southward African Coastal Current flows along the West African shoreline in winter and spring. During summer and fall, a northward flow, the Mauritania Current, exists along the coast (e. g. Stramma and Schott, 1999), transporting warm surface waters influenced

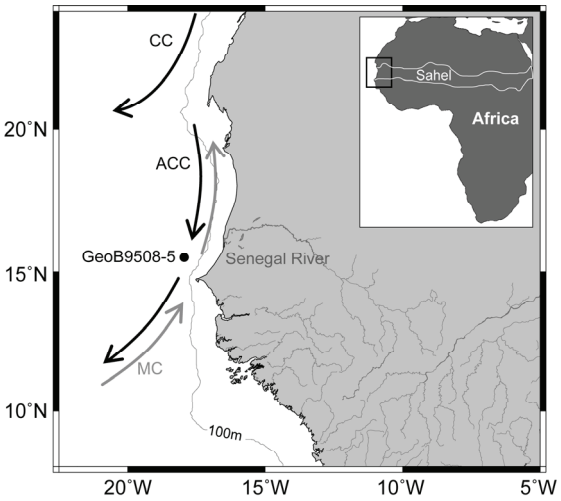

Fig. 6.1-1: Position of marine gravity core GeoB9508-5 in the tropical NE Atlantic off Senegal. Black curved arrows indicate surface currents during winter and spring, gray curved arrows indicate surface currents in summer and fall: CC: Canary Current (winter and spring); ACC: African Coastal Current (winter and spring); MC: Mauritania Current (summer and fall). A detailed map of tropical Atlantic currents systems can be found in Stramma and Schott (1999).

by the North Equatorial Countercurrent and the Guinea Dome.

The area of our study site experiences weak upwelling in winter and spring and no upwelling throughout the rest of the year (Mittelstaedt, 1991). Seasonally averaged SSTs range from 19°C during winter to 28°C during summer (National Virtual Ocean Data System, http://ferret.pmel.noaa.gov/NVODS). Alkenone derived SST estimates off NW Africa represent the yearly average of the mixed layer temperature (Müller and Fischer, 2001).

At present, the core site is bathed by North Atlantic deepwater (NADW) (Sarnthein et al., 1994). During glacial times the core site was most likely located close to the boundary between the glacial North Atlantic deepwater and Antarctic Bottom Water (Sarnthein et al., 1994, Lynch-Stieglitz et al., 2007) which makes the core a sensitive recorder of vertical changes in the distribution of both water masses.

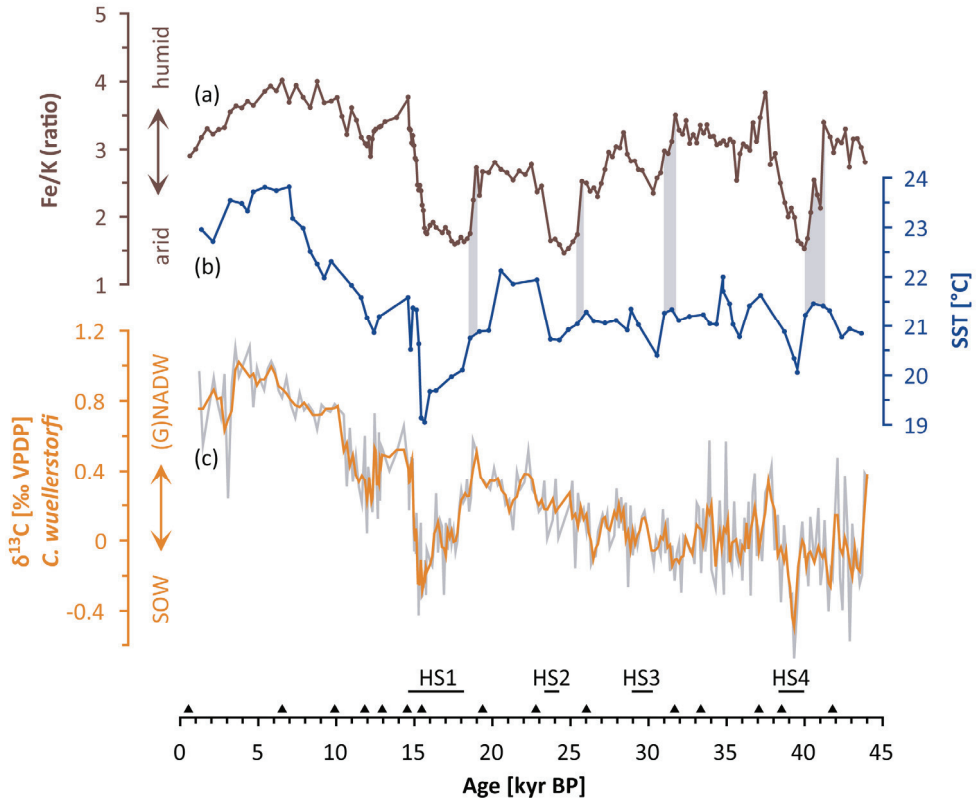

Fig. 6.1-2: Records of GeoB9508-5: (a) $\delta^{13}C$ of *C. wuellerstorfi* and (b) SST plotted together with (c) Fe/K ratios from Mulitza et al. (2008). Gray bars indicate intervals of abrupt transitions toward lower values seen in the Fe/K record. Ages of North Atlantic HS after Sarnthein et al. (2001). Triangles indicate AMS radiocarbon datings. (G)NADW: (glacial) North Atlantic Deepwater; SOW: deep Southern Ocean Water.

6.1.3 Methods

Alkenones were extracted as described by Müller and Fischer (2001) on 73 samples from the upper 692 cm of the core. $U^{K'}_{37}$ was calculated as described by Prahl and Wakeham (1987) and SST was estimated according to Prahl et al. (1988). The analytical precision was determined by co-extracting and analyzing a reference sediment every 11 samples, revealing a standard deviation (1σ) of 0.7°C.

Changes in the stable carbon isotopic composition ($\delta^{13}C$) of bottom water total dissolved inorganic carbon (ΣCO_2) were traced by measuring $\delta^{13}C$ of the benthic foraminifer *Cibicidoides wuellerstorfi*. Sample preparation and analytical procedures for isotopic and XRF data are described in Mulitza et al. (2008).

The age model of the core is based on 11 AMS radiocarbon dates on planktic foraminifera and a correlation of the benthic $\delta^{18}O$ record with core MD95-2042 (Shackleton et al., 2004, Mulitza et al., 2008). The resulting average sampling interval is ~600 years.

A freshwater-hosing experiment with the NCAR (National Center for Atmospheric Research) coupled climate model CCSM2/T31x3a (Prange, 2008) was performed as described in Mulitza et al. (2008) to obtain further insight into physical mechanisms that lead to tropical and extratropical NE Atlantic SST changes and Sahel aridity in response to a slowdown of the AMOC. In this experiment, a present-day control run was perturbed by a freshwater flux of 0.1 Sv into the northern North Atlantic. The continuously perturbed model was integrated for ~400 years.

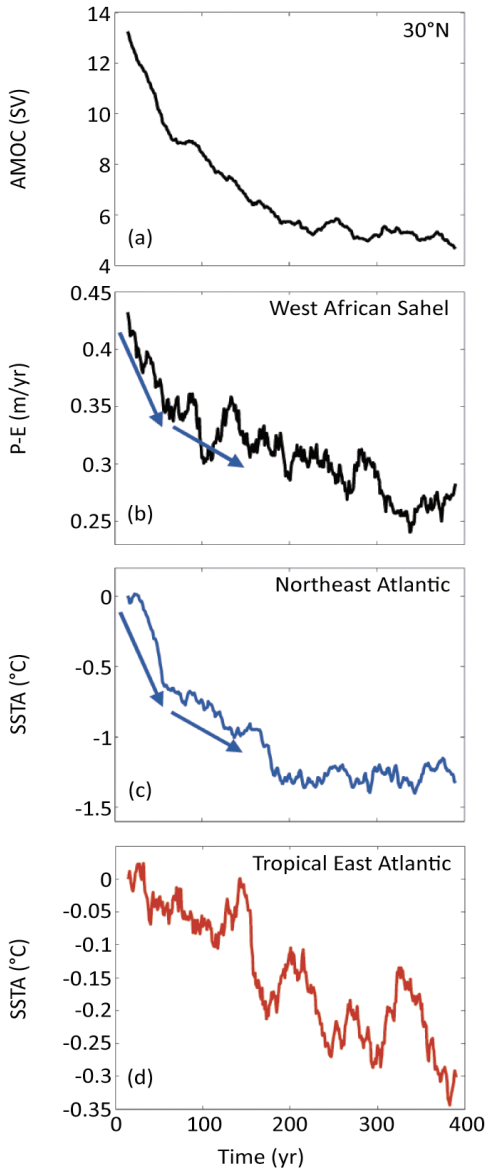

Fig. 6.1-3: Simulated climate response to a North Atlantic freshwater perturbation (all timeseries are smoothed by a 30-yr boxcar average and start from the equilibrium climate of the control run). (a) Temporal evolution of the AMOC at 30°N given as the streamfunction maximum below 800 m, (b) summer (July–September) precipitation minus evapotranspiration (i.e. runoff) averaged over the West African Sahel (15°W–10°E, 10–20°N), (c) mid-latitude NE Atlantic SST anomaly (SSTA, average over 30–50°N, east of 40°W) relative to the control run climatology, and (d) tropical NE Atlantic SSTA (average over 10–20°N, east of 25°W, i.e. around core location). Arrows are drawn as a visual guide and highlight synchronous rapid drops in Sahel runoff and mid-latitude NE Atlantic SST directly after the beginning of the freshwater injection.

6.1.4 Results

Alkenone-based SST estimates at the study site (Fig. 6.1-2b) generally decrease during North Atlantic Heinrich stadials (HS) 1-4. The most prominent coolings occur during HS1 (> 2°C) and HS4 (1.5°C). Despite the different minimum SST during HS, the decrease (except for HS2) generally takes place with a cooling rate between 0.1 and 0.2°C per 100 years.

The $\delta^{13}C$ of *C. wuellerstorfi* (Fig. 6.1-2c) shows more depleted values during HS1 and 4. These excursions toward lower values parallel the decreases in SST. Moreover, during HS1 both records show a gradual decline followed by an abrupt increase. From the beginning of the Holocene to 5.5 kyr BP, the $\delta^{13}C$ increase from 0.6 ‰ up to 0.9 ‰ is followed by a decrease to 0.7 ‰, closely matching the temporal evolution of the SST record.

The Fe/K ratios (Fig. 6.1-2a) show a similar pattern as the SST estimates. Minimum Fe/K ratios coincide with lower SST during HS1-4 (Fig. 6.1-2b). A closer inspection of the records, however, reveals that the transitions of the Fe/K ratios to lower values during the onset of HS (indicated by the gray bars in Fig. 6.1-2) are completed (HS1 and 4) or have already started (HS3), when SST still shows relatively high values. For HS2, however, it is not possible to properly define the onset of the SST decrease given the very small total variation. For the other HS, the decrease of SST lags the abrupt transitions seen in the Fe/K record by ~400 years during HS1 and 3, and even by 1,000 years during HS4. We note that these estimates are limited by the sampling frequency and that the real time lag might be smaller.

6.1.5 Discussion

Our data show coolings of tropical NE Atlantic SST during HS1-4 that coincide with decreased Fe/K ratios. As Mulitza et al. (2008) demonstrated, variations of Fe/K within sediment core GeoB9508-5 can be used to trace climatic conditions over the western Sahel. Lower Fe/K ratios correspond to decreased riverine input and enhanced dust supply, suggesting drier conditions during these intervals.

The variation in $\delta^{13}C$ recorded by *C. wuellerstorfi* can be used to monitor bottom water $\delta^{13}C_{\Sigma CO2}$ and water mass structure, based on the link between biological productivity at the surface and deepwater $\delta^{13}C_{\Sigma CO2}$ that leads to relatively low $\delta^{13}C_{\Sigma CO2}$ of the 'old' southern component water as compared to the better ventilated northern component water (Duplessy et al., 1988, Sarnthein et al., 1994). The $\delta^{13}C$ signature of deep Southern Ocean Water has been found extending to 60°N at water depths as shallow as 2000 m during the last glaciation (Sarnthein et al., 1994, Elliot et al., 2002, Lynch-Stieglitz et al., 2007). We interpret the decrease in $\delta^{13}C$ during HS4 and HS1 to represent a retreat of glacial North Atlantic deepwater in favour of an expansion of deep Southern Ocean Water to the core location, associated with a reduction in the AMOC (e.g. Sarnthein et al., 1994, McManus et al., 2004).

Climatic variations over the western Sahel are marked by abrupt transitions with the decrease of SST lagging the onset of drought during HS1, HS3 and HS4 by some centuries. The tight coupling of $\delta^{13}C$ and SST variation argues for a link between glacial North Atlantic deepwater formation and tropical NE Atlantic SST. These findings are consistent with our model results. A slowdown of the AMOC (Fig. 6.1-3a) reduces the northward transport of warm tropical surface waters within the western branches of the subtropical North Atlantic Gyre, leading to a temperature drop by ~0.7°C in the mid-latitude North Atlantic within ~60 years (Fig. 6.1-3c). After 200 years, mid-latitude SST is virtually equilibrated. By contrast, SST in the tropical NE Atlantic (Fig. 6.1-3d) decreases at a slower rate and lags the extratropical temperature evolution possibly even beyond the 400 years of the model run. The modelled temperature decrease in the tropical NE Atlantic is partly attributable to a cooling and strengthening of the Canary Current which delivers extratropical waters towards the tropical region. Such a cooling and strengthening of the Canary Current in response to AMOC weakening has already been described in previous model studies (Schiller et al., 1997, Prange et al., 2004). Further, an anomalous supply of relatively warm waters from the South (not shown) counteracts the cooling of the tropical NE Atlantic, leading to delayed SST decrease. The timeseries of Sahel runoff (precipitation minus evapotranspiration; Fig. 6.1-3b) follows the abrupt SST drop in the mid-latitude NE Atlantic (Fig. 6.1-3c) during the first ~150 years of the experiment (arrows in Fig. 6.1-3) when SST anomalies in the tropical NE Atlantic are still negligible (Fig. 6.1-3d). After 400 years, runoff in the western Sahel is almost 50 % lower than at the beginning of the experiment. About 75 % of this drying takes place within the first ~150 years and is associated with the rapid SST drop in the extratropical NE Atlantic.

The modelled cooling rate of the tropical NE Atlantic is about 0.1°C per 100 years and is consistent with the alkenone-derived cooling rates for HS1, HS3, and HS4. The strong cooling associated with HS1 (> 2°C), however, is exceptional among the HS and cannot be simulated by the model. As Bard et al. (2000) point out, HS1 is marked by two

subsequent events of ice rafting. Indeed, the existence of two distinct events during HS1 is indicated in the $\delta^{13}C$ record (Fig. 6.1-2c). The seemingly gradual decrease of SST during HS1 might represent two subsequent cooling events that are not resolved by the sampling frequency of the record. We further surmise that enhanced coastal upwelling (a process not properly resolved in the coarse-resolution ocean component of the climate model) influenced the core site during HS1, when due to a low sea-level (ca. 120-110 m lower than today; Lambeck and Chappell (2001)) the core location was closer to the shoreline and anomalous southward winds along the West African coast (simulated in our freshwater hosing experiment; not shown) resulted in stronger Ekman pumping. Lowering of surface solar radiation by Saharan dust (not included in the climate model) might have further contributed to the observed sea-surface cooling (Lau and Kim, 2007, Evan et al., 2009).

However, one might argue that for HS1 tropical SST does not lag but precede Sahel aridity if the decrease in SST between 20.5 and 19.7 kyr BP is taken into account. This would imply that the onset of Sahel aridity during HS1 would lag the decrease of SST (which is as large as 1°C) by 1.5 kyr which we do not consider physically reasonable and therefore unlikely to have occurred.

Taken together, our study indicates that the tropical North Atlantic SST is not the initial trigger for abrupt Sahel climate change during HS, corroborating the conclusion of Mulitza et al. (2008) that millennial-scale Sahel aridity was induced by an abrupt drop in extratropical NE Atlantic SST. This cooling created a positive sea-level pressure anomaly over northern North Africa and hence led to a southward shift of the monsoon trough. The Sahel drying was further amplified by an intensification of the African Easterly Jet.

In contrast to this study, Sutton and Hodson (2005) did not find a significant influence of extratropical North Atlantic SST on Sahel rainfall in their model. We suspect that this discrepancy is due to the different SST forcing amplitudes, i.e. northern North Atlantic SST anomalies during HS were much larger than the anomalies considered by Sutton and Hodson (2005). This suggests that extratropical North Atlantic SST anomalies have to exceed a certain threshold value in order to exert a significant influence on West African climate.

6.1.6 Conclusions

Our data show that millennial-scale sea-surface cooling off Senegal largely concurs with decreased bottom water $\delta^{13}C_{\Sigma CO2}$ that coincide with drying events in the western Sahel during HS1-4. We suggest that the SST decrease results from a reduced northward heat transport within the subtropical North Atlantic Gyre due to a reduced AMOC. Our data indicate that tropical NE Atlantic surface cooling lags the onset of Sahel aridity during HS. A freshwater hosing experiment supports the conclusion that the tropical NE Atlantic SST off Senegal is not the initial trigger of millennial-scale Sahel aridity. Glacial Sahel droughts were most likely induced by extratropical coolings in the North Atlantic.

Acknowledgements

This work was funded by the DFG through the Research Center/Excellence Cluster „The Ocean in the Earth System“ at MARUM, through GLOMAR (EMN), and project SCHE903/8 (ES). The climate model experiments were performed on the IBM pSeries 690 Supercomputer of the HLRN. We are grateful for comments of two anonymous reviewers that greatly improved this study. We thank James Collins for linguistic support.

6.2 Orbital- and millennial-scale changes in the hydrologic cycle and vegetation in the western African Sahel: Insights from plant wax δD and $\delta^{13}C$

Eva M. Niedermeyer[1], Enno Schefuß[1], Alex L. Sessions[2], Stefan Mulitza[1], Gesine Mollenhauer[1,3,4], Michael Schulz[1,4], Gerold Wefer[1,2]

[1] *MARUM–Center for Marine Environmental Sciences, University of Bremen, P.O. Box 330 440, D-28334 Bremen, Germany (eniedermeyer@marum.de)*

2 California Institute of Technology, Department of Geological and Planetary Sciences, 17 Mail Stop 100-23, Pasadena, CA 91125

[3] *Alfred Wegener Institute, Am Handelshafen 12, D-27570 Bremerhaven, Germany*

[4]*Department of Geosciences, University of Bremen, P.O. Box 330 440, D-28334 Bremen, Germany*

Submitted to *Quaternary Science Reviews*

To reconstruct variability of the West African monsoon and vegetation changes on precessional and millennial time scales, we analyzed a marine sediment core from the continental slope off Senegal spanning the past 44,000 years (44 ka). We used the stable hydrogen isotopic composition (δD) of individual terrestrial plant wax *n*-alkanes as a proxy for past rainfall variability. The abundance and stable carbon isotopic composition ($\delta^{13}C$) of the same compounds were analyzed to assess changes in vegetation composition (C_3/C_4 plants) and density. The δD record reveals two wet periods that coincide with local maximum summer insolation from 38-28 ka and 15-4 ka and that are separated by a less wet period during minimum summer insolation. Additional dry intervals are identified that coincide with North Atlantic Heinrich stadials and the Younger Dryas interval, indicating that the West African monsoon over tropical northwest Africa is linked to both insolation forcing and high-latitude climate variability. The $\delta^{13}C$ record indicates that vegetation of the western Sahel was consistently dominated by C_4 plants during the past 44 ka, possibly stabilized by low atmospheric pCO_2, whereas C_3-type vegetation increased during the Holocene. Moreover, we observe a gradual ending of the Holocene humid period together with unchanging vegetation composition, indicating that an abrupt aridification due to vegetation feedbacks is not a general characteristic of this time interval.

6.2.1 Introduction

Tropical monsoon variability and associated rain belt migration is a prominent feature of global atmospheric circulation and the resulting heat distribution over the globe. As part of the global monsoon system, the West African monsoon has been linked to the precessional cycle of the Earth's orbit and related variability in insolation through associated changes in the land-ocean pressure gradient and sea-surface temperature (e. g. Kutzbach, 1981, Rossignol-Strick, 1983, Pokras and Mix, 1987, Kutzbach and Liu, 1997). Internal non-linear responses such as vegetation-albedo feedbacks (e. g. Charney, 1975, Kutzbach et al., 1996, Ganopolski et al., 1998) may induce abrupt climate shifts despite a gradual insolation forcing (e. g. Claussen et al., 1999, deMenocal et al., 2000). The most recent wet phase of

northwest Africa, the so-called African humid period (14.8-5.5 ka), occurred during a period of maximal summer insolation and is regarded as an example of the insolation-driven intensity of the West African monsoon (Gasse, 2000). Studies of marine records from the continental slope off west Africa by Weldeab et al. (2007) (Niger) and Tjallingii et al. (2008) (Mauritania) show a general correlation between the West African monsoon and insolation intensity, but also a decreased monsoonal response to insolation forcing during the last glacial period. This latter feature is attributed to a lower amplitude of insolation variability and increasing global ice sheet coverage. Other studies of marine cores collected from off Senegal (Mulitza et al., 2008) and Mauritania (Jullien et al., 2007) also show sensitivity of northwest African climate to high-latitude climate variations during North Atlantic Heinrich stadials, indicating multiple controls on the West African monsoon. These stadials are less pronounced in the humidity index of Tjallingii et al. (2008) and are absent in estimates of the intensity of the West African monsoon inferred from fluvial runoff variation (Weldeab et al., 2007).

To provide a better understanding of long term variability of the West African monsoon, we used the stable hydrogen and carbon isotopic composition (δD and $\delta^{13}C$) and abundance of terrestrial plant wax *n*-alkanes in a marine sediment core from the continental slope off Senegal as proxies for past changes in continental hydrology, vegetation composition and density. The δD value of plant waxes has been applied successfully in earlier studies e. g. on marine sediments off the Congo basin (Schefuß et al., 2005) and on lacustrine sediments from Lake Tanganyika (Tierney et al., 2008), revealing valuable insights into the controls of the central and southeast African monsoon.

Our data show that the West African monsoon over tropical northwest Africa is linked to both insolation forcing and high-latitude climate variability during the Younger Dryas and North Atlantic Heinrich stadials of the past 44 ka.

6.2.2 Study area

Core location

Marine sediment core GeoB9508-5 was retrieved during RV Meteor cruise M65/1 (Mulitza et al., 2006). The core location (15° 29.90' N, 17° 56.88' W) is ~160 km southwest of the Senegal River mouth on the continental slope off Senegal at 2384 m water depth (Fig. 6.2-1). The terrigenous fraction of continental slope sediments at this location is derived from both Senegal River suspended load and from aeolian dust (Sarnthein et al., 1981, Mulitza et al., 2008).

Environmental setting

Western Sahel precipitation derives from the Gulf of Guinea and, to a lesser extent, from the tropical Atlantic off northwest Africa (Gong and Eltahir, 1996). It is transported to the Sahel by the West African monsoon and is further recycled by cloud convective systems and evapotranspiration over the continent (Nicholson, 2009). The amount of rainfall in the Sahel (Fig. 6.2-2) depends on the moisture content of the West African monsoon and the position of the tropical rain belt, moving between 10-20°N following seasonal changes in maximum solar insolation. As a result, total annual rainfall and duration of the rainy season decrease from the Guinea coast (>3000 mm yr^{-1}) to the Sahara desert (0-100 mm yr^{-1}) (compare Willmott and Matsuura database, http://climate.geog.udel.edu/~climate).

Maximum precipitation over the Sahel (100-500 mm yr^{-1}) occurs during the northern

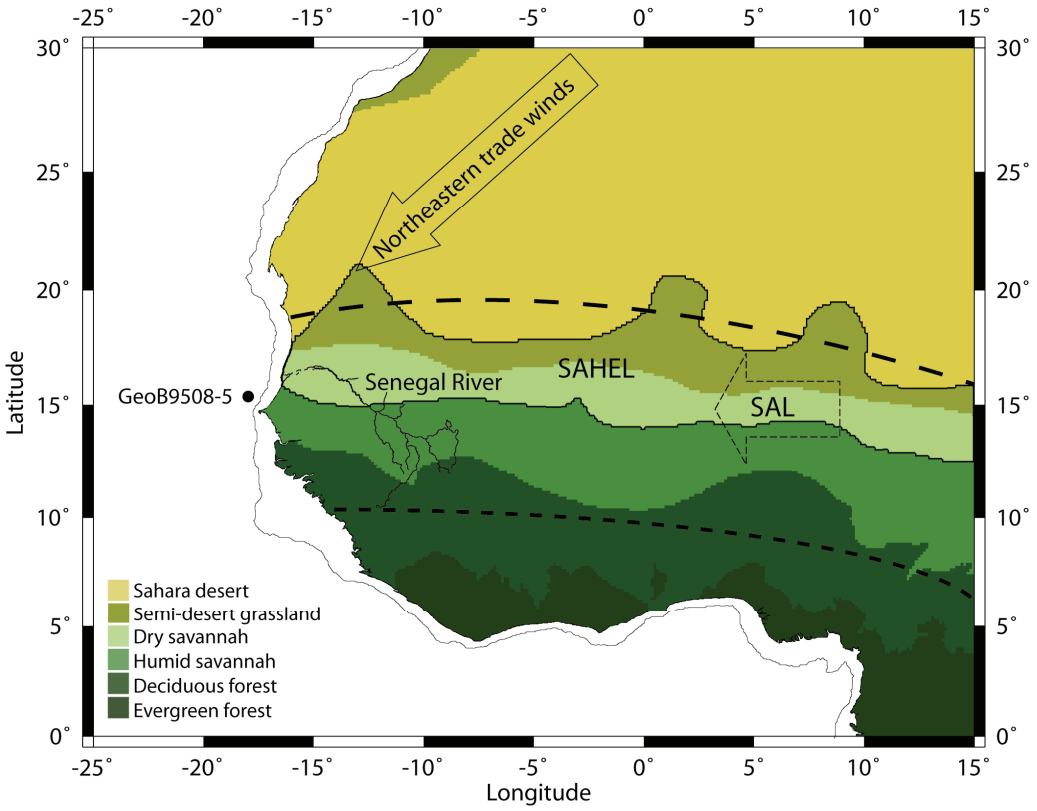

Fig. 6.2-1: Position of core GeoB9508-5 and vegetation zones of tropical Northwest Africa (after White, 1983). Upper (lower) dashed line indicates the approximate northernmost (southernmost) position of the tropical rain belt during northern hemisphere summer (winter). Arrows indicate dominant direction of northeastern trade winds and the Saharan Air Layer (SAL).

hemisphere summer from July to September when the rain belt reaches its northernmost position, followed by a long dry season for the rest of the year when the rain belt moves southward. The north-south rainfall gradient is reflected by decreasing rain water δD values (Fig. 6.2-2) from the Sahara desert to 10°N (due to the amount effect (Dansgaard, 1964)) where they form a "bullseye", and decrease again southward to the Guinea coast (reflecting the continental effect (Dansgaard, 1964)).

Following the seasonal migration of the rain belt and the associated rainfall gradient, vegetation (Fig. 6.2-1) gradually shifts from desert to dense tropical vegetation forming latitudinal bands oriented almost parallel to the equator (White, 1983). The Sahara desert is sparsely vegetated by few C_4 grasses and to a lesser extent by CAM plants. The adjacent Sahel comprises both semi-desert grassland (100-250 mm yr^{-1}) dominated by C_4 grasses and dry savannah (250-500 mm yr^{-1}) with sporadic C_3 trees. Due to its transitional nature, the Sahel is a sensitive ecosystem that is highly susceptible to even small climatic changes (Dupont, 1993). It is bordered by the humid savannah (500-1000 mm yr^{-1}) which receives sufficient rainfall to maintain a higher vegetation cover consisting of both tall C_4 grasses and trees (C_3). It shifts to tropical deciduous forests (1000-2000 mm yr^{-1}) toward the equator that become evergreen forests (2000-3000 mm yr^{-1}; both dominated by C_3 plants) at the Guinea coast.

During the dry season, the northwest African continent is dominated by low-level (≥ 900hPa) northeastern trade winds

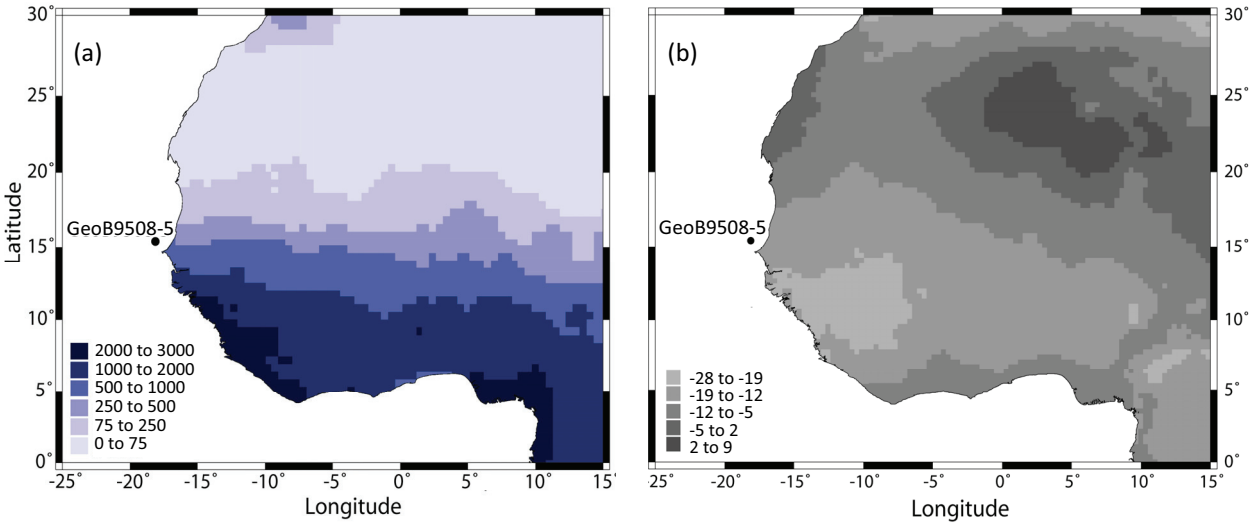

Fig. 6.2-2: (a) Mean annual rainfall [mm yr^{-1}] over tropical northwest Africa. Graphic is based on a compilation of rainfall data from the period 1950 to 1999 available on the Willmott, Matsuura and Collaborators Global Resources Pages (http://climate.geog.udel.edu/~climate/), Center for Climatic Research at University of Delaware. (b) Stable hydrogen isotopic composition (δD) of precipitation over tropical northwest Africa during the growing season [‰]. Graphic is based on data from www.waterisotopes.org (Bowen and Revenaugh, 2003, Bowen, 2009).

(Sarnthein et al., 1981) (Fig. 6.2-1) that blow almost parallel to the West African coast. An additional wind system, the high-level atmospheric African Easterly Jet, is most intense during northern-hemisphere summer and carries dust within the so-called Saharan Air Layer. Dust of the Saharan Air Layer originates from the southern Sahara and the Sahel, and is uplifted to higher atmospheric levels and deposited in the Atlantic between 10 and 25°N. These two regimes are the most important agents of aeolian plant wax transport (Huang et al., 2000) to the ocean off West Africa. However, due to the fine grain size and widespread distribution of dust in the Saharan Air Layer its contribution to sediments at the core location is relatively low compared to dust transported from more proximal regions by the northeastern trade winds (Stuut et al., 2005).

The study site also receives terrigenous material transported by the Senegal River (Sarnthein et al., 1981, Mulitza et al., 2008) located between ~11-16°N and 10-16°W with a total drainage area of approximately 350,000 km^2 (Fig. 6.2-1). Given the north-south precipitation gradient, the major portion of Senegal River discharge is generated in the tropical deciduous forests of the Guinea Mountains and southern Mali, whereas the contribution from higher tropical latitudes is small. Sedimentary discharge is closely related to water runoff (Gac and Kane, 1986) and thus is highest during the rainy season from June to October and drops to almost zero during the end of the dry season.

6.2.3 Methods

The age model of the core is based on a combination of radiocarbon dating and benthic stable oxygen isotope stratigraphy (Mulitza et al., 2008). A total of 94 samples was collected from the upper 692 cm of the core at 4-20 cm intervals, resulting in an

average temporal resolution of about 460 years.

Lipid extraction, identification and quantitation

Lipids were extracted from freeze-dried and finely ground sediment samples by ultrasonication in methanol (MeOH), 1:1 MeOH/dichloromethane (DCM), and DCM. An internal standard (squalane) was added to the total lipid extracts. Each total lipid extract was then washed with bi-distilled water (Seralpur) to remove salts, dried over anhydrous Na_2SO_4, and concentrated by evaporation under N_2. Next, total lipid extracts were saponified with 0.5 M KOH in MeOH at 80°C for 3h. Neutral lipids were extracted with hexane and separated by silica-gel column chromatography. Alkanes were eluted with hexane, then further purified by $AgNO_3$-silica gel column chromatography again using hexane as eluent.

n-Alkanes were identified by gas chromatography/flame ionization detector (GC/FID) by comparing their retention times to a standard mixture containing the corresponding *n*-alkanes at known concentrations. Alkane abundances were quantified using the FID peak areas calibrated against the standard mixture. Final *n*-alkane concentrations in the sediment were corrected for losses during sample preparation using the internal standard by assuming identical losses of standard and sample *n*-alkanes. Repeated analyses of a reference sediment yielded a mean precision of 0.2 µg g^{-1} for *n*-alkane abundance.

δD measurements

The δD values of individual *n*-alkanes were measured using a Thermo Trace GC^{ULTRA} coupled to a Finnigan $Delta^{+}XP$ isotope-ratio mass spectrometer via a pyrolysis furnace operated at 1430°C. Data processing and the daily H_3^+ correction were accomplished using Isodat v2.5 software as described by Sessions et al. (2001). An external standard containing 15 homologous *n*-alkanes (from C_{16} to C_{30}) with known δD values was analyzed repeatedly with the samples, and yielded a standard deviation (1σ) of 2.7 ‰ and root-mean-squared accuracy of 2.7 ‰. In addition, an internal standard (C_{36} *n*-alkane) was coinjected with all samples and yielded a standard deviation (1σ) of 1.8 ‰ with a mean deviation from the known δD value of 9 ‰. Due to a limited sample size, replicate analyses were not possible for every sample. Those that were analyzed in replicate yielded a mean standard deviation (1σ) of 2.3 ‰.We report δD values only for the C_{31}-*n*-alkane which was the most cleanly separated compound of adequate abundance. All δD values are reported in permil [‰] relative to the V-SMOW standard.

To account for ice volume effects on the δD value of meteoric water, the *n*-alkane δD record was corrected for glacial-interglacial changes in seawater isotopic composition as follows. The average global change in seawater $\delta^{18}O$ since the last glacial maximum is about 1.0 ‰ (e. g. Schrag et al., 2002, Waelbroeck et al., 2002). To account for additional seawater $\delta^{18}O$ variability prior to the last glacial maximum, we corrected the *n*-alkane δD record using the benthic $\delta^{18}O$ record obtained from tests of *Cibicidoides wuellerstorfi* from the same core (Mulitza et al., 2008). The benthic $\delta^{18}O$ record was scaled to the last glacial interglacial shift of 1 ‰, (set after Schrag et al. (2002) as the maximal amplitude of the $\delta^{18}O$ decrease between the last glacial maximum and the Holocene), and the equivalent δD variability was calculated using the global meteoric water line (Craig, 1961). This correction does not account for

changes caused by variability of deuterium excess which comprises a range of ~4 ‰ within the past 45 ka (Masson-Delmotte et al., 2005).

$\delta^{13}C$ measurement

The $\delta^{13}C$ values of individual *n*-alkanes were measured using a Thermo Trace GC^{ULTRA} coupled to a Finnigan MAT 252 IRMS via a Finnigan GC/C III combustion interface operated at 960°C. To monitor the system's performance, a standard mixture containing squalane and 16 homologous *n*-alkanes (C_{20} to C_{36}) with known $\delta^{13}C$ values was analyzed repeatedly. The $\delta^{13}C$ values of sample analytes were calibrated against CO_2 with known isotopic composition and the internal standard (squalane, see section 4.1). Samples were analyzed in duplicate or triplicate with a standard deviation (1σ) for the C_{31} *n*-alkane of 0.5 ‰. Values of $\delta^{13}C$ are reported relative to the V-PDB standard.

6.2.4 Results

The δD values of the *n*-C_{31} alkane (Fig. 6.2-3c, pink line) vary between -163 and -124 ‰. Values of δD corrected for ice volume (Fig. 6.2-3c, black line) are generally lower during the last glacial interval with a somewhat smaller amplitude of variability between -167 and -133 ‰. The overall structure of both records exhibits a periodic pattern that is correlated with variations in intensity of local summer insolation at 15°N (Fig. 6.2-3d, insolation values are shown for July 21 after Berger (1978)). Lowest δD values are observed during periods of highest insolation between 38-28 ka and 15-4 ka, whereas periods of reduced insolation coincide with higher δD values. In order to analyze the δD record for variations other than those linked to the insolation pattern we applied a high-pass filter (Rybicki and Press, 1995) with a cut-off frequency of 1/(10,000 yr). The filtered data (Fig. 6.2-4) indicate an excursion toward higher values between 9 and 7 ka and further enrichments that coincide with the intervals of the Younger Dryas interval and Heinrich stadials (HS) 1, 3 and 4.

All HS intervals reflected in the δD record coincide with decreased plant wax *n*-alkane concentrations (Fig. 6.2-3a) which exhibit considerable variation between 1.7 and 0.4 $\mu g\ g^{-1}$. HS2, which is only weakly expressed in the δD record, can be clearly identified in the record of *n*-alkane concentration.

The $\delta^{13}C$ values of *n*-C_{31} alkanes (Fig. 6.2-3b) vary between -26 and -21 ‰ and show no overall variation attributable to either insolation or HS. Generally, the $\delta^{13}C$ record varies between about -21 and -24 ‰ during the last glacial period and gradually decreases to -26 ‰ starting at around 18 ka. We used a two-component mixing calculation to estimate the contribution of *n*-C_{31} from C_4 plants by assuming $\delta^{13}C$ values of -21 ‰ and -36 ‰ for the C_4 and C_3 end members, respectively (Rieley et al., 1993, Collister et al., 1994). This calculation reveals a C_4 contribution of between 85 and 100 % during the last glacial, and a gradual decrease to 75 % toward the end of the record. During HS2 the $\delta^{13}C$ record indicates an increase of C_4 plant waxes up to 100 %. This is the HS with the least variability in the δD record.

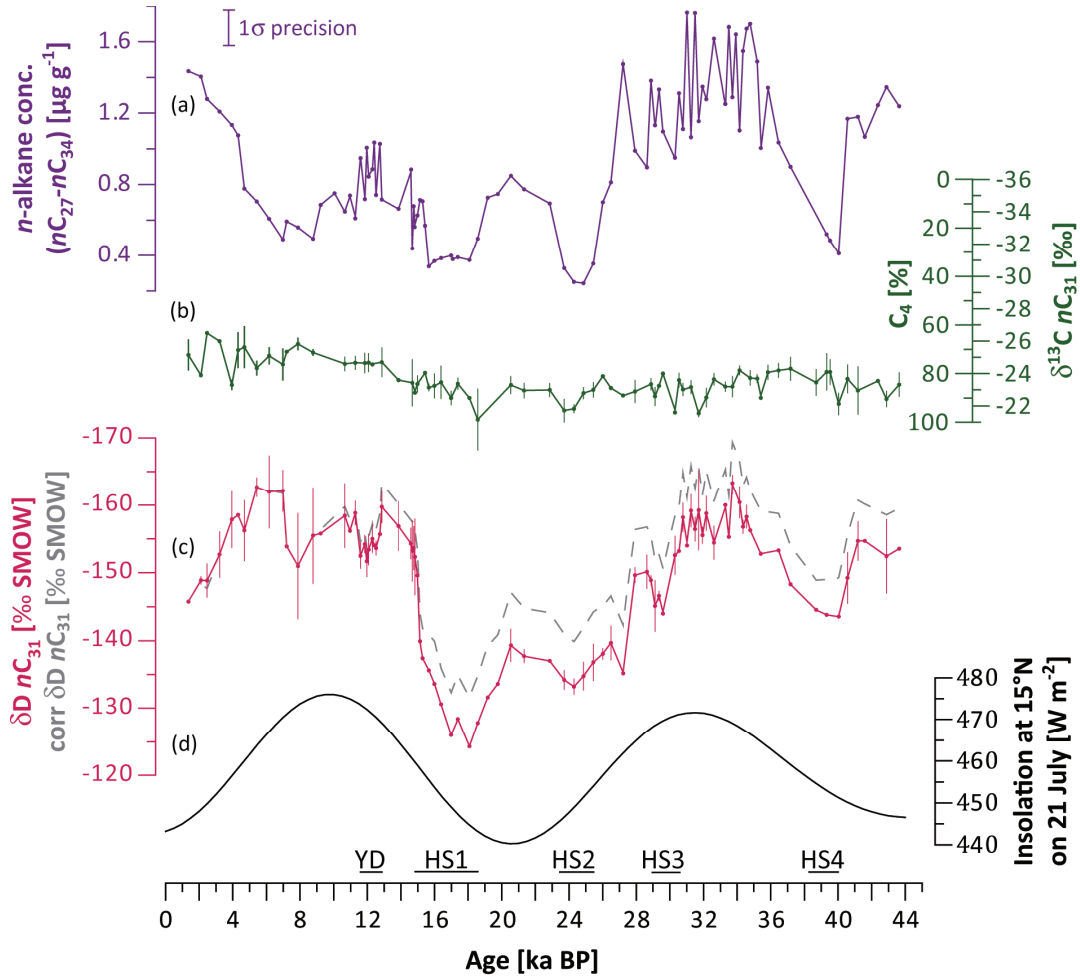

Fig. 6.2-3: Temporal evolution of (a) sedimentary *n*-alkane concentration; (b) stable carbon isotopic composition ($\delta^{13}C$) of the C_{31} *n*-alkane (right axis) and fractional contribution of C_4 vegetation (left axis); (c) pink line: stable hydrogen isotopic composition (δD) of the C_{31} *n*-alkane (nC_{31}); (c) black dashed line: δD of the C_{31} *n*-alkane corrected for ice volume effects; (d) insolation at 15°N on 21 July after Berger (1978). General note: Error bar in a) reflects the average precision as deduced from the internal standard. Error bars (1σ) for (b) and (c) are given for multiple-measurement samples. Datapoints without error bars derive from single measurements.

6.2.5 Discussion

Sources of long-chain sedimentary n-alkanes

Long-chain *n*-alkanes are integral parts of epicuticular waxes from vascular plant leaves (Eglinton and Hamilton, 1967). They have typical chain lengths ranging from C_{25} to C_{35} and exhibit a dominance of odd-carbon numbered *n*-alkanes over even-numbered homologues (Eglinton and Hamilton, 1967, Kolattukudy, 1976). The extent of this odd-over-even predominance can be quantified as the carbon preference index (CPI) with generally high values (>5) (e. g. Collister et al., 1994) for *n*-alkanes from higher plant waxes. Long-chain *n*-alkanes that derive from other sources such as petroleum or that are released from other carbon pools through diagenetic processes exhibit lower to negligible chain-length predominance and have a low CPI (<1) (Kolattukudy, 1976). We report a range of CPI between 5.3 to 7.8 with an average CPI of 6.6 and a standard deviation (1σ) of 0.6 for *n*-alkanes at the

study site indicating higher terrestrial plants as the major source throughout the entire record.

Provenance of sedimentary plant wax n-alkanes

The study site receives terrigenous sediment contributions from both aeolian dust and Senegal River suspended load (Sarnthein et al., 1981, Mulitza et al., 2008). Today, aeolian dust deposited at the study site is mainly carried by the northeastern trade winds (Stuut et al., 2005), whereas the Senegal River basin drains more humid areas southward. Thus, the possibility must be considered that the plant waxes originate from different geographic sources and that the contribution of these sources may vary depending on climate. To date there are no studies examining the contribution of fluvial vs. aeolian derived plant waxes to sediments off northwest Africa. Pronounced fluvial input of plant wax *n*-alkanes should be indicated in the $\delta^{13}C$ record by enhanced contribution of C_3 derived *n*-alkanes during wet periods because the Senegal River drains more humid areas with increasing C_3 vegetation toward the south. As will be described in more detail in the following section, this pattern is not observed suggesting that riverine transport of plant wax *n*-alkanes from its southern catchment to the study site is of minor importance. However, minor plant wax contributions from the northern catchment draining parts of the Sahel may still occur. In summary, we suppose that the transport of plant waxes to the study site is mainly by aeolian dust (Huang et al., 2000, Schefuß et al., 2003). Plant waxes transported by the low-level northeastern trade winds (Schefuß et al., 2003) most likely represent the vegetation type underlying the final section of the air-mass trajectory (Simoneit et al., 1989, Schefuß et al., 2003) rather than the vegetation along the entire path. Because the northeastern trade winds blow almost parallel to the northwest African coast, plant waxes deposited at the study site are likely abraded from the vegetation of northern Senegal, south-western Mauritania and western central Mali and therefore reflect an integrated signal of the climatic conditions in these areas. Depending on Senegal River discharge, plant wax contribution extends to the northern drainage basin (northern Senegal).

Controls on plant wax δD variability

Variability in the δD values of plant wax *n*-alkanes has been shown to relate to the δD value of the plant source water (Sessions et al., 1999, Chikaraishi and Naraoka, 2003, Huang et al., 2004, Sachse et al., 2004, Sachse et al., 2006, Hou et al., 2008). Today, the dominant effect controlling precipitation δD over the study area is the "amount effect" (Dansgaard, 1964, Worden et al., 2007, Risi et al., 2008a, Risi et al., 2008b) leading to lower values (stronger D depletion) in areas of high precipitation and higher values (D enrichment) when precipitation is low. Significant influence through large temperature changes is (at present) restricted to the extremely cold polar regions (Alley and Cuffey, 2001). We therefore suppose that a potential influence of temperature variability during the past 44 ka on the isotopic composition of precipitation at the study site is small compared to the amount effect. Provided that the local controls on the δD value of precipitation are stable over time, changes in the isotopic composition of plant wax *n*-alkanes reflect changes in the amount of precipitation.

Strictly speaking it is not the isotopic composition of precipitation that is recorded by plant waxes but rather that of leaf water (e. g. Pendall et al., 2005). This water source may be D-enriched relative to precipitation by soil evaporation and leaf transpiration (e. g. Dongmann et al., 1974, Epstein et al., 1977, Flanagan et al., 1991), suggesting an additional influence of relative humidity on leaf wax δD. Such a link has been suggested in studies of recent lake surface sediments along a north-south European transect (Sachse et al., 2004) and grasses from greenhouse and natural environments across the central USA (Smith and Freeman, 2006). A recent survey of lake-surface sediments across a transect of southwestern USA by Hou et al. (2008), however, found no correlation between in situ source-water/leaf wax fractionation and relative humidity, in contrast to their greenhouse experiment. The question of how much relative humidity influences D enrichment in leaf waxes thus remains unresolved. Regardless, both effects (leaf water transpiration and the amount effect on precipitation) should point in the same climatic direction, causing D enrichment of leaf waxes during more arid conditions (Worden et al., 2007).

There is also debate about whether vegetation type has an influence on leaf wax δD through differences in leaf anatomy, photosynthetic pathway or rooting depth (Chikaraishi and Naraoka, 2003, Liu et al., 2006, Smith and Freeman, 2006, Hou et al., 2007, Liu and Yang, 2008). Values of $\delta^{13}C$ for the C_{31}-*n*-alkane in our record (Fig. 6.2-3b) do not vary considerably during the last glacial and show no correlation with the δD record, suggesting that plant type variability likely exerts little influence on the δD signal at the study site.

Influence on plant wax δD other than West African monsoon intensity is exerted by ice volume effects on the δD value of meteoric water. The corrected data (Fig. 6.2-3c, black dashed line) account for an approximation of

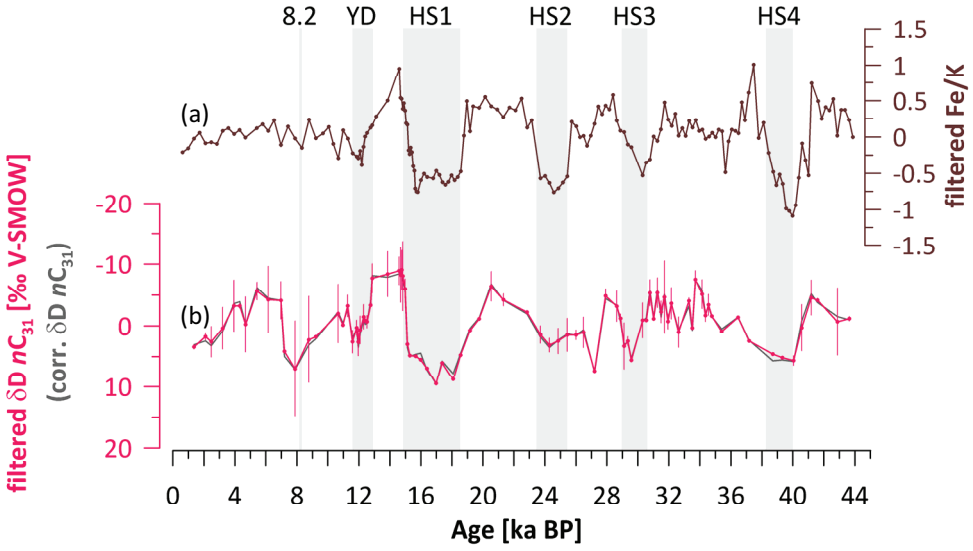

Fig. 6.2-4: Temporal variability of (a) the Fe/K record from the same core (Mulitza et al, 2008) and (b) the δD record both after high-pass filtering (Rybicki and Press, 1995) with a cut-off frequency of 1/(10,000 yr) to show variability other than linked to insolation. Gray bars indicate periods of Heinrich stadials (HS, after Sarnthein et al (2001)), the Younger Dryas interval (YD) and the 8.2 ka event. Error bars (1σ) are given for multiple-measurements only.

these effects and show lower δD values during the last glacial but no changes in the overall temporal structure.

Taken together, we interpret lower plant wax δD values in our record as reflecting periods of enhanced precipitation and/or higher humidity ('wetter'), though we cannot specifically disentangle those two effects. Similarly, higher δD values likely reflect intervals of drier conditions. In addition, since plant wax *n*-alkane production occurs during the growing season, we infer that δD variability likely corresponds to climatic variability during the growing (wet) season and, hence, to West African monsoon intensity. However, we cannot distinguish West African monsoon variability relating to a shortening of the rainy season vs. a decrease in precipitation intensity.

Orbital-scale climate variability

The large-scale variability of both δD records (raw and ice-volume corrected, Fig. 6.2-3c) matches the temporal structure of variations in local summer insolation at 15°N (Fig. 6.2-3d), exhibiting two wetter periods between 38-28 and 15-4 ka that coincide with highest summer insolation. This suggests a link between insolation variability and the West African monsoon. Indeed, such a link has been described by earlier studies (Wang et al., 2001, Yuan et al., 2004, Weldeab et al., 2007, Tjallingii et al., 2008) as a global feature of monsoon systems. However, Tjallingii et al. (2008) recently presented grain-size data from a marine core off of Mauritania indicating a decreased influence of insolation on the West African monsoon during the last glacial period. They attribute their findings to the generally weaker amplitude of insolation variability during marine isotope stage 3 of the last glacial period in combination with an expansion of the northern hemisphere ice caps. This leads to an intensification of the dry northeastern trade winds that limits the northward extension of the West African monsoon. Our data, however, indicate that the current study site – which is located ~3° further south – was under the climatic influence of an insolation forced West African monsoon during the last glacial period. This may suggest that the border between the two wind systems was located between 17° and 20°N during this period.

The δD record indicates insolation forcing of the West African monsoon between 38 and 28 ka which corresponds to earlier evidence for a wet interval between about 40 and 30 ka from lake level variability of paleolake Chad (Durand, 1982). Although plant wax δD is a sensitive proxy for the isotopic composition of precipitation it is not yet possible to quantify the changes with respect to rainfall amounts. Still, δD values indicate similar precipitation during the last glacial wet period and the wet period during the Holocene. However, the $\delta^{13}C$ record (Fig. 6.2-3b) does not show an increase of C_3 plants during the last glacial wet period (the proportion of about 90 % C_4 plants remains almost constant), indicating that precipitation was not high enough to sustain significant C_3 vegetation. Today, in order to support a woodland-grass savannah (humid savannah) with considerable contribution of C_3 shrubs and trees, rainfall in northwest Africa must exceed 400 mm $year^{-1}$ (Walter, 1970). From this, one might infer that during the last glacial wet period rainfall over the source area was below 400 mm $year^{-1}$ and did not support significant C_3 vegetation. Continuously high sedimentary *n*-alkane concentrations (Fig. 6.2-3a) although wind intensity and aeolian dust supply were lower during this period (Jullien et al., 2007), point to increased terrestrial biomass possibly related to an increase in C_4 grass abundance.

We note that changes in sediment *n*-alkane concentration can be caused by both variability of plant wax availability (vegetation density) and dust flux intensity (dilution effect) (compare Adkins et al., 2006), respectively. However, a modern analog of this scenario would be the northern area of the humid savannah (Fig. 6.2-1) which comprises tall C_4 grasses and sporadic C_3 plants (trees). Accordingly, the last glacial wet period likely was associated with a northward shift of the humid savannah vegetation belt. Low atmospheric pCO_2 during the last glacial period (Indermühle et al., 2000) may have further stabilized the dominance of C_4 grasses (Collatz et al., 1998, Bond et al., 2003).

The second wet period identified within the δD record reaches its maximum from 15-4 ka. This agrees with earlier studies that describe an insolation-forced African humid period during the Holocene (e. g. deMenocal et al., 2000, Gasse, 2000, Salzmann et al., 2002). In contrast to studies by e. g. deMenocal et al. (2000) we do not observe an abrupt end of the African humid period but a gradual decrease of precipitation starting around 5 ka. Surprisingly, the vegetation type shows no significant response to the decrease in precipitation but perhaps a slight increase of C_3-type plants. This might be explained by the increased glacial-to-interglacial difference in atmospheric pCO_2 levels (Monnin et al., 2001), allowing for higher water use efficiencies (Policy et al., 1993, Street-Perrott et al., 1997). Furthermore, *n*-alkane abundances (Fig. 6.2-3a) during the Holocene indicate an increase in vegetation density though we note that this may be partly due to increasing wind intensity (Jullien et al., 2007) amplifying leaf wax abrasion. deMenocal et al. (2000) attribute the abruptness to nonlinear vegetation and albedo feedbacks (Charney, 1975, Kutzbach, 1981, Kutzbach et al., 1996). For this to occur, vegetation cover needs to fall below a certain threshold to produce an abrupt non-linear response to the gradual orbital forcing (Claussen et al., 1999). The gradual decrease observed within this study agrees with observations of Mulitza et al. (2008) from the same core as well as with studies from the Lake Tilla crater (northeastern Nigeria) (Salzmann et al., 2002) and Lake Yoa (northern Chad) (Kröpelin et al., 2008). Thus an abrupt termination is not a general characteristic of the Holocene African humid period, possibly because vegetation density at some locations did not fall below the threshold value required for an abrupt climate transition. We suggest that the ecosystem documented by this study was stabilized by higher pCO_2, compensating for the effect of decreasing precipitation (Policy et al., 1993, Street-Perrott et al., 1997, Ghannoum et al., 2000).

Millennial-scale climate variability

The high-pass filtered δD record (Fig. 6.2-4b) reveals climate forcing of arid intervals other than linked to insolation. Millennial-scale dry periods coincide with North Atlantic Heinrich stadials (HS) which is in agreement with other studies from near Senegal (Mulitza et al., 2008, Itambi et al., 2009) and Mauritania (Jullien et al., 2007). Whereas most of the proxies applied in these studies likely reflect enhanced dust input during the dry season, we ascribe plant wax *n*-alkane δD to climatic conditions during the wet growing season. Our data therefore indicate that climate variability during HS also affected the rainy season toward drier conditions. In order to depict the distinct responses of the growing season and the dry season, we show Fe/K ratios from the same core (Fig. 6.2-4a) (Mulitza et al., 2008) using the same high-pass filtering as for the δD record. Lower

Fe/K ratios correspond to decreased riverine input and enhanced dust supply, suggesting drier conditions during these intervals (Mulitza et al., 2008).

HS2 seems to be anomalous in its weak response (if at all) in the δD record. Sedimentary *n*-alkanes (Fig. 6.2-3a), in contrast, show a pronounced decrease in abundance. This may derive from both lowered plant wax production and increased dust input (as reconstructed by Jullien et al. (2007)) and points toward intensification of the dry season. Fe/K ratios in sediments from the same core (Fig. 6.2-4a) (Mulitza et al., 2008) also indicate intensification of the dry season during HS2. The δD record, however, exhibits only slight variation during this period, whereas the $\delta^{13}C$ values (Fig. 6.2-3b) suggest an increase in C_4 plant abundance. We speculate that this possibly reflects a shortening of the rainy season without a concomitant change in precipitation rate. This would lead to an extended dry season favoring grasses (C_4 plants) but with little change in precipitation δD values during the growing season.

The filtered data indicate additional aridification between 13 and 11.5 ka. Such a drying event has been widely observed in tropical Northwest Africa e. g. in lacustrine sediments from Lake Tilla (northeastern Nigeria) (Salzmann et al., 2002), Lake Bosumtwi (Ghana) (Talbot and Johannessen, 1992, Peck et al., 2004, Shanahan et al., 2006) and Lake Barombi Mbo (western Cameroon) (Maley and Brenac, 1998), and is attributable to the Younger Dryas interval.

The δD record indicates a further excursion toward dry conditions between 9 and 7 ka. The data for this period have large error bars, complicating the interpretation. However, aridification of tropical African climate within this interval is reported in a range of studies (e. g. Gasse and Van Campo, 1994, Gasse, 2000, Shanahan et al., 2008) which supports the persistance of drier conditions in the western Sahel around 8 ka as indicated by the δD record. This interval possibly coincides with the "8.2 ka" event, a period of colder conditions in the high-latitude North Atlantic realm and beyond (Alley et al., 1997, Alley and Ágústsdóttir, 2005, Ellison et al., 2006).

The dry episodes during Heinrich stadials, the Younger Dryas interval and the 8.2 ka event coincide with reduced Atlantic overturning circulation (McManus et al., 2004, Ellison et al., 2006) and are probably induced by cool North Atlantic sea-surface temperatures (Mulitza et al., 2008, Niedermeyer et al., submitted to Geophysical Research Letters). In the model of Mulitza et al (2008), an abrupt drop in extratropical northeast Atlantic sea-surface temperature creates a positive sea level pressure anomaly over northern North Africa. This leads to a southward shift of the monsoon trough, with the Sahel drying further being amplified by an intensification of the African Easterly Jet. The intervals of lowered precipitation identified within the δD record indicate that this mechanism is important for tropical West African climate throughout the seasons.

6.2.6 Conclusions

The pattern of δD variability in terrestrial leaf wax *n*-alkanes suggests permanent local insolation forcing of the West African monsoon during the past 44 ka. We identify two wet periods from 38 to 28 ka and from 15 to 4 ka that coincide with maximal local summer insolation. Millennial scale intervals of reduced precipitation/humidity are identified that coincide with North Atlantic Heinrich stadials 1, (2), 3 and 4, the Younger Dryas interval and the "8.2 ka" event. We therefore conclude that the West African monsoon is susceptible to both local

insolation and North Atlantic climate. Furthermore, we propose that, in addition to the dry season, also the growing season is affected by Atlantic overturning circulation and associated extratropical sea-surface temperatures. This suggests a crucial role of the North Atlantic in controlling tropical northwest African climate.

We observe a gradual end of the Holocene African humid period which implies that decreasing precipitation did not initiate non-linear vegetation feedbacks as suggested for an abrupt climate transition during this period. Vegetation variability at the study site generally shows low correlation to changes in hydrology indicating that additional controls such as atmospheric pCO_2 may have been relevant during the time window of this record.

Acknowledgements

This work was funded by the German Science Foundation (DFG) through the Research Center / Excellence Cluster „The Ocean in the Earth System“ at MARUM – Center for Marine Environmental Sciences, University of Bremen and by the U.S. National Science Foundation grant EAR-0645502 to ALS. ES is funded through DFG grant Sche 903/8. EMN acknowledges additional support by GLOMAR – Bremen International Graduate School for Marine Sciences. The German academic exchange service (DAAD) is acknowledged for funding a research stay at Caltech. We thank Jan-Berend Stuut (MARUM) for providing information on the provenance of aeolian dust at the study site. Martin Erbs (Bundesforschungsinsitut Braunschweig) is acknowledged for helpful discussions on the ecology of plants. We thank Robert J. Holmes for editorial assistance.

6.3 18th century onset of aridification toward modern drought in the western Sahel Region

Eva M. Niedermeyer[1], Enno Schefuß[1], Stefan Mulitza[1], Alex L. Sessions[2], Gesine Mollenhauer[1,3,4], Gerold Wefer[1,2]

[1] *MARUM–Center for Marine Environmental Sciences, University of Bremen, P.O. Box 330 440, D-28334 Bremen, Germany (eniedermeyer@marum.de)*

[2] *California Institute of Technology, Department of Geological and Planetary Sciences, 17 Mail Stop 100-23, Pasadena, CA 91125*

[3] *Alfred Wegener Institute, Am Handelshafen 12, D-27570 Bremerhaven, Germany*

[4]*Department of Geosciences, University of Bremen, P.O. Box 330 440, D-28334 Bremen, Germany*

In preparation for *Science*

Western Sahel hydrology has been linked to the pattern of global ocean surface temperatures through land-sea atmospheric interactions and feedbacks of vegetation on moisture and albedo (Folland et al., 1986, Xue and Shukla, 1993, Bader and Latif, 2003, Giannini et al., 2003). It is still not well understood to what extend human induced vegetation change contributed to the 20th century Sahel drought and whether the recent drought marks the onset of a progressive aridification process. We reconstructed the history of western Sahel hydrology and adjacent ocean-surface temperature of the past 2900 years from marine sediments deposited off the coast of Senegal. We used Deuterium/Hydrogen ratios and the stable carbon isotopic composition of plant wax *n*-alkanes to assess changes in precipitation and vegetation, and estimated sea-surface temperatures by alkenone paleothermometry. We present evidence that aridification in the western Sahel started 250 years ago. Variability of local sea-surface temperature shows low correlation to changes in precipitation, suggesting little impact on Sahel climate. Instead, we propose that early agricultural activity has contributed to the present-day semi-arid Sahel climate. Our data show that the modern drought in the western Sahel is part of a multi-centennial aridification trend.

The western Sahel region has experienced severe drought from the early 1960s to the late 1980s with dramatic socio-economic consequences. Two main hypotheses have been proposed for the cause of drought. One focuses on recent human impact on vegetation cover through agricultural clearing and overgrazing affecting monsoon circulation through moisture and albedo feedbacks (Otterman, 1974, Charney, 1975, Xue and Shukla, 1993, Kutzbach et al., 1996, Claussen et al., 1999). The other emphasizes the role of sea-surface temperature (SST) patterns across the Atlantic and associated atmospheric feedbacks (Folland et al., 1986, Rowell et al., 1995, Fontaine et al., 1998, Hoerling et al., 2006). Modeling studies combining ocean- and land-feedbacks suggest ocean temperatures to be the dominating factor with vegetation changes acting as amplifier (Rowell et al., 1995, Zheng and Eltahir, 1998, Giannini et al., 2003). Furthermore, controversial debate since exists since whether this drought marks the onset of an expansion of the Sahara. Modern dry conditions are suggested to have established 2000 years ago (Lézine and Casanova, 1989), and Satellite images

indicate no southward expansion of the Sahara desert during the past years (Anyamba and Tucker, 2005) . A recent study on sediments from Lake Bosumtwi (Ghana) (Shanahan et al., 2009) indicates that tropical West African climate today is even wetter than during the past 1000 years. In contrast, historical sources suggest progressive drying in the western Sahel starting in the late 16th to early 17th century (Webb, 1994). If this to be true, a climatic shift occurred within the past centuries that separated climate controls over the western Sahel and the southward Lake Bosumtwi area.

Here, we reconstruct the history of western Sahel hydrology, vegetation composition (C_3/C_4 plants) and tropical northeast Atlantic SST of the past 2900 years. We worked on sediments from the marine site GeoB9504 (15°41.00'N 16°43.88'W) using a gravity- and a multi core retrieved at 36 m water depth from the mudbelt of the Senegal River (Mulitza et al., 2006) (Fig. 6.3-1). The age model of the two cores is based on 7 (2) radiocarbon dates of bivalve shells of the gravity core (multi core) spanning from 2900 to 650 years before present (yrs BP) (480 until present) (Supplementary Methods).

We used $U^{K'}_{37}$ based alkenone paleo-thermometry to reconstruct adjacent ocean SST. The stable carbon isotopic composition ($\delta^{13}C$) and Deuterium/Hydrogen ratios (δD) of compound specific plant wax *n*-alkanes were used to estimate changes in vegetation type and precipitation. Sedimentary abundance of *n*-alkanes was used as a proxy for fluvial discharge (Supplementary Methods).

The Senegal River is located in tropical northwest Africa between about 16°-11°N and 10-16°W (Fig. 6.3-1). It drains the vegetation of the humid savannah and the dry savannah of the western Sahel on its way north to the Atlantic and is expected to deposit an integrated climate signal from its course at the study site. Sedimentary discharge is closely related to water runoff (Gac and Kane, 1986) and thus is highest during the rainy season and drops to almost zero during the dry season.

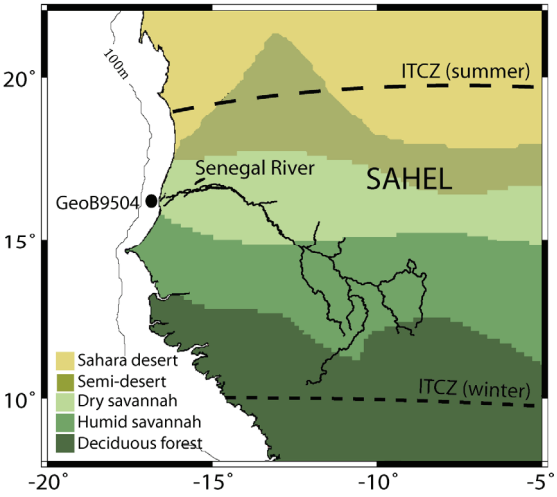

Fig. 6.3-1: Map indicating study site GeoB9504 and regional setting. Vegetation changes from Sahara desert to deciduous forest as indicated by colour coding (White, 1983). The Senegal River is indicated draining the humid and dry savannah. Dashed lines indicate northernmost (southernmost) ITZC position during northern hemisphere summer (winter).

Rainfall in the western Sahel is brought by the West African monsoon with a significant portion of Sahel precipitation deriving from continental rainwater recycling through evapotranspiration and cloud convective systems (Nicholson, 2009). The seasonal migration of the tropical rain belt leads to increasing annual precipitation from the Sahara desert toward the equator. Sahel vegetation (Fig. 6.3-1) changes accordingly from C_4 grasses adapted to dry conditions and sporadic shrubs and trees (C_3) to the C_3/C_4 mixed humid savannah with increasing contribution of C_3 plants with increasing precipitation (White, 1983).

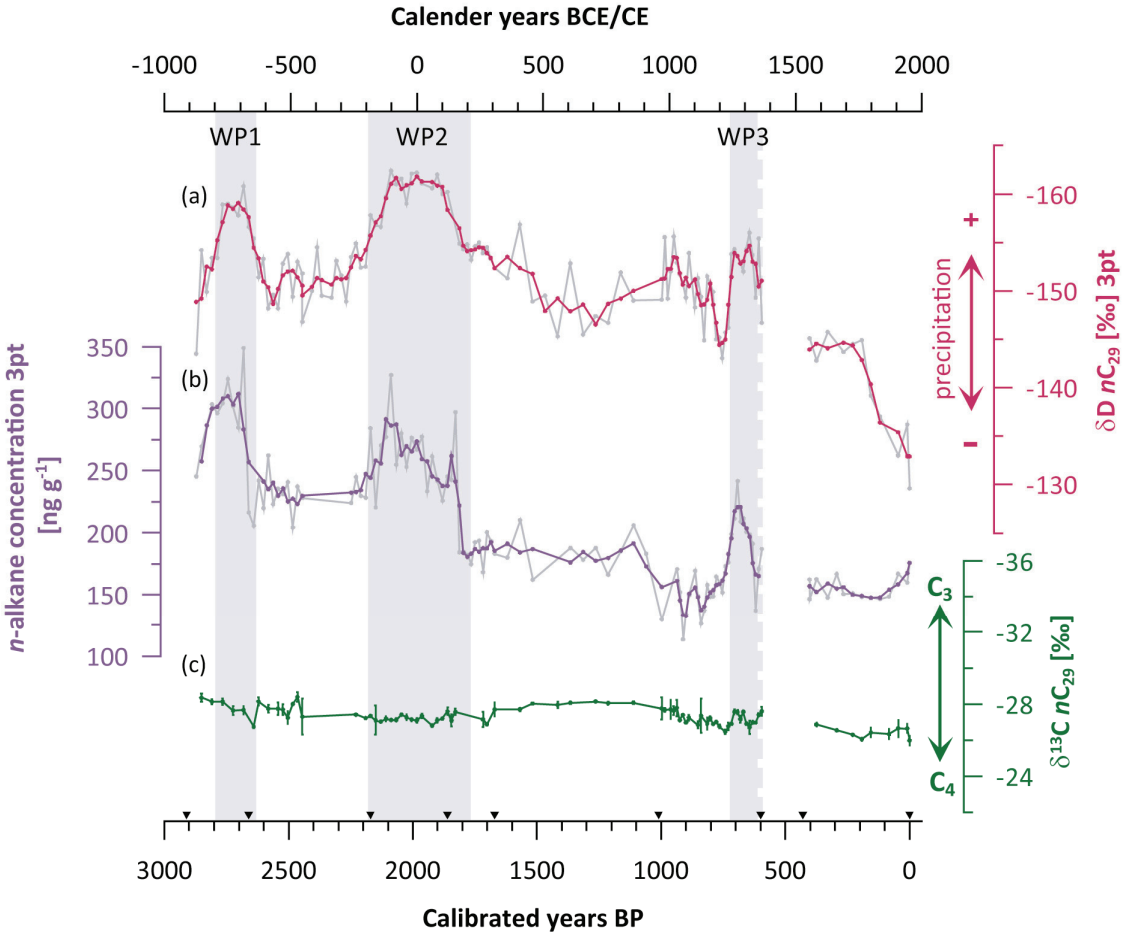

Fig. 6.3-2: Temporal evolution of (a) stable hydrogen isotopic composition (δD) of the nC_{29}-alkane; (b) sedimentary *n*-alkane concentration; c) stable carbon isotopic composition of the nC_{29}-alkane. Gray bars indicate onset and ending of wet periods as inferred from the δD record.

Long-chain *n*-alkanes are integral parts of the epicuticular wax layer of terrestrial higher plants (Eglinton and Hamilton, 1967) and their δD value has been found to relate to the isotopic composition of precipitation (Sachse et al., 2004, Sm... and Freeman, 2006). Over the study area, the δD value of precipitation is dominated by the amount effect (Dansgaard, 1964, Worden et al., 2007) with high tropical rainfall leading to Deuterium depletion of precipitation and vice versa (amount effect, Dansgaard, 1964, Worden et al., 2007). Strictly speaking it is the isotopic composition of leafwater that is recorded by plant waxes, hence, modification of rainwater may occur through humidity driven evapotranspiration. Regardless, both effects should point in the same climatic direction, causing Deuterium enrichment during more arid conditions. We therefore interpret lower plant wax δD values in our record as reflecting periods of enhanced precipitation ("wetter conditions"). Similarly, higher δD values likely reflect intervals of drier conditions.

The δD record of the nC_{29}-alkane (Fig. 6.3-2a) varies between -160 and 130 ‰ (relative to the V-SMOW standard) with a general trend toward higher values, which is drier conditions, to the end of the combined records. This trend is not straightforward but interrupted by three excursions peaking in lower values interpreted to reflect wetter

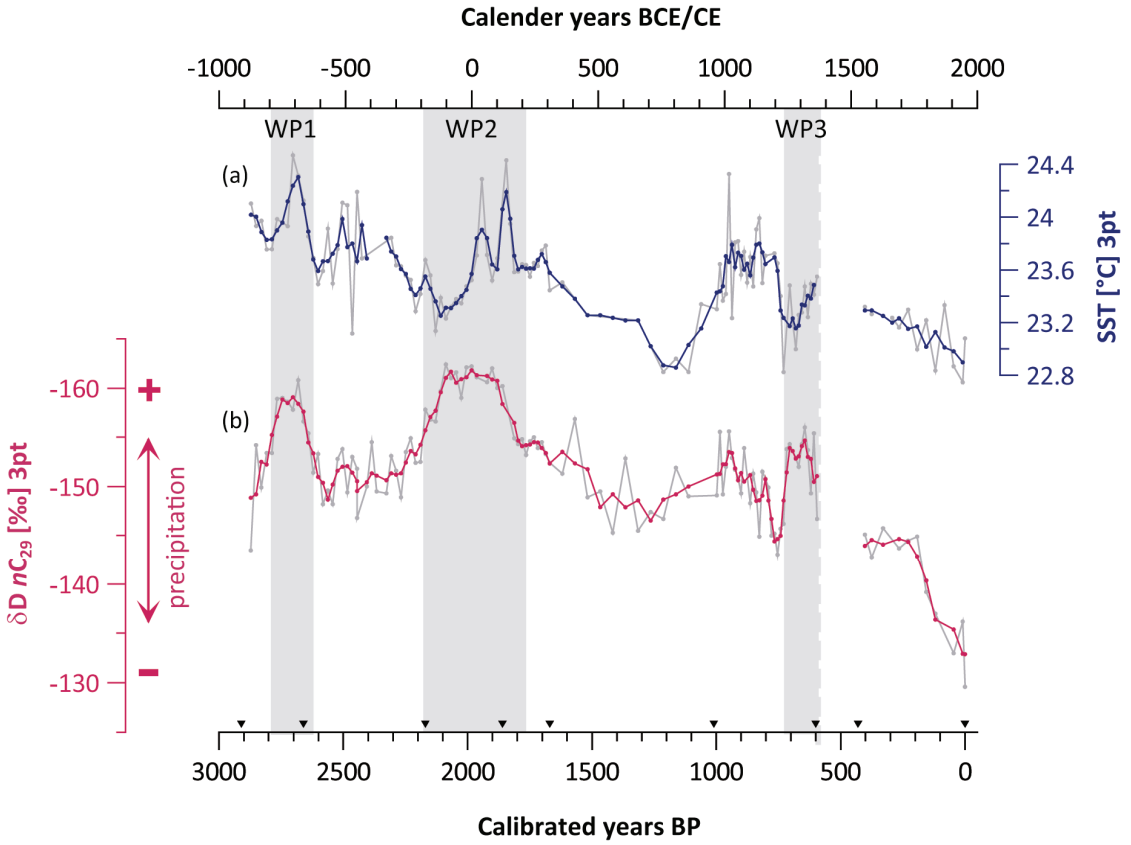

Fig. 6.3-3: Temporal evolution of a) alkenone-derived sea-surface temperature (SST) and b) stable hydrogen isotopic composition (δD) of the nC$_{29}$-alkane. Gray bars indicate onset and ending of wet periods as inferred from the δD record.

conditions. We define onset and termination of the wet periods as the point when the δD value reaches half of the maximal decrease/increase inferred from a 3 point running mean. This yields three wet periods from 2900 to 2550, 2200 to 1800 and from 700 to at least 600 years BP, hereafter referred to as wet periods (WP) 1, 2 and 3. The end of the WP 3 cannot be properly defined because the two records do not overlap leaving a gap between 650 and 450 yr BP.

The $\delta^{13}C$ of plant waxes relates to the photosynthetic pathway (C_3 or C_4) (O'Leary, 1981). $\delta^{13}C$ values of plant wax n-alkanes typically range from about -21 to -36 ‰ with higher values deriving from C_4 photosynthesis and lower values from the C_3 pathway (Rieley et al., 1993). The $\delta^{13}C$ values recorded by the nC$_{29}$-alkane (Fig. 6.3-2c) vary between -28 and -26 ‰ (relative to the V-PDB), indicating that the Senegal River drains C_3/C_4 mixed vegetation dominated by C_4 plants as expected for a Savannah ecosystem (White, 1983). The small range of $\delta^{13}C$ variation suggests only minor changes in the relative proportions of C_3 and C_4. However, a slight (about 1 ‰) but systematic increase in C_3 plants is indicated during the dry interval between WP 2 and 3. This is contrasting on a first view only because the relative contribution of C_3 plants from the southern catchment of the river should increase if drier conditions cause a retreat of C_4 vegetation in the western Sahel.

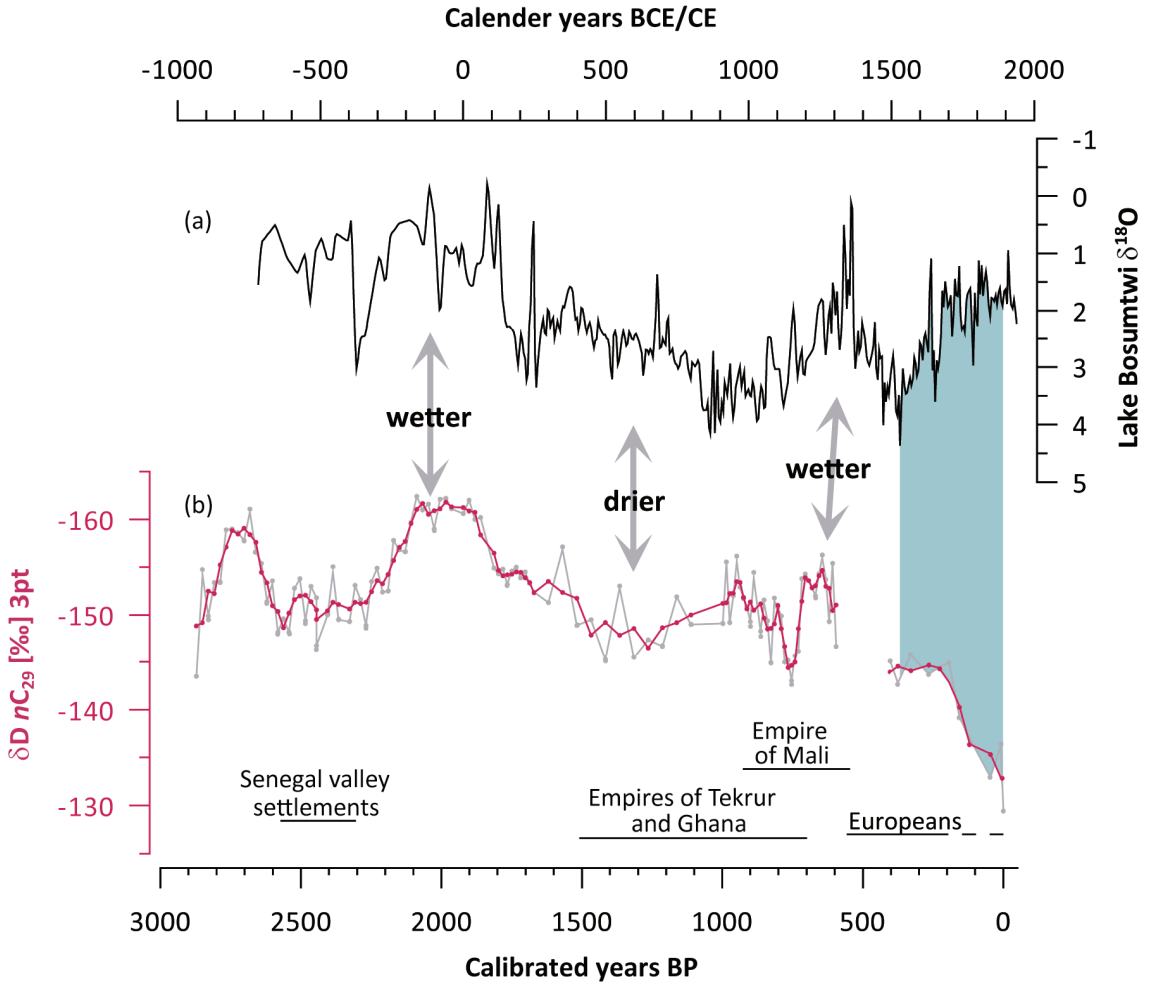

Fig. 6.3-4: (a) Authigenic lake carbonate $\delta^{18}O$ from Lake Bosumtwi (Ghana) (Shanahan et al., 2009) plotted together with (b) δD of the nC_{29}-alkane from study site GeoB9504. Gray arrows indicate synchronistic variability of precipitation at both study sites. Blue bar depicts divergence of West African monsoon and Sahelian precipitation. Black lines indicate intervals of enhanced human activity in the western Sahel.

The wet periods indicated by the δD record go along with increased sedimentary *n*-alkane concentrations (Fig. 6.3-2b) which we interpret to reflect enhanced riverine runoff and fluvial discharge as expected for wet intervals (Gac and Kane, 1986). *n*-Alkane abundance is independent of the local sedimentation rate, and therefore supposed to be largely unaffected by spatial dynamics of sediment deposition. Increasing precipitation may have stimulated vegetation density, further contributing to higher sedimentary *n*-alkane concentrations. The wetter conditions in the western Sahel suggested during WP 1 and 2 agree with a study on pollen and dinoflagellate cyst assemblages in a neighbouring coastal core about 250 m north (Bouimetarhan et al., 2009) which supports our interpretation of the δD record. Further independent evidence for a drying in Senegal between WP 2 and 3 has been reported based on ostracod and foraminifera assemblages in lacustrine sediments derived north of Dakar (Senegal) (Sarr et al., 2008, Sarr et al., 2009). Taken together, these findings corroborate our interpretation of plant wax δD as a proxy for past rainfall variability.

The changes of precipitation deduced from the hydrogen isotope record largely match the changes in hydrology of tropical West Africa inferred from the oxygen isotope record from Lake Bosumtwi (Ghana) (Shanahan et al., 2009) (Fig. 6.3-4) during the period from 2000 to 650 yr BP. The common pattern of the two records decouples latest 400 yr BP (this can not be further clarified since the δD record gaps between 650 and 400 yr BP). Decreasing $\delta^{18}O$ values indicate the onset of wetter conditions in the Lake Bosumtwi area 450 years ago (Fig. 6.3-4a). In the western Sahel, however, the δD record shows constant rainfall intensity from 450 to 300 yr BP (Fig. 6.3-4b), followed a persistent decrease of precipitation starting 250 years ago. Furthermore, increasing sedimentary *n*-alkane abundance about 150 years ago likely reflects increasing eolian dust flux and associated enhanced plant wax abrasion, responding to dry conditions. Independent historical evidence for drying comes from European merchants reporting progressive aridification in the western Sahel 250 years ago (Webb, 1994). The diverging trends in hydrology indicated by the two records strongly suggest decoupling of West African and Sahelian precipitation.

It has been suggested that tropical Atlantic SST exerts considerable control on western Sahel climate (Folland et al., 1986). We reconstructed adjacent ocean SST revealing a small range of temperature fluctuations between about 24 and 23°C (Fig. 6.3-3a). In order to work out a possible link between adjacent ocean temperature and continental hydrology we compare the onset of SST changes to the onset of wet periods defined within the δD record (Fig. 6.3-3b). If Sahel hydrology was driven by changes in adjacent ocean temperature we would expect sea-surface cooling to precede precipitation changes, or at least to appear simultaneously in the paleo-record in case the feedback exceeds the temporal resolution of our sediments. We notice a general cooling trend but no such a lead-lag relation can be identified. Warm SST excursions lag Sahel precipitation on a centennial- to multi-decadal scale. We therefore suggest that adjacent ocean SST was of minor importance for western Sahel precipitation during the past 2900 years.

Archaeological evidence exists for increasing human activities in the western Sahel during the time covered by our record. Human settlements have been found in the middle Senegal valley from about 2000 to 1100 yrs BP (McIntosh 1999), when drying of the Senegal Delta (Sarr et al., 2008, Sarr et al., 2009) allowed agriculture in formerly flooded plains, followed by the Empires of Tekrur (located in the Senegal Valley) and Ghana (southeastern Mauritania and southwestern Mali). The large Empire of Mali flourished between about 900 and 550 yr BP comprising the present-day countries of southern Mauritania, Senegal, Gambia, Guinea-Bissau, Guinea, southern Mali, and parts of Niger. The decoupling of hydrologic patterns recorded for the western Sahel and around Lake Bosumtwi about 400 years ago coincides with historical evidence of systematic agricultural overproduction in the western Sahel to produce grain, a major trading good during this time (Webb, 1994). Agricultural clearing of Savannah vegetation dramatically destabilized the ecosystem leading to barren soils (Schlesinger et al., 1990, Mbow et al., 2008). We suggest that anthropogenic degradation of the western Sahel ecosystem lead to a less developed low pressure system over the western Sahel through decreased evapotranspiration and albedo feedbacks, reducing the northward

expansion of the tropical rain belt (Charney, 1975, Ganopolski et al., 1998, Renssen et al., 2006).

However, we note that it is difficult to separate "natural" from anthropogenically induced desertification, since the biologic and climatic feedbacks acting as self-accelerators do not necessarily need a human hand to be set on. Though, it is conspicuous that the decoupling of West African and Sahelian rainfall was preceded by enhanced human activity. Whatever the ultimate cause of aridification, our data indicate that it started about 250 years ago and that the western Sahel today is experiencing the driest conditions within the past 2900 years. Therefore, the recent Sahel drought is part of a multi-centennial aridification trend. Our data suggest that tropical climate is even more sensitive to human impact than previously assumed.

Further remarks on the manuscript

Since this manuscript is still in preparation it is subject to further revision.

By now, the age model of the multi core is based on linear interpolation between two ^{14}C ages. An additional ^{14}C age at the climatic change toward modern Sahel climate will provide more detailed information about the onset of this transition (Dr. Mahyar Mohtadi). Moreover, grain-size analyses of the multi core sediments should reveal potential changes in the source region of plant waxes (riverine transport vs. eolian dust) during aridification.

The study site is close to the Senegal River mouth. Therefore, the SST record potentially reflects a local signal rather than representing temperatures of the tropical northeast Atlantic. Since the multi core records overlap with the instrumental record, the SST record is to be compared to the instrumental data in order to estimate its relation to more offshore SST.

Moreover, detailed information about agricultural changes will be provided

Supporting Material

Radiocarbon dating

Nine AMS radiocarbon dates (seven for the gravity core and two for the multi core) on bivalve shells were analyzed at the Leibniz-Laboratory for Radiometric Dating and Stable Isotope Research, Kiel, Germany. The conventional radiocarbon ages were calibrated using the radiocarbon calibration program Calib5.0.2 (Stuiver and Reimer, 1993) with the marine04 calibration dataset (Hughen et al., 2004). We corrected for a marine reservoir age of 550 years, composed of the global marine reservoir age (400 years) plus a regional difference (ΔR) of ~150 years (compare Ndeye, 2008). The ages of the sediment between the dated depths were calculated by linear interpolation between the referring calibrated ages (1σ, Table 1).

The calibrated ages suggest an age of 2910 years at the base and 600 years at the top of the gravity core. The multi core has an age of 430 years before present (yr BP) at the base and a post-atomic age at the core top. Together, they extend from the past 2900 years to the end of the 20th century with a gap of 230 years between 600 and 430 yr BP.

Table S1: Conventional ^{14}C ages together with calibrated ages (yr BP) and calendar ages (BCE/CE), respectively, which were used to construct the age model by linear interpolation.

Core depth (cm)	Lab code	Conventional ^{14}C age	Calibrated age range (cal. yr BP)	Calibrated age (cal. yr BP)	Calendar age range (CE/BCE)	Calendar age (CE/BCE)
Multi core						
0-1	KIA 3733	>AD 1954	-	-	1950	1950 CE
47-48	KIA 3734	945 ±30	357-499	430	1451-1593	1520 CE
Gravity core						
5	KIA 0522	1175 ±40	535-659	600	1291-1415	1350 CE
173	KIA 3727	1605 ±45	916-1105	1010	845-1034	940 CE
238	KIA33728	2240 ±45	1563-1777	1670	173-387	280 CE
298	KIA 3729	2400 ±45	1751-1967	1860	18 BCE -199 CE	90 CE
373	KIA 3730	2640 ±30	2066-2276	2170	327-117 BCE	220 BCE
498	KIA 3731	3060 ±30	2558-2770	2660	821-609 BCE	720 BCE
557	KIA 0521	3275 ±45	2796-3018	2910	1069-847 BCE	960 BCE

Conventional ages were calibrated using the radiocarbon calibration program Calib5.0.2 (Stuiver and Reimer, 1993) with the marine04 calibration dataset (Hughen et al., 2004). All ages were corrected for a marine reservoir age of 550 years (after Ndeye, 2008).

Lipid extraction, identification and abundance

The two cores were sampled every 5 cm with a total sample size of 110. Lipids were extracted from freeze-dried and fine ground sediment samples with Methanol (MeOH), MeOH/Dichloromethanol (DCM) (1:1), and DCM using ultrasonic. We added Squalane (2, 6, 10, 15, 19, 23-hexamethyltetracosane) as internal standard to the total lipid extracts to trace eventual losing of lipids during the procedure and to monitor precision of stable isotope analyses. Total lipid extracts were washed with bi-distilled water (Seralpur) to remove salts and were further dried with anhydrous Na_2SO_4; excess solvent was evaporated. Total lipid extracts were saponified with 0.5 M KOH/MeOH at 80°C for 3 h. Lipids were separated in two fractions by column chromatography with 1 % water-deactivated silica gel. *n*-Alkanes were eluted with hexane and further purified by $AgNO_3$-$SiSO_2$ column chromatography using hexane as solvent. The alkenone containing ketone fraction was eluted with DCM/hexane (2:1).

n-Alkanes were identified by gas chromatography/flame ionization detector (GC/FID) by comparing their retention times to a standard mixture containing the corresponding *n*-alkanes at known concentrations. Alkane abundances were quantified using the FID peak areas calibrated against the standard mixture. Final *n*-alkane concentrations in the sediment were corrected for losses during sample preparation using the internal standard by supposing identical losses of standard and sample *n*-alkanes.

Deuterium/Hydrogen ratios – δD

The δD values of individual *n*-alkanes were measured using a Thermo Trace GC^{ULTRA} coupled to a Finnigan $Delta^{+}XP$ isotope-ratio mass spectrometer via a pyrolysis furnace operated at 1430°C. Data processing and the daily H_3^+ correction were done as described by Sessions et al. (2001). A standard mixture containing 15 homologous *n*-alkanes (from C_{16} to C_{30}) with known δD values was analyzed repeatedly with the samples and yielded a standard deviation (1σ) of 2.7 ‰ and a standard error of 2.7 ‰. Due to low *n*-alkane concentrations, replicate analyses were not possible. However, the internal standard (squalane) showed a standard deviation (1σ) of 1.7 ‰. Moreover, an external standard (C_{36} *n*-alkane) was coinjected with the samples yielding a standard deviation (1σ) of 1.8 ‰ and a standard error of 9 ‰. δD values are reported for the *n*C_{29}-alkane which was the most abundant compound. All δD values are noted in permil [‰] relative to the V-SMOW standard.

Stable carbon isotopic composition – $\delta^{13}C$

The $\delta^{13}C$ values of individual *n*-alkanes were measured using a Thermo Trace GC^{ULTRA} coupled to a Finnigan MAT 252 IRMS via a Finnigan GC/C III combustion interface operated at 960°C. A standard mixture containing 16 homologous *n*-alkanes (C_{20} to C_{36}) was analyzed repeatedly to monitor system performance. The $\delta^{13}C$ values of the sample-analytes were calibrated against a CO_2 standard gas with known isotopic composition and the internal standard (squalane). Samples were analyzed in duplicate or triplicate revealing a mean standard deviation (1σ) of 0.5 ‰ for the nC_{29}-alkane. Values are reported relative to the V-PDB standard.

Sea-surface temperature

Alkenones were extracted and purified as described above. Alkenone identification and peak area calculation was performed using gas chromatography/flame ionization detector (GC/FID) in combination with the HPChem Station software by comparing their retention to the alkenone fraction of a standard sediment. Sea-surface temperatures were calculated by peak areas after Prahl et al. (1988) using the alkenone unsaturation index $U^{K'}_{37}$ defined by Prahl & Wakeham (1987). The precision of the method was checked by co-extracting and analyzing a reference standard repeatedly with the samples yielding a standard deviation (1σ) of 0.7°C.

7 SYNTHESIS

This study investigated the last 44 kyr of Late Quaternary changes in West African monsoon intensity and vegetation, and their potential link to Atlantic meridional overturning circulation and sea-surface temperatures (SST) of the adjacent ocean. Analyses were done using marine cores retrieved from the continental slope off the coast of Senegal. Changes in West African monsoon intensity and vegetation (that is C_3 vs. C_4 plants) were estimated using Deuterium/Hydrogen ratios (δD) and the stable carbon isotopic composition ($\delta^{13}C$) of individual plant wax *n*-alkanes. Deepwater ventilation at the study site was assessed through $\delta^{13}C$ of tests from benthic foraminifera and sea-surface temperatures (SSTs) were estimated using alkenone-paleothermometry based on the $U^{K'}_{37}$ index.

7.1 West African monsoon and tropical northeast Atlantic SST

Variability of δD in individual plant wax *n*-alkanes indicates that rainfall over the western Sahel responds to a variety of controls (MANUSCRIPT II). On orbital timescales, West African monsoon intensity matches variation of precession forced local summer season insolation. Additional forcing is recorded during Heinrich stadials implemented by drier conditions than expected from insolation forcing alone. This suggests, together with studies of Jullien et al. (2007) and Mulitza et al. (2008), that climate variability during Heinrich stadials affected both seasons since the proxy applied in the present study is linked to precipitation changes. As discussed in MANUSCRIPT I, tropical northeast SST is likely not the trigger of western Sahel drought during Heinrich stadials. This was inferred from the temporal relation of changes in SST and Fe/K ratios in sediments from the same core (Mulitza et al., 2008), a proxy that probably relates to the dry season. At this point it would be interesting to compare the SST record also to the δD record to assess potentially different responses of the seasons. Unfortunately, the temporal resolution of both the SST and the δD Late Quaternary records is too low to investigate a lead-lag relation with confidence. However, a distinct lag of SST variation to changes of plant wax δD of about 100-200 years is identified in the Holocene records (MANUSCRIPT III), indicating extratropical forcing of western Sahel climate to be a robust feature throughout the seasons on millennial to multi decadal timescales.

This contrasts with studies on modern Sahel climate which suggest tropical Atlantic SST to be a driving force of modern Sahel rainfall variability (Hastenrath, 1984). A reason for this discrepancy may be the different timescales addressed. Studies of modern Sahel climate address annual rainfall variability, whereas the climate reconstruction in the present study

approximates long-term changes with the single datapoints reflecting a decadal to centennial scale "averaged" climate.

As Nicholson (2009) pointed out, rainfall resulting directly from surface convection affects only the southern Sahara and the northernmost Sahel. Rainfall generation within this system appears to be independent of that which produces most of the rainfall within the tropical rain belt (compare Fig. 1.1-2). It is speculated that AMOC and associated extratropical SST variation exert dominant control on ITCZ and rain belt position, whereas tropical Atlantic SST may trigger rainfall generation within the surface convergence. Therefore, modern western Sahel rainfall variability may be triggered by adjacent ocean temperature, but the general "long-term" climate is coupled to high-latitude climate.

7.2 Vegetation feedbacks

The $\delta^{13}C$ record of individual plant wax *n*-alkanes indicates major contribution of C_4 plants throughout the past 44,000 years (MANUSCRIPTS II and III). This complicates identification of potential vegetation precipitation feedbacks, since aridification would not go along with a shift in vegetation. Instead, this should be indicated by changes in vegetation density. Although sedimentary plant wax abundances were analyzed within this study they cannot be unambiguously linked to changes in vegetation density because this would require continuous quantitative plant wax transport. This is not expected because wind intensity and fluvial discharge depend on climate. It is therefore not possible to work out a potential lead-lag relation between *n*-alkane abundance and hydrology, indicative for vegetation-precipitation feedbacks. However, the results discussed within Manuscript II indicate that Late Quaternary natural climate variability was not controlled by abrupt changes in vegetation. This does not imply that these feedbacks are generally negligible, as indicated in MANUSCRIPT III. This study suggests that anthropogenic agricultural clearing triggered western Sahel aridification 250 years ago. This suggests that the relative importance of feedback-mechanisms within the climatic system is highly dynamic.

7.3 Plant wax δD

Studies investigating the link between the source-water and leaf wax δD found a range of different responses on the individual plant level (e. g. Chikaraishi and Naraoka, 2003, Liu et al., 2006, Smith and Freeman, 2006, Hou et al., 2007). As Sachse et al. (2004) demonstrated in a study on lacustrine core top sediments, these differences seem to be "smoothed" in an integrated record. For marine sediments, however, no such study exists so far. Part of this PhD project was to examine the link between the δD value of plant waxes from core top

sediments along a transect off the West African coast and precipitation over the adjacent continent. Unfortunately, analytical difficulties did not allow an interpretation of the results of this project with confidence. However, comparing the core-top value of the Holocene δD record (which is about -135 ‰, MANUSCRIPT III) to that of another marine plant wax δD record (about -140 ‰, Schefuß et al., 2005) from the Congo basin reveals good agreement. Since the isotopic composition of precipitation over the Sahel and the Congo basin is within the same range (compare http://www.waterisotopes.org), this suggests that an integrated plant wax signal deposited in a marine environment is a good proxy for precipitation δD. The similar δD values of precipitation over the semi-arid Sahel and the wet Congo basin, in turn, emphasize the need to carefully interpret plant wax δD with respect to the underlying rainfall intensity and to thoroughly assess the local controls of the isotopic composition of precipitation. Provided that the spatial controls do not vary considerably over time, the δD value of individual plant wax *n*-alkanes is an applicable tool to assess past variations in hydrology.

Comparing the core-top δD value of the Holocene record (MANUSCRIPT III) to the time series of the Late Quaternary δD record (MANUSCRIPT II) suggests that modern precipitation in the western Sahel compares to West African monsoon intensity between the last glacial maximum and Heinrich stadial 1. This appears reasonable since with ongoing aridification the next "climatic step" of the semi-arid western Sahel would be Sahara desert conditions. This indicates that the plant wax δD provides reasonable estimates of past rainfall variability, supporting confidence in the application of plant wax δD as a proxy for precipitation changes for Late Quaternary environments.

8 OUTLOOK

The present study indicates that Atlantic Ocean circulation had considerable impact on Late Quaternary western Sahel climate. At this point it would be of interest to asses the impact of this mechanism under modern boundary conditions. The study of the past 2900 years indicates a similar SST-precipitation relation as during the past 44 kyr suggesting a corresponding link between Late Holocene Sahelian climate and the AMOC. This approach, however, is limited by the availability of high-resolution deep sea sediments that are suited to estimate (small) changes in ocean ventilation. Such sediments were not available at the study site and information about Late Holocene changes of the AMOC is sparse. Therefore, the potential link between ocean circulation and precipitation changes during the past 2900 years could not be investigated in this study. This study further demonstrates the difficulty to assess the potential link between vegetation dynamics and precipitation. Modelling studies suggest significant feedbacks between vegetation and precipitation (Kutzbach, 1981, Kutzbach et al., 1996, Ganopolski et al., 1998, Claussen et al., 1999). Evidence from the paleo record, however, remains elusive due to the lack of a direct proxy for vegetation density.

The present study applied plant wax δD as a proxy for past rainfall variability. Calibration of this proxy is subject to ongoing research and will require deeper knowledge about the impact of different ecological strategies of plants like changes of source water through different rooting depths (Larcher, 2001) and the impact of evapotranspiration on leaf water enrichment (e. g. Flanagan et al., 1991, Sachse et al., 2004, Smith and Freeman, 2006). The application of plant wax δD as a quantitative proxy may further require information about continental temperature to estimate additional modification of rainwater δD through evapo(transpi)ration. Continental temperature may potentially be assessed using a recently developed method that is based on differences in the methylation and cyclisation ratio of specific branched tetraethers (Weijers et al., 2007a). These compounds are produced by soil bacteria and found in coastal marine sediments (Weijers et al., 2007b).

As indicated in MANUSCRIPT II, rainfall over the western Sahel decreased during Heinrich stadials. This, however, may derive from both a southward shift of the tropical rain belt or a weakened monsoon in general. Reconstructing West African monsoon intensity along a north-south transect off subtropical and tropical West Africa could reveal detailed insight to the spatial dynamics of the northern- and southernmost position of the tropical rain belt and the precipitation gradient in between. This may provide valuable insights to global climate dynamics since ITZC position and monsoon intensity are important features of atmospheric circulation and the hydrologic cycle.

9 REFERENCES

Adegbie, A. T., R. R. Schneider, U. Röhl and G. Wefer (2003), Glacial millenial-scale fluctuations in central African precipitation recorded in terrigenous sediment supply and freshwater signals offshore Cameroon, *Palaeogeogr. Palaeoclimatol. Palaeoecol. 197*, 323-333.

Adkins, J., P. B. DeMenocal and G. Eshel (2006), The "African humid period" and the record of marine upwelling from excess ^{230}Th in Ocean Drilling Program Hole 658C, *Paleoceanography 21*, PA4203.

Alley, R. B. and K. M. Cuffey (2001), Oxygen- and hydrogen-isotopic ratios of water in precipitation: Beyond paleothermometry, *Reviews in Mineralogy & Geochemistry 43*, 527-553.

Alley, R. B. and A. M. Ágústsdóttir (2005), The 8k event: cause and consequences of a major Holocene abrupt climate change, *Quat. Sci. Rev. 24*, 1123-1149.

Alley, R. B., P. A. Mayewski, T. Sowers, M. Stuiver, K. C. Taylor and P. U. Clark (1997), Holocene climatic instability: A prominent, widespread event 8200 yr ago, *Geology 25*, 483-486.

Altabet, M. A., M. J. Higginson and D. W. Murray (2002), The effect of millennial-scale changes in Arabian Sea denitrification on atmospheric CO_2, *Nature 415*, 159-162.

Anyamba, A. and C. J. Tucker (2005), Analysis of Sahelian vegetation dynamics using NOAA-AVHRR NDVI data from 1981-2003, *J. Arid Environ. 63*, 596-614.

Bader, J. and M. Latif (2003), The impact of decadal-scale Indian Ocean sea surface temperature anomalies on Sahelian rainfall and the North Atlantic, *Geophys. Res. Lett. 30*, 2169.

Baker, P. A., C. A. Rigsby, G. O. Seltzer, S. C. Fritz, T. K. Lowenstein, N. P. Bacher and C. Veliz (2001), Tropical climate changes at millennial and orbital timescales on the Bolivian Altiplano, *Nature 409*, 698-701.

Bard, E., F. Rostek, J.-L. Turon and S. Gendreau (2000), Hydrological impact of Heinrich events in the suptropical Northeast Atlantic, *Science 289*, 1321-1324.

Berger, A. L. (1978), Long-term variations of daily insolation and Quaternary climatic changes, *J. Atmos. Sci. 35*, 2362-2367.

Bond, G., W. Broecker, S. Johnsen, J. McManus, L. Labeyrie, J. Jouzel and G. Bonani (1993), Correlations between climate records from North Atlantic sediments and Greenland ice, *Nature 365*, 143-147.

Bond, G., H. Heinrich, W. Broecker, L. Labeyrie, J. McManus, J. Andrews, S. Huon, R. Jantschik, S. Clasen, C. Simet, K. Tedesco, M. Klas, G. Bonani and S. Ivy (1992), Evidence for massive

discharges of icebergs into the north Atlantic ocean during the last glacial period, *Nature 360*, 245-249.

Bond, W. J., G. F. Midgley and F. I. Woodward (2003), The importance of low atmospheric CO_2 and fire in promoting the spread of grasslands and savannas, *Global Change Biology 9*, 973-982.

Bouimetarhan, I., L. Dupont, E. Schefuß, G. Mollenhauer, S. Mulitza and K. Zonneveld (2009), Palynological evidence for climatic and oceanic variability off NW Africa during the late Holocene, *Quaternary Research 72*, 188-197.

Bowen, G. J. (2009): Gridded maps of the isotopic composition of meteoric precipitation. www.waterisotopes.org.

Bowen, G. J. and J. Revenaugh (2003), Interpolating the isotopic composition of modern meteoric precipitation, *Water Resour. Res. 39*, 1299.

Boyle, E. A. and L. Keigwin (1987), North Atlantic thermohaline circulation during the past 20,000 years linked to high-latitude surface temperature, *Nature 330*, 35-40.

Brassel, S. C., G. Eglinton, I. T. Marlowe, U. Pflaumann and M. Sarnthein (1986), Molecular stratigraphy: a new tool for climatic assessment, *Nature 320*, 129-133.

Broccoli, A. J., K. A. Dahl and R. J. Stouffer (2006), Response of the ITCZ to northern hemisphere cooling, *Geophys. Res. Lett. 33*, L01702.

Broecker, W., G. Bond, M. Klas, E. Clark and J. McManus (1992), Origin of the northern Atlantic's Heinrich events, *Climate Dynamics 6*, 265-273.

Charney, J. G. (1975), Dynamics of deserts and drought in the Sahel, *Q. J. R. Meteorol. Soc. 101*, 193-202.

Chiang, J. C. H., M. Biasutti and D. S. Battisti (2003), Sensitivity of the Atlantic intertropical convergence zone to last glacial maximum boundary conditions, *Paleoceanography 18*, 1094.

Chikaraishi, Y. and H. Naraoka (2003), Compound-specific $\delta D - \delta^{13}C$ analyses of *n*-alkanes extracted from terrestrial and aquatic plants, *Phytochemistry 63*, 361-371.

Claussen, M., C. Kubatzki, V. Brovkin, A. Ganopolski, P. Hoelzmann and H.-J. Pachur (1999), Simulation of an abrupt change in Saharan vegetation in the mid-Holocene, *Geophys. Res. Lett. 26*, 2037-2040.

Collatz, G. J., J. A. Berry and J. S. Clark (1998), Effects of climate and atmospheric CO_2 partial pressure on the global distribution of C_4 grasses: present, past, and future, *Oecologia 114*, 441-454.

Collister, J. W., G. Rieley, B. Stern, G. Eglinton and F. Brian (1994), Compound-specific $\delta^{13}C$ analyses of leaf lipids from plants with differing carbon dioxide metabolism, *Org. Geochem. 21*, 619-627.

Combourieu Nebout, N., J. L. Turon, R. Zahn, L. Capotondi, L. Londeix and K. Pahnke (2002), Enhanced aridity and atmospheric high-pressure stability over the western Mediterranean during the North Atlantic cold events of the past 50 k.y., *Geology 30*, 863-866.

Conte, M., H., M.-A. Sicre, C. Rühlemann, J. C. Weber, S. Schulte, D. Schulz-Bull and T. Blanz (2006), Global temperature calibration of the alkenone unsaturation index ($U^{K'37}$) in surface waters and comparison with surface sediments, *Geochemistry Geophysics Geosystems 7*, Q02005.

Conte, M. H., G. Eglinton and L. A. S. Madureira (1992), Long-chain alkenones and alkyl alkenoates as palaeotemperature indicators: their production, flux and early sedimentary diagenesis in the Eastern North Atlantic, *Org. Geochem. 19*, 287-298.

Craig, H. (1961), Isotopic variations in meteoric waters, *Science 133*, 1702-1703.

Curry, W. B., J.-C. Duplessy, L. Labeyrie and N. J. Shackleton (1988), Changes in the distribution of $\delta^{13}C$ of deep water ΣCO_2 between the last glaciation and the Holocene, *Paleoceanography 3*, 317-341.

Daansgard, W., S. Johnsen, H. B. Clausen, D. Dahl-Jensen, N. S. Gundestrup, C. U. Hammer, C. S. Hvidberg, J. P. Steffensen, A. E. Sveinbjörnsdottir, J. Jouzel and G. Bond (1993), Evidence for general instability of past climate from a 250-kyr ice-core record, *Nature 364*, 218-220.

Dansgaard, W. (1964), Stable isotopes in precipitation, *Tellus 16*, 436-68.

deMenocal, P. B., J. Ortiz, T. Guilderson, J. Adkins, M. Sarnthein, L. Baker and M. Yarusinsky (2000), Abrupt onset and termination of the African humid period: rapid climate response to gradual insolation forcing, *Quat. Sci. Rev. 19*, 347-361.

Dongmann, G., H. W. Nürnberg, H. Förstel and K. Wagener (1974), On the enrichment of $H_2{}^{18}O$ in the leaves of transpiring plants, *Radiat. Environ. Biophys. 11*, 41-52.

Druyan, L. M. (1991), The sensitivity of sub-Saharan precipitation to Atlantic SST, *Clim. Change 18*, 17-36.

Duplessy, J. C., N. J. Shackleton, R. G. Fairbanks, L. Labeyrie, D. Oppo and N. Kallel (1988), Deepwater source variations during the last climatic cycle and their impact on the global deepwater circulation, *Paleoceanography 3*, 343-360.

Dupont, L. M. (1993), Vegetation zones in NW Africa during the brunhes chron reconstructed from marine palynological data, *Quat. Sci. Rev. 12*, 189-202.

Durand, A. (1982), Oscillations of lake chad over the past 50,000 years: New data and new hypothesis, *Palaeogeogr. Palaeoclimatol. Palaeoecol. 39*, 37-53.

Eglinton, G. and R. J. Hamilton (1967), Leaf epicuticular waxes, *Science 156*, 1322-1335.

Elliot, M., L. Labeyrie and J.-C. Duplessy (2002), Changes in North Atlantic deep-water formation associated with the Dansgaard-Oeschger temperature oscillations (60-10 ka), *Quat. Sci. Rev. 21*, 1153-1165.

Ellison, C. R. W., M. R. Chapman and I. R. Hall (2006), Surface and deep ocean interactions during the cold climate event 8200 years ago, *Science 312*, 1929-1932.

Epstein, S., P. Thompson and C. J. Yapp (1977), Oxygen and hydrogen isotopic ratios in plant cellulose, *Science 198*, 1209-1215.

Evan, A. T., D. J. Vimont, A. K. Heidinger, J. P. Kossin and R. Bennartz (2009), The role of aerosols in the evolution of tropical North Atlantic ocean temperature anomalies, *Science*, published online March 26, doi: 10.1126/science.1167404.

Flanagan, L. B., J. F. Bain and J. R. Ehleringer (1991), Stable oxygen and hydrogen isotope composition of leaf water in C_3 and C_4 plant species under field conditions, *Oecologia 88*, 394-400.

Folland, C. K., T. N. Palmer and D. E. Parker (1986), Sahel rainfall and worldwide sea temperatures, 1901-85, *Nature 320*, 602-607.

Fontaine, B. and S. Bigot (1993), West African rainfall deficits and sea surface temperatures, *Int. J. Climatol. 13*, 271-285.

Fontaine, B., S. Trzaska and S. Janicot (1998), Evolution of the relationship between near global and Atlantic SST modes and the rainy season in West Africa: statistical analyses and sensitivity experiments, *Climate Dynamics 14*, 353-368.

Gac, J.-Y. and A. Kane (1986), Le fleuve Sénégal: I. Bilan hydrologique et flux continentaux de matières particulaires a l'embouchure, *Sciences Géologiques Bulletin 39*, 99-130.

Ganachaud, A. and C. Wunsch (2000), Improved estimates of global ocean circulation, heat transport and mixing from hydrographic data, *Nature 408*, 453-457.

Ganopolski, A., C. Kubatzki, M. Claussen, V. Brovkin and V. Petoukhov (1998), The influence of vegetation-atmosphere-ocean interaction on climate during the mid-Holocene, *Science 280*, 1916-1919.

Gasse, F. (2000), Hydrological changes in the African tropics since the last glacial maximum, *Quat. Sci. Rev. 19*, 189-211.

Gasse, F. and E. van Campo (1994), Abrupt post-glacial climate events in West Asia and North Africa monsoon domains, *Earth Planet. Sci. Lett. 126*, 435-456.

Gat, J. R. (1996), Oxygen and hydrogen isotopes in the hydrological cycle, *Annu. Rev. Earth Planet. Sci. 24*, 225-262.

Ghannoum, O., S. V. Caemmerer, L. H. Ziska and J. P. Conroy (2000), The growth response of C_4 plants to rising atmospheric CO_2 partial pressure: a reassessment, *Plant, Cell & Environment 23*, 931-942.

Giannini, A., R. Saravanan and P. Chang (2003), Oceanic forcing of Sahel rainfall on interannual to interdecadal time scales, *Science 302*, 1027-1030.

Gong, C. and E. Eltahir (1996), Sources of moisture for rainfall in West Africa, *Water Resour. Res. 32*, 3115-3121.

Grimm, E. C., G. L. J. Jacobson, W. A. Watts, B. C. S. Hansen and K. A. Maasch (1993), A 50,000-year record of climate oscillations from Florida and its temporal correlation with the Heinrich Events, *Science 261*, 198-200.

Grimm, E. C., W. A. Watts, G. L. Jacobson Jr, B. C. S. Hansen, H. R. Almquist and A. C. Dieffenbacher-Krall (2006), Evidence for warm wet Heinrich events in Florida, *Quat. Sci. Rev. 25*, 2197-2211.

GRIP (1993), Climate instability during the last interglacial period recorded in the GRIP ice core, *Nature 364*, 203-207.

Grootes, P. M., M. Stuiver, J. W. C. White, S. Johnsen and J. Jouzel (1993), Comparison of oxygen isotope records from the GISP2 and GRIP Greenland ice cores, *Nature 366*, 552-554.

Hastenrath, S. (1984), Interannual variability and annual cycle: Mechanisms of circulation and climate in the tropical Atlantic sector, *Mon. Weather Rev. 112*, 1097-1107.

Heinrich, H. (1988), Origin and consequences of cyclic ice rafting in the Northeast Atlantic Ocean during the past 130,000 years, *Quaternary Research 29*, 142-152.

Herbert, T. D., J. D. Schuffert, D. Thomas, C. Lange, A. Weinheimer, A. Peleo-Alampay and J. C. Herguera (1998), Depth and Seasonality of alkenone production along the california margin inferred from a core top transect, *Paleoceanography 13*, 263-271.

Hoerling, M., J. Hurrell, J. Eischeid and A. Phillips (2006), Detection and attribution of twentieth-century northern and southern african rainfall change, *Journal of Climate 19*, 3989-4008.

Hou, J., W. J. D'Andrea and Y. Huang (2008), Can sedimentary leaf waxes record D/H ratios of continental precipitation? Field, model, and experimental assessments, *Geochim. Cosmochim. Acta 72*, 3503-3517.

Hou, J., W. J. D'Andrea, D. MacDonald and Y. Huang (2007), Hydrogen isotopic variability in leaf waxes among terrestrial and aquatic plants around Blood Pond, Massachusetts (USA), *Org. Geochem. 38*, 977-984.

Huang, Y., B. Shuman, Y. Wang and T. Webb (2004), Hydrogen isotope ratios of individual lipids in lake sediments as novel tracers of climatic and environmental change: a surface sediment test, *Journal of Paleolimnology 31*, 363-375.

Huang, Y., L. Dupont, M. Sarnthein, J. M. Hayes and G. Eglinton (2000), Mapping of C_4 plant input from north west Africa into north East Atlantic sediments, *Geochimica et Cosmochimica 64*, 3505-3513.

Hughen, K. A., M. G. L. Baillie, E. Bard, J. W. Beck, C. J. H. Bertrand, P. G. Blackwell, C. E. Buck, G. S. Burr, K. B. Cutler, P. E. Damon, R. L. Edwards, R. G. Fairbanks, M. Friedrich, T. P.

Guilderson, B. Kromer, G. McCormac, S. Manning, C. B. Ramsey, P. J. Reimer, R. W. Reimer, S. Remmele, J. R. Southon, M. Stuiver, S. Talamo, F. W. Taylor, J. van der Plicht and C. E. Weyhenmeyer (2004), Marine04 marine radiocarbon age calibration, 0-26 cal kyr BP, *Radiocarbon 46*, 1059-1086.

Hulbe, C. L., D. R. MacAyeal, G. H. Denton, J. Kleman and T. V. Lowell (2004), Catastrophic ice shelf breakup as the source of Heinrich event icebergs, *Paleoceanography 19*, PA1004.

Indermühle, A., E. Monnin, B. Stauffer, T. F. Stocker and M. Wahlen (2000), Atmospheric CO_2 concentration from 60 to 20 kyr BP from the Taylor Dome ice core, Antarctica, *Geophys. Res. Lett. 27*, 735–738.

Indermühle, A., T. F. Stocker, F. Joos, H. Fischer, H. J. Smith, M. Wahlen, B. Deck, D. Mastroianni, J. Tschumi, T. Blunier, R. Meyer and B. Stauffer (1999), Holocene carbon-cycle dynamics based on CO_2 trapped in ice at Taylor Dome, Antarctica, *Nature 398*, 121-126.

Itambi, A. C., T. Von Dobeneck, S. Mulitza, T. Bickert and D. Heslop (2009), Millennial-scale northwest African droughts related to Heinrich events and Dansgaard-Oeschger cycles: Evidence in marine sediments from offshore Senegal, *Paleoceanography 24*, PA1205.

Ivanochko, T. S., R. S. Ganeshram, G.-J. A. Brummer, G. Ganssen, S. J. A. Jung, S. G. Moreton and D. Kroon (2005), Variations in tropical convection as an amplifier of global climate change at the millennial scale, *Earth Planet. Sci. Lett. 235*, 302-314.

Johnsen, S. J., H. B. Clausen, W. Dansgaard, K. Fuhrer, N. Gundestrup, C. U. Hammer, P. Iversen, J. Jouzel, B. Stauffer and J. P. steffensen (1992), Irregular glacial interstadials recorded in a new Greenland ice core, *Nature 359*, 311-313.

Jullien, E., F. Grousset, B. Malaize, J. Duprat, M.-F. Sánchez-Goni, F. Eynaud, K. Charlier, R. Schneider, A. Bory, V. Bout and J. A. Flores (2007), Low-latitude "dusty events" vs. high latitude "icy Heinrich events", *Quaternary Research 68*, 379-386.

Kaufman, Y. J., D. Tanre and O. Boucher (2002), A satellite view of aerosols in the climate system, *Nature 419*, 215-223.

Kolattukudy, P. E. (1976), *Chemistry and biochemistry of natural waxes*, Elsevier Scientific Pub. Co., Amsterdam New York.

Kroopnick, P. M. (1985), The distribution of ^{13}C of ECO_2 in the world oceans, *Deep Sea Research Part A. Oceanographic Research Papers 32*, 57-84.

Kröpelin, S., D. Verschuren, A.-M. Lézine, H. Eggermont, C. Cocquyt, P. Francus, J.-P. Cazet, M. Fagot, B. Rumes, J. M. Russel, F. Darius, D. J. Conley, M. Schuster, H. von Suchodoletz and D. R. Engstrom (2008), Climate-driven ecosystem succession in the Sahara: The past 6000 years, *Science 320*, 765-768.

Kutzbach, J., G. Bonan, J. Foley and S. P. Harrison (1996), Vegetation and soil feedbacks on the response of the African monsoon to orbital forcing in the early to middle Holocene, *Nature 384*, 623-626.

Kutzbach, J. E. (1981), Monsoon climate of the early Holocene: Climate experiment with the earth's orbital parameters for 9000 years ago, *Science 214*, 59-61.

Kutzbach, J. E. and Z. Liu (1997), Response of the African monsoon to orbital forcing and ocean feedbacks in the middle Holocene, *Science 278*, 440-443.

Lamb, P. J. and R. A. Peppler (1992), Further case Studies of tropical Atlantic surface atmospheric and oceanic patterns associated with sub-Saharan drought, *Journal of Climate 5*, 476-488.

Lambeck, K. and J. Chappell (2001), Sea level change through the last glacial cycle, *Science 292*, 679-686.

Larcher, W. (2001), *Ökophysiologie der Pflanzen: Leben, Leistung und Streßbewältigung der Pflanzen in ihrer Umwelt*, Ulmer, Stuttgart.

Lau, K. M. and K. M. Kim (2007), Cooling of the Atlantic by Saharan dust, *Geophys. Res. Lett. 34*, L23811.

Lézine, A.-M. (1989), Late quaternary vegetation and climate of the Sahel, *Quaternary Research 32*, 317-334.

Lézine, A.-M. and J. Casanova (1989), Pollen and hydrological evidence for the interpretation of past climates in tropical west Africa during the holocene, *Quat. Sci. Rev. 8*, 45-55.

Liu, W. and H. Yang (2008), Multiple controls for the variability of hydrogen isotopic compositions in higher plant n-alkanes from modern ecosystems, *Global Change Biology 14*, 2166-2177.

Liu, W., H. Yang and L. Li (2006), Hydrogen isotopic compositions of *n*-alkanes from terrestrial plants correlate with their ecological life forms, *Oecologia 150*, 330-338.

Lu, J. and T. L. Delworth (2005), Oceanic forcing of the late 20th century Sahel drought, *Geophys. Res. Lett. 32*, L22706.

Lynch-Stieglitz, J., J. F. Adkins, W. B. Curry, T. Dokken, I. R. Hall, J. C. Herguera, J. J.-M. Hirschi, E. V. Ivanowa, C. Kissel, O. Marchal, T. M. Marchitto, I. N. McCave, J. F. McManus, S. Mulitza, U. Ninnemann, F. Peeters, E.-F. Yu and R. Zahn (2007), Atlantic meridional overturning circulation during the last glacial maximum, *Science 316*, 66-69.

MacAyeal, D. R. (1993), Binge/purge oscillations of the Laurentide ice sheet as a cause of the North Atlantic's Heinrich events, *Paleoceanography 8*, 775-784.

Mackensen, A. and T. Bickert (1999), Stable carbon isotopes in benthic foraminifera: Proxies for deep and bottom water circulation and new production, in *Use of proxies in paleoceanography: Examples from the South Atlantic*, 229-254, Springer, Berlin Heidelberg

Makou, M., K. A. Hughen, L. Xu, S. P. Sylva and T. I. Eglinton (2007), Isotopic records of tropical vegetation and climate change from terrestrial vascular plant biomarkers preserved in Cariaco Basin sediments, *Org. Geochem. 38*, 1680-1691.

Maley, J. and P. Brenac (1998), Vegetation dynamics, palaeoenvironments and climatic changes in the forests of western Cameroon during the last 28,000 years B.P, *Review of Palaeobotany and Palynology 99*, 157-187.

Manabe, S. and R. J. Stouffer (1995), Simulation of abrupt climate change induced by freshwater input to the North Atlantic Ocean, *Nature 378*, 165-167.

Marchal, O., T. F. Stocker and F. Joos (1998), Impact of Oceanic Reorganizations on the Ocean Carbon Cycle and Atmospheric Carbon Dioxide Content, *Paleoceanography 13*, 225–244.

Masson-Delmotte, V., J. Jouzel, A. Landais, M. Stievenard, S. J. Johnsen, J. W. C. White, M. Werner, A. Sveinbjornsdottir and K. Fuhrer (2005), GRIP deuterium excess reveals rapid and orbital-scale changes in Greenland moisture origin, *Science 309*, 118-121.

Mbow, C., O. Mertz, A. Diouf, K. Rasmussen and A. Reenberg (2008), The history of environmental change and adaptation in eastern Saloum-Senegal--Driving forces and perceptions, *Global and Planetary Change 64*, 210-221.

McIntosh, S. K. and R. J. McIntosh (1983), Current directions in West African prehistory, *Annu. Rev. Anthropol. 12*, 215-258.

McIntyre, A. and B. Molfino (1996), Forcing of atlantic equatorial and subpolar millennial cycles by precession, *Science 274*, 1867-1870.

McManus, J. F., R. Francois, J. M. Gherardi, L. D. Keigwin and S. Brown-Leger (2004), Collapse and rapid resumption of Atlantic meridional circulation linked to deglacial climate changes, *Nature 428*, 834-837.

Mittelstaedt, E. (1991), The ocean boundary along the Northwest African coast: Circulation and oceanographic properties at the sea surface, *Prog. Oceanog. 26*, 307-355.

Mix, A. C., W. F. Ruddiman and A. McIntyre (1986), Late quaternary paleoceanography of the tropical Atlantic, 1: Spatial variability of annual Mean sea-surface temperatures, 0-20,000 years B.P, *Paleoceanography 1*, 43-66.

Monnin, E., A. Indermuhle, A. Dallenbach, J. Fluckiger, B. Stauffer, T. F. Stocker, D. Raynaud and J.-M. Barnola (2001), Atmospheric CO_2 concentrations over the last glacial termination, *Science 291*, 112-114.

Moreno, A., I. Cacho, M. Canals, M. A. Prins, M. F. Sánchez Goni, L. O. Grimalt and G. J. Weltje (2002), Saharan dust transport and high-latitude glacial climatic variability: The Alboran Sea record, *Quaternary Research 58*, 318-328.

Mulitza, S., M. Prange, J.-B. Stuut, M. Zabel, T. von Dobeneck, A. C. Itambi, J. Nizou, M. Schulz and G. Wefer (2008), Sahel megadroughts triggered by glacial slowdowns of Atlantic meridional overturning, *Paleoceanography 23*, PA4206.

Mulitza, S., I. Bouimetarhan, M. Brüning, A. Freesemann, N. Gussone, H. Filipsson, G. Heil, S. Hessler, A. Jaeschke, H. Johnstone, M. Klann, F. Klein, K. Küster, C. März, H. McGregor, M. Minning, H. Müller, W.-T. Ochsenhirt, A. Paul, F. Schewe, M. Schulz, J. Steinlöchner, J.-B. Stuut, R. Tjallingii, T. von Dobeneck, S. Wiesmaier, M. Zabel and K. Zonneveld, (2006), Report and preliminary results of METEOR Cruise M65/1, Dakar-Dakar, 11.06 – 1.07.2005. Berichte, Fachbereich Geowissenschaften, Universität Bremen. No. 252, Bremen.

Müller, P. J. and G. Fischer (2001), A 4-year sediment trap record of alkenones from the filamentous upwelling region off Cape Blanc, NW Africa and a comparison with distributions in underlying sediments, *Deep Sea Research Part I: Oceanographic Research Papers 48*, 1877-1903.

Müller, P. J., G. Kirst, G. Ruhland, I. von Storch and A. Rosell-Melé (1998), Calibration of the alkenone paleotemperature index $U^{K'37}$ based on core-tops from the eastern South Atlantic and the global ocean (60°N-60°S), *Geochimica et Cosmochimica 62*, 1757-1772.

Ndeye, M. (2008), Marine reservoir ages in northern Senegal and Mauritania coastal waters, *Radiocarbon 50*, 281-288.

Nicholson, S. (2000), Land surface processes and Sahel climate, *Rev. Geophys. 38*, 117-139

Nicholson, S. (2009), A revised picture of the structure of the “monsoon” and land ITCZ over West Africa, *Climate Dynamics 32*, 1155-1171.

Nicholson, S. E. and J. P. Grist (2003), The seasonal evolution of the atmospheric circulation over West Africa and equatorial Africa, *Journal of Climate 16*, 1013-1030.

Niedermeyer, E. M., M. Prange, S. Mulitza, G. Mollenhauer, E. Schefuß and M. Schulz Extratropical forcing of Sahel aridity during Heinrich Stadials *submitted to Geophys. Res. Lett.*

O'Leary, M. H. (1981), Carbon isotopic fractionation in plants, *Phytochemistry 20*, 553-567

Oppo, D. W. and S. J. Lehman (1995), Suborbital timescale variability of North Atlantic Deep Water during the past 200,000 years, *Paleoceanography 10*, 901-910.

Otterman, J. (1974), Baring high-albedo soils by overgrazing: A hypothesized desertification mechanism, *Science 186*, 531-533.

Peck, J. A., R. R. Green, T. Shanahan, J. W. King, J. T. Overpeck and C. A. Scholz (2004), A magnetic mineral record of Late Quaternary tropical climate variability from Lake Bosumtwi, Ghana, *Palaeogeogr. Palaeoclimatol. Palaeoecol. 215*, 37-57.

Pendall, E., D. Williams and S. Leavitt (2005), Comparison of measured and modeled variations in piñon pine leaf water isotopic enrichment across a summer moisture gradient, *Oecologia 145*, 605-618.

Peterson, L. C., G. H. Haug, K. A. Hughen and U. Rohl (2000), Rapid changes in the hydrologic cycle of the tropical Atlantic during the last glacial, *Science 290*, 1947-1951.

Pokras, E. M. and A. C. Mix (1987), Earth's precession cycle and quaternary climatic change in tropical Africa, *Nature 326*, 486-487.

Policy, H. W., H. B. Johnson, B. D. Marinot and H. S. Mayeux (1993), Increase in C3 plant water-use efficiency and biomass over glacial to present CO_2 concentrations, *Nature 361*, 61-64.

Prahl, F. G. and S. G. Wakeham (1987), Calibration of unsaturation patterns in long-chain ketone compositions for palaeotemperature assessment, *Nature 330*, 367-369.

Prahl, F. G., L. A. Muehlhausen and D. L. Zahnle (1988), Further evaluation of long-chain alkenones as indicators of paleoceanographic conditions, *Geochim. Cosmochim. Acta 52*, 2303-2310.

Prange, M. (2008), The low-resolution CCSM2 revisited: new adjustments and a present-day control run, *Ocean Science 4*, 151-181.

Prange, M., G. Lohmann, V. Romanova and M. Butzin (2004), Modelling tempo-spatial signatures of Heinrich Events: influence of the climatic background state, *Quat. Sci. Rev. 23*, 521-527.

Prell, W. L. and E. van Campo (1986), Coherent response of Arabian Sea upwelling and pollen transport to late Quaternary monsoonal winds, *Nature 323*, 526-528.

Prospero, J. M. and P. J. Lamb (2003), African droughts and dust transport to the Caribbean: Climate change implications, *Science 302*, 1024-1027.

Raymo, M. E., W. F. Ruddiman, N. J. Shackleton and D. W. Oppo (1990), Evolution of Atlantic-Pacific $\delta^{13}C$ gradients over the last 2.5 m.y, *Earth Planet. Sci. Lett. 97*, 353-368.

Reed, R. J., D. C. Norquist and E. E. Recker (1977), The structure and properties of African wave disturbances as observed during phase III of GATE, *Mon. Weather Rev. 105*, 317-333.

Renssen, H., V. Brovkin, T. Fichefet and H. Goosse (2006), Simulation of the Holocene climate evolution in northern Africa: The termination of the African humid period, *Quaternary International 150*, 95-102.

Rieley, G., J. W. Collister, B. Stern and G. Eglinton (1993), Gas chromatography/isotope ratio mass spectrometry of leaf wax *n*-alkanes from plants of differing carbon dioxide metabolism, *Rapid Communication in Mass Spetrometry 7*, 488-491.

Risi, C., S. Bony and F. Vimeux (2008a), Influence of convective processes on the isotopic composition ($\delta^{18}O$ and δD) of precipitation and water vapor in the tropics: 2. Physical interpretation of the amount effect, *J. Geophys. Res. 113*, D19306.

Risi, C., S. Bony, F. Vimeux, L. Descroix, B. Ibrahim, E. Lebreton, I. Mamadou and B. Sultan (2008b), What controls the isotopic composition of the African monsoon precipitation? Insights from event-based precipitation collected during the 2006 AMMA field campaign, *Geophys. Res. Lett. 35*, L24808.

Romero, O. E., J.-H. Kim and B. Donner (2008), Submillenial-to-millenial variability of diatom production off Mauritania, NW Africa, during the last glacial cycle, *Paleoceanography 23*, PA3218.

Rossignol-Strick, M. (1983), African monsoons, an immediate climate response to orbital insolation, *Nature 304*, 46-49.

Rowell, D. P., C. K. Folland, K. Maskell and M. N. Ward (1995), Variability of summer rainfall over tropical North Africa (1906-92): Observations and modelling, *Q. J. R. Meteorol. Soc. 121*, 669-704.

Rühlemann, C., S. Mulitza, P. J. Müller, G. Wefer and R. Zahn (1999), Warming of the tropical Atlantic Ocean and slowdown of thermohaline circulation during the last deglaciation, *Nature 402*, 511-514.

Rühlemann, C., S. Mulitza, G. Lohmann, A. Paul, M. Prange and G. Wefer (2004), Intermediate depth warming in the tropical Atlantic related to weakened thermohaline circulation: Combining paleoclimate data and modeling results for the last deglaciation, *Paleoceanography 19*, PA1025.

Rybicki, G. B. and W. H. Press (1995), Class of fast methods for processing irregularly sampled or otherwise inhomogeneous one-dimensional data, *Phys. Rev. Lett. 74*, 1060.

Sachse, D., J. Radke and G. Gleixner (2004), Hydrogen isotope ratios of recent lacustrine sedimentary n-alkanes record modern climate variability, *Geochim. Cosmochim. Acta 68*, 4877-4889.

Sachse, D., J. Radke and G. Gleixner (2006), dD values of individual n-alkanes from terrestrial plants along a climatic gradient - Implications for the sedimentary biomarker record, *Org. Geochem. 37*, 469-483.

Salzmann, U., P. Hoelzmann and I. Morczinek (2002), Late quaternary climate and vegetation of the Sudanian zone of Northeast Nigeria, *Quaternary Research 58*, 73-83.

Sánchez-Goñi, M.-F., A. Landais, W. J. Fletcher, F. Naughton, S. Desprat and J. Duprat (2008), Contrasting impacts of Dansgaard-Oeschger events over a Western European latitudinal transect modulated by orbital parameters, *Quat. Sci. Rev. 27*, 1136-1151.

Sánchez-Goñi, M. F., J.-L. Turon, F. Eynaud and S. Gendreau (2000), European climatic response to millennial-scale changes in the atmosphere-ocean system during the last glacial period, *Quaternary Research 54*, 394-403.

Sarnthein, M., G. Tetzlaff, B. Koopmann, K. Wolter and U. Pflaumann (1981), Glacial and interglacial wind regimes over the eastern subtropical Atlantic and North-West Africa, *Nature 293*, 193-196.

Sarnthein, M., K. Winn, S. J. A. Jung, J.-C. Duplessy, L. Labeyrie, H. Erlenkeuser and G. Ganssen (1994), Changes in East Atlantic deepwater circulation over the last 30,000 years: Eight time slice reconstructions, *Paleoceanography 9*, 209-267.

Sarr, R., E. H. Sow and B. Sarr (2008), Holocene marine intrusions in Retba and Mbawane lakes (Senegal) evidenced by ostracod faunas, *Rev. Micropaleontol. 51*, 327-338.

Sarr, R., J.-P. Debenay and E. H. Sow (2009), Enregistrement des fluctuations du niveau marin dans l'Holocène supérieur du lac Retba (Sénégal) par les foraminifères, *Rev. Micropaleontol. 52*, 31-41.

Sauer, P. E., T. I. Eglinton, J. M. Hayes, A. Schimmelmann and A. L. Sessions (2001), Compound-specific D/H ratios of lipid biomarkers from sediments as a proxy for environmental and climatic conditions, *Geochimica et Cosmochimica 65*, 213-222.

Schefuß, E., S. Schouten and R. R. Schneider (2005), Climatic controls on central African hydrology during the past 20,000 years, *Nature 437*, 1003-1006.

Schefuß, E., V. Ratmeyer, J.-B. W. Stuut, J. H. F. Jansen and J. S. Sinnighe Damsté (2003), Carbon isotope analyses of *n*-alkanes in dust from the lower atmosphere over the central eastern Atlantic, *Geochim. Cosmochim. Acta 67*, 1757-1767.

Schiller, A., U. Mikolajewicz and R. Voss (1997), The stability of the North Atlantic thermohaline circulation in a coupled ocean-atmosphere general circulation model, *Climate Dynamics 13*, 325-347.

Schlesinger, W. H., J. F. Reynolds, G. L. Cunningham, L. F. Huenneke, W. M. Jarrell, R. A. Virginia and W. G. Whitford (1990), Biological feedbacks in global desertification, *Science 247*, 1043-1048.

Schmittner, A., M. Yoshimori and A. J. Weaver (2002), Instability of glacial climate in a model of the ocean- atmosphere-cryosphere system, *Science 295*, 1489-1493.

Schrag, D. P., J. F. Adkins, K. McIntyre, J. L. Alexander, D. A. Hodell, C. D. Charles and J. F. McManus (2002), The oxygen isotopic composition of seawater during the last glacial maximum, *Quat. Sci. Rev. 21*, 331-342.

Sessions, A. L. (2006), Isotope-ratio detection for gas chromatography, *J. Sep. Sci. 29*, 1946-1961.

Sessions, A. L., T. W. Burgoyne and J. M. Hayes (2001), Correction of H_3^+ contributions in hydrogen isotope ratio monitoring mass spectrometry, *Anal. Chem. 73*, 192-199.

Sessions, A. L., T. W. Burgoyne, A. Schimmelmann and J. M. Hayes (1999), Fractionation of hydrogen isotopes in lipid biosynthesis, *Org. Geochem. 30*, 1193-1200.

Severinghaus, J. P., T. Sowers, E. J. Brook, R. B. Alley and M. L. Bender (1998), Timing of abrupt climate change at the end of the Younger Dryas interval from thermally fractionated gases in polar ice, *Nature 391*, 141-146.

Shackleton, N. J., R. G. Fairbanks, T.-C. Chiu and F. Parrenin (2004), Absolute calibration of the Greenland time scale: implications for Antarctic time scales and for $\Delta^{14}C$, *Quat. Sci. Rev. 23*, 1513-1522.

Shanahan, T. M., J. T. Overpeck, C. A. Scholz, J. W. Beck, J. Peck and J. W. King (2008), Abrupt changes in the water balance of tropical west Africa during the late Quaternary, *J. Geophys. Res. 113*, D12108.

Shanahan, T. M., J. T. Overpeck, C. W. Wheeler, J. W. Beck, J. S. Pigati, M. R. Talbot, C. A. Scholz, J. Peck and J. W. King (2006), Paleoclimatic variations in West Africa from a record of late Pleistocene and Holocene lake level stands of Lake Bosumtwi, Ghana, *Paleogeography, Paleoclimatology, Paleoecology 242*, 287-302.

Shanahan, T. M., J. T. Overpeck, K. J. Anchukaitis, J. W. Beck, J. E. Cole, D. L. Dettman, J. A. Peck, C. A. Scholz and J. W. King (2009), Atlantic forcing of persistent drought in West Africa, *Science 324*, 377-380.

Simoneit, B. R. T., R. E. Cox and L. J. Standley (1989), Organic matter of the troposphere—IV. Lipids in harmattan aerosols of nigeria, *Atmos. Environ. 22*, 983-1004.

Singh, R. P., A. K. Prasad, V. K. Kayetha and M. Kafatos (2008), Enhancement of oceanic parameters associated with dust storms using satellite data, *J. Geophys. Res. 113*, C11008.

Smith, F. A. and K. H. Freeman (2006), Influence of physiology and climate on δD of leaf wax *n*-alkanes from C_3 and C_4 grasses, *Geochimica et Cosmochimica 70*, 1172-1187.

Stocker, T. F. and D. G. Wright (1991), Rapid transitions of the ocean's deep circulation induced by changes in surface water fluxes, *Nature 351*, 729-732.

Stott, L., C. Poulsen, S. Lund and R. Thunell (2002), Super ENSO and global climate oscillations at millennial time scales, *Science 297*, 222-226.

Stramma, L. and F. Schott (1999), The mean flow field of the tropical Atlantic Ocean, *Deep Sea Research Part II: Topical Studies in Oceanography 46*, 279-303.

Street-Perrott, F. A., Y. Huang, R. A. Perrott, G. Eglinton, P. Barker, L. B. Khelifa, D. D. Harkness and D. O. Olago (1997), Impact of lower atmospheric carbon dioxide on tropical mountain ecosystems, *Science 278*, 1422-1426.

Stuiver, M. and P. J. Reimer (1993), Extended ^{14}C database and revised Calib 3.0 ^{14}C age calibration program, *Radiocarbon 35*, 215-230.

Stuut, J.-B., M. Zabel, V. Ratmeyer, P. Helmke, E. Schefuß, G. Lavik and R. Schneider (2005), Provenance of present-day eolian dust collected off NW Africa, *J. Geophys. Res. 110*, D04202.

Sutton, R. T. and D. L. R. Hodson (2005), Atlantic ocean forcing of North American and European summer climate, *Science 309*, 115-118.

Swap, R., S. Ulanski, M. Cobbett and M. Garstang (1996), Temporal and spatial characteristics of Saharan dust outbreaks, *J. Geophys. Res. 101*, 4205-4220.

Talbot, M. R. and T. Johannessen (1992), A high resolution palaeoclimatic record for the last 27,500 years in tropical West Africa from the carbon and nitrogen isotopic composition of lacustrine organic matter, *Earth Planet. Sci. Lett. 110*, 23-37.

Teece, M. A., J. M. Getliff, J. W. Leftley, R. J. Parkes and J. R. Maxwell (1998), Microbial degradation of the marine prymnesiophyte Emiliania huxleyi under oxic and anoxic conditions as a model for early diagenesis: long chain alkadienes, alkenones and alkyl alkenoates, *Org. Geochem. 29*, 863-880.

Thompson, R. M., S. W. Payne, E. E. Recker and R. J. Reed (1979), Structure and Properties of Synoptic-Scale Wave Disturbances in the Intertropical Convergence Zone of the Eastern Atlantic, *J. Atmos. Sci. 36*, 53-72.

Tierney, J. E., J. M. Russell, Y. Huang, J. S. S. Damste, E. C. Hopmans and A. S. Cohen (2008), Northern hemisphere controls on tropical Southeast African climate during the past 60,000 Years, *Science 322*, 252-255.

Tjallingii, R., M. Claussen, J.-B. W. Stuut, J. Fohlmeister, A. Jahn, T. Bickert, F. Lamy and U. Röhl (2008), Coherent high- and low-latitude control of the northwest African hydrological balance, *Nature Geoscience 1*, 670-675.

Toggweiler, J. R., J. L. Russell and S. R. Carson (2006), Midlatitude westerlies, atmospheric CO_2, and climate change during the ice ages, *Paleoceanography 21,* PA2005.

Tomczak, M. and J. S. Godfrey (1994), *Regional oceanography: An introduction*, Pergamon.

Turney, C. S. M., A. P. Kershaw, S. C. Clemens, N. Branch, P. T. Moss and L. Keith Fifield (2004), Millennial and orbital variations of El Nino/Southern Oscillation and high-latitude climate in the last glacial period, *Nature 428*, 306-310.

Tyrrell, T. and A. Merico (2004), Emiliania huxleyi: bloom observations and the conditions that indice them, in *Coccolithophores - From molecular processes to to global impact*, edited by Thierstein;, H. R. and J. R. Young, pp. 75-97, Springer.

Vidal, L., L. Labeyrie, E. Cortijo, M. Arnold, J. C. Duplessy, E. Michel, S. Becqué and T. C. E. van Weering (1997), Evidence for changes in the North Atlantic deep water linked to meltwater surges during the Heinrich events, *Earth Planet. Sci. Lett. 146*, 13-27.

Voelker, A. H. L. (2002), Global distribution of centennial-scale records for Marine Isotope Stage (MIS) 3: a database, *Quat. Sci. Rev. 21*, 1185-1212.

Waelbroeck, C., L. Labeyrie, E. Michel, J. C. Duplessy, J. F. McManus, K. Lambeck, E. Balbon and M. Labracherie (2002), Sea-level and deep water temperature changes derived from benthic foraminifera isotopic records, *Quat. Sci. Rev. 21*, 295-305.

Walter, H. (1970), Klimatisch bedingte Savannen. Gräser und Holzarten als Antagonisten, *Vegetationszonen und Klima*, Ulmer, Stuttgart.

Wang, X., A. S. Auler, R. L. Edwards, H. Cheng, P. S. Cristalli, P. L. Smart, D. A. Richards and C.-C. Shen (2004), Wet periods in northeastern Brazil over the past 210 kyr linked to distant climate anomalies, *Nature 432*, 740-743.

Wang, Y. J., H. Cheng, R. L. Edwards, Z. S. An, J. Y. Wu, C. C. Shen and J. A. Dorale (2001), A high-resolution absolute-dated late pleistocene monsoon record from Hulu Cave, China, *Science 294*, 2345-2348.

Webb, J. L. (1994), *Desert Frontier: Ecological and Economic Change along the Western Sahel, 1600-1850*, University of Wisconsin.

Weijers, J. W. H., S. Schouten, J. C. van den Donker, E. C. Hopmans and J. S. Sinninghe Damsté (2007a), Environmental controls on bacterial tetraether membrane lipid distribution in soils, *Geochim. Cosmochim. Acta 71*, 703-713.

Weijers, J. W. H., E. Schefuss, S. Schouten and J. S. S. Damste (2007b), Coupled Thermal and Hydrological Evolution of Tropical Africa over the Last Deglaciation, *Science 315*, 1701-1704.

Weldeab, S., D. W. Lea, R. R. Schneider and N. Andersen (2007), 155,000 years of West African monsoon and ocean thermal evolution, *Science 316*, 1303-1307.

White, F. (1983), The vegetation of Africa, *Natural Resources Research*, UNESCO, Paris.

Worden, J., D. Noone and K. Bowman (2007), Importance of rain evaporation and continental convection in the tropical water cycle, *Nature 445*, 528-532.

Xue, Y. and J. Shukla (1993), The Influence of land surface properties on Sahel climate. Part 1: Desertification, *Journal of Climate 6*, 2232-2245.

Yuan, D., H. Cheng, R. L. Edwards, C. A. Dykoski, M. J. Kelly, M. Zhang, J. Qing, Y. Lin, Y. Wang, J. Wu, J. A. Dorale, Z. An and Y. Cai (2004), Timing, duration, and transitions of the last interglacial Asian monsoon, *Science 304*, 575-578.

Zhang, R. and T. L. Delworth (2005), Simulated tropical response to a substantial weakening of the Atlantic thermohaline circulation, *Journal of Climate 18*, 1853-1860.

Zhao, M., N. A. S. Beveridge, N. J. Shackleton, M. Sarnthein and G. Eglinton (1995), Molecular stratigraphy of cores off Northwest Africa: Sea surface temperature history over the last 80 ka, *Paleoceanography 10*, 661-675.

Zheng, X. and E. A. B. Eltahir (1998), The role of vegetation in the dynamics of West African monsoons, *Journal of Climate 11*, 2078-2096.